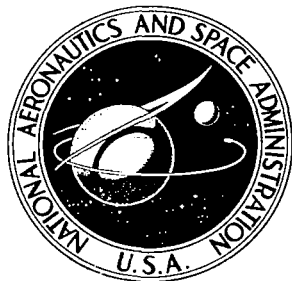


**NASA CONTRACTOR  
REPORT**

NASA CR-1401



NASA CR-1401

0.1

LOAN COPY: RETURN TO  
AFWL (WLIL-2)  
HARTLAND AFB, N MEX

0060534



TECH LIBRARY KAFB, NM

**DESIGN OF BRAYTON ROTATING UNIT  
ON ROLLING-ELEMENT BEARINGS**

*by R. Cohen and J. Clausi*

*Prepared by*

**UNITED AIRCRAFT CORPORATION**

East Hartford, Conn.

*for Lewis Research Center*

NATIONAL AERONAUTICS AND SPACE ADMINISTRATION • WASHINGTON, D. C. • AUGUST 1969

NASA CR-1401

TECH LIBRARY KAFB, NM



0060534

## DESIGN OF BRAYTON ROTATING UNIT ON ROLLING-ELEMENT BEARINGS

By R. Cohen and J. Clausi

Distribution of this report is provided in the interest of information exchange. Responsibility for the contents resides in the author or organization that prepared it.

Prepared under Contract No. NAS 3-10949 by  
PRATT & WHITNEY AIRCRAFT  
Division of United Aircraft Corporation  
East Hartford, Conn.

for Lewis Research Center

NATIONAL AERONAUTICS AND SPACE ADMINISTRATION

---

For sale by the Clearinghouse for Federal Scientific and Technical Information  
Springfield, Virginia 22151 - CFSTI price \$3.00

## ABSTRACT

The National Aeronautics and Space Administration is developing a Brayton-cycle space power system as part of its evaluation of potential long-life nuclear and solar electrical power sources. The candidate Brayton-cycle system under active investigation incorporates a single-shaft rotating unit consisting of a compressor, turbine and alternator rotating on gas bearings. This study was conducted to design such a Brayton rotating unit operating on oil-lubricated rolling-element bearings. Design of the bearing system was based on the technology demonstrated in two 2500-hour endurance tests successfully conducted in previous programs. Therefore, the bearing system design should be capable of development for mission lifetimes in excess of 10,000 hours with no significant oil contamination of the power system.

## FOREWORD

The research described herein, which was conducted by Pratt & Whitney Aircraft, Division of United Aircraft Corporation, was performed under NASA Contract NAS 3-10949. The work was done under the direction of Mr. C. L. O'Dear, Space Power Systems Division, NASA Lewis Research Center, as project manager. The report was originally issued as Pratt & Whitney report PWA-3549, November 1968.



## TABLE OF CONTENTS

	<u>Page</u>
Foreword	iii
Table of Contents	v
List of Figures	vi
List of Tables	ix
I. Summary	1
II. Introduction	2
III. Brayton Rotating Unit Design	5
A. General Arrangement of Brayton Rotating Unit	5
B. Rolling-Element Bearing Lubrication System Design	8
1. Lubrication System	8
2. Separator	22
3. Heat Exchanger	25
4. Lubricant Selection	25
5. Adsorber	27
C. Bearing Design	30
D. Seal Design	40
E. Oil Contamination of Power System	44
F. Temperature Maps	46
G. Critical Speed Analysis	49
Appendix – Alternate Configurations of Brayton Rotating Unit	52

## LIST OF FIGURES

<u>Number</u>	<u>Title</u>	<u>Page</u>
1	Brayton Rotating Unit	4
2	BRU with Rolling-Contact Bearings	6
3	BRU Lubrication System Schematic	10
4	Turbine-End Bearing Compartment	11
5	Compressor-End Bearing Compartment	12
6	Scavenge Pump	13
7	Scavenge Impeller Performance	14
8	BRU with Rolling-Contact Bearings	16
9	BRU Lubrication System Flow Rates	17
10	Two-Phase Flows	18
11	BRU Lubrication System Pressures	20
12	Turboalternator Design	23
13	Rotating Parts of Separator	24
14	Heat Exchanger Design	26
15	Tested Adsorber Configurations	28
16	Adsorber Configuration	29
17	20 mm Angular-Contact Ball Bearing	32
18	Bearing Performance	33
19	Bearing Cage Speeds	34
20	BRU Bearing Load Diagram	35
21	BRU Bearing Life	37

## LIST OF FIGURES (Cont'd)

<u>Number</u>	<u>Title</u>	<u>Page</u>
22	Dry-Face Seal and Sealplate (Seal in 20 mm Bearing Compartment)	41
23	Carbon Face Seal Gas Leakage	42
24	Carbon Face Seal Power Consumption (Seal in 20 mm Bearing Compartment)	43
25	Seal Wear	45
26	Thermal Map of Compressor End (6 KW)	47
27	Thermal Map of Turbine End (6 KW)	48
28	Mass Distribution of Rotor Assembly	50
29	Distribution of Polar Moment of Inertia of Rotor Assembly	51
30	Gas Bearing BRU	55
31	BRU Turbine Wheel	56
32	BRU Compressor Wheel	57
33	BRU Alternator	58
34	BRU with Rolling-Contact Bearings	62
35	Gas Make-up System Weight	64
36	BRU with Rolling-Contact Bearings	67
37	BRU with Rolling-Contact Bearings	68
38	BRU with Rolling-Contact Bearings	69
39	BRU Lubrication System Schematic - Inboard Bearings	70
40	BRU with Rolling-Contact Bearings	71
41	BRU with Rolling-Contact Bearings	73



## LIST OF FIGURES (Cont'd)

<u>Number</u>	<u>Title</u>	<u>Page</u>
42	BRU with Rolling-Contact Bearings	74
43	BRU with Rolling-Contact Bearings	76
44	BRU with Rolling-Contact Bearings	77
45	BRU with Rolling-Contact Bearings	79
46	BRU with Rolling-Contact Bearings	80
47	BRU with Rolling-Contact Bearings	82
48	BRU with Rolling-Contact Bearings	83
49	Shaft Section of BRU with Inboard Bearings	85
50	BRU with Rolling-Contact Bearings	86
51	BRU Lubrication System Schematic - Outboard Bearings (Externally-Driven Separator)	87
52	BRU Lubrication System Schematic - Outboard Bearings (No Separator)	88

## LIST OF TABLES

<u>Number</u>	<u>Title</u>	<u>Page</u>
1	Parasitic Power Losses	15
2	Lubrication System Flow Rates	19
3	Lubrication System Pressure Levels	19
4	Buffer-Gas Oil-Vapor Transport Capacity	21
5	Separator Performance	22
6	Adsorber Performance Comparison	27
7	Adsorber Design	30
8	Bearing B <sub>1</sub> Lifetime	36
9	Requirements for Compressor-End Bearing	39
10	Requirements for Turbine-End Bearing	39
11	Solar Heat Receiver Design	46
12	BRU Design Requirements	60
13	Rotor Dynamic Characteristics of Inboard-Bearing Configuration	65
14	Rotor Dynamic Characteristics. Inboard-Bearing Configuration (No Separator on Shaft)	72
15	Rotor Assembly Critical Speeds	78
16	Rotor Assembly Critical Speeds	78
17	Parasitic Power Losses for 40mm Outboard-Mounted Rolling-Contact Bearings	81



## I. SUMMARY

Pratt & Whitney Aircraft has conducted a preliminary design study of a single-shaft Brayton-cycle rotating unit (BRU) incorporating a radial compressor, a radial turbine and a four -pole radial gap alternator supported on a common shaft rotating at 36,000 rpm, and supported on oil-lubricated, rolling-element bearings. The design of the rolling-element bearing and lubrication system is based on the flight-type technology previously demonstrated by Pratt & Whitney Aircraft for Brayton-cycle turbomachinery under NASA Contract NAS3 -7635, and other programs. During the earlier programs, two 2500-hour endurance tests successfully demonstrated the integrity of the rotor support system at 50,000 rpm, and demonstrated the excellent performance of the gas cleanup system.

The Brayton Rotating Unit design resulting from the present study supports the rotor assembly with bearing compartments located outboard of the major rotating components. A separator is located at the compressor end of the rotor assembly, overhung from the bearing. This bearing is 35 mm in diameter, while the turbine-end bearing is 20 mm. Both bearing compartments are sealed from the working cycle by carbon face seals and labyrinth buffer seals. With the larger bearing controlling life, predicted  $B_1$  and  $B_{10}$  lives for this bearing are 13,400 and 58,000 hours, respectively. Face-seal life based on carbon wear, falls within the same life range. The total parasitic power loss predicted for the lubrication system is about 1260 watts. Oil contamination of the power system is estimated to be about 0.05 gram in 10,000 hours, well within allowable limits for the columbium alloy heat receiver of a Brayton-cycle system with a solar heat source.

## II. INTRODUCTION

The National Aeronautics and Space Administration is developing a Brayton-cycle space power system as part of its evaluation of potential long-life nuclear and solar electrical power sources. The candidate Brayton-cycle system under active investigation incorporates a heat source, a rotating unit, a recuperator and a cooler in the power-conversion loop. The rotating unit is a single-shaft combined rotating unit consisting of a single-stage radial compressor, a single-stage radial turbine and a high-frequency alternator operating on gas bearings. It became the desire of the National Aeronautics and Space Administration to design a backup Brayton Rotating Unit (BRU) operating on oil-lubricated rolling-element bearings. Pratt & Whitney Aircraft, under Contract NAS3-10949, conducted a preliminary design study of a BRU incorporating designs of the rotor-support system and lubrication system based on the flight-type technology developed by Pratt & Whitney Aircraft previously under NASA Contract NAS3-7635\* and other programs.

The Brayton Rotating Unit is designed to operate using a helium-xenon gas mixture combined in proportions resulting in a molecular weight of 83.8, similar to krypton. The lubricant used in the design is 5P4E polyphenyl ether (PWA-524). Designs of the radial-inflow turbine, alternator and radial compressor were furnished by the National Aeronautics and Space Administration. The unit was designed to be capable of more than 10,000 hours of operating life with the following conditions used in the design of the unit:

### Turbine

weight flow	0.8 lb/sec
inlet total temperature	2060°R
inlet total pressure	25.8 psia
pressure ratio, total-to-total	1.75
rotative speed, design	36,000 rpm
speed capability, percent of design	0 to 120%

### Alternator

design power, net	6.0 KW
number of poles	4
voltage	120/208 volts
frequency	1200 Hertz
coolant	Dow-Corning 200
coolant temperature	530°R

### Compressor

inlet total temperature	540°R
inlet total pressure	14.2 psia
pressure ratio, total-to-total	1.90

\*Cohen, R., H. Means and P. Heyl, Brayton-Cycle Turbomachinery on Rolling-Element Bearings, Report PWA-3277, Pratt & Whitney Aircraft, Contract NAS3-7635, March 1968, NASA Report CR-1229

The study covered three phases:

- 1) Preliminary design studies of the BRU to evaluate alternate candidate configurations.
- 2) Selection of the most promising of the candidate configurations for further design evaluation with particular emphasis on the rotor support and lubrication system.
- 3) Establishment of preliminary design drawings, temperature maps, flow and pressure schematics, critical stresses, component life, rotor dynamic behavior, and parasitic power loss and cycle gas bleed flow estimates for the bearing and lubrication system.

The first phase of this study which evaluated many alternate configurations is presented in the Appendix, along with a brief description of the gas-bearing version. The design and analysis results of the selected configuration are presented in the following sections.

The BRU incorporating oil-lubricated rolling-element bearings is shown in Figure 1. The overall length of the unit is about 2.5 feet.

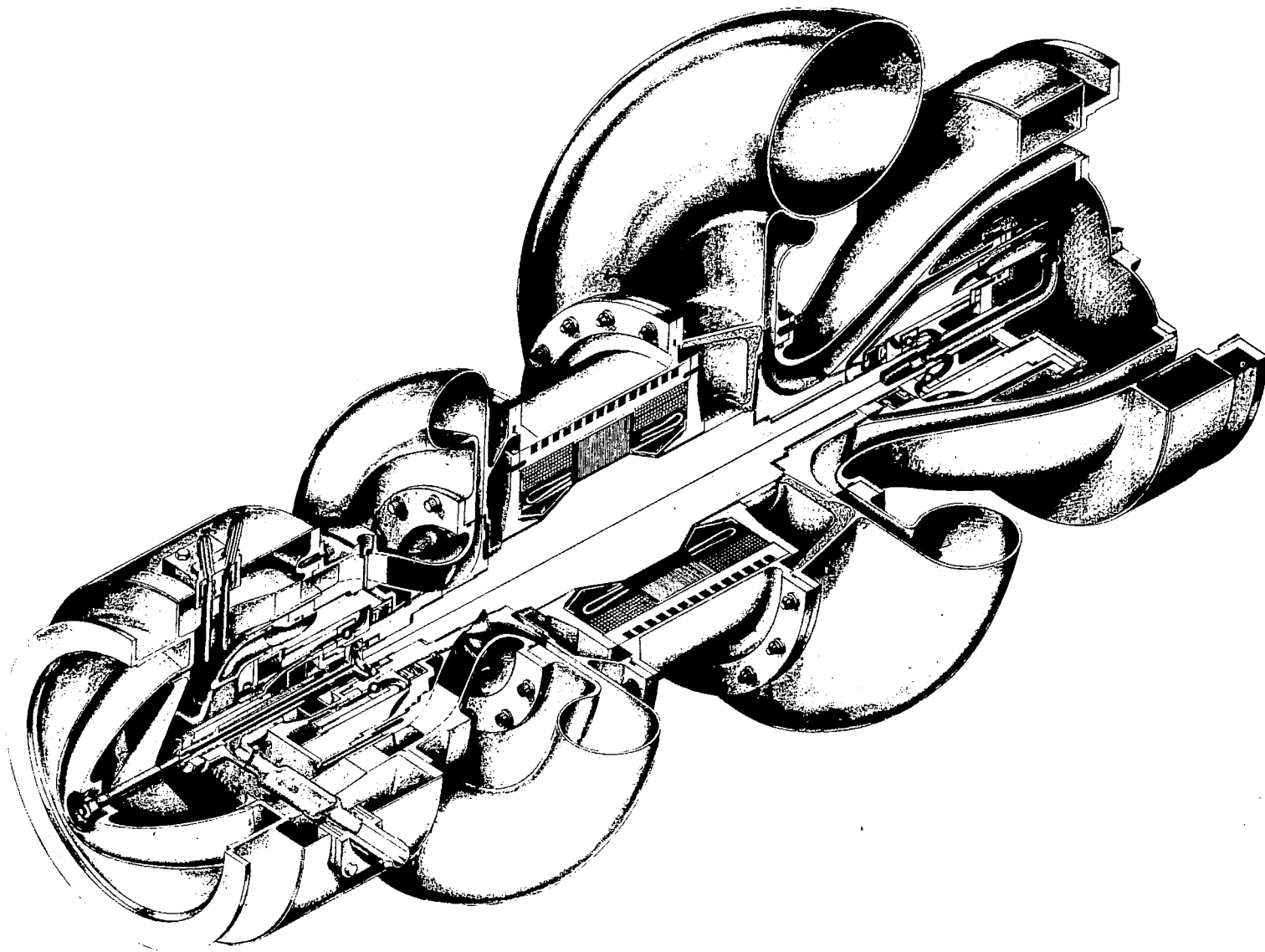


Figure 1 Brayton Rotating Unit

### III. BRAYTON ROTATING UNIT DESIGN

The overall objectives and considerations of the BRU preliminary design study were: 1) to design a bearing, seal and lubrication system that would provide a high probability of successful operation for a mission duration of at least 10,000 hours, and would be compatible with the weight objectives of the Brayton-cycle power system, 2) to retain, as far as practicable, the mechanical configuration and performance objectives of the gas-bearing BRU by utilizing the existing turbine and compressor aerodynamic designs and the alternator electrical design, 3) to minimize the parasitic power losses of the oil-lubricated rolling-element bearing system, including that of any required auxiliaries (such as a separately-driven separator) within the limits of the life, reliability and design objectives, and 4) to use the technology developed and utilized by Pratt & Whitney Aircraft under Contract NAS3-7635.

#### A. General Arrangement of Brayton Rotating Unit

The BRU design shown in Figure 2 includes, from left to right, an overhung separator, a 35 mm bore bearing, a 5.25 inch diameter radial-flow compressor wheel, a modified Lundell alternator rotor, a 5.0 inch diameter radial-inflow turbine wheel, and a 20 mm bore bearing at the turbine end. The two ball bearings which support the rotor assembly are thrust-loaded against each other by springs to preclude skidding which could occur in a lightly-loaded high-speed application such as this. Both of these angular-contact ball bearings are of the extra-light series constructed of M-50 steel with one-piece cages.

The bearing compartments are sealed from the powerplant cycle by carbon face seals with a mean seal diameter of 2.0 inches at the compressor end and 1.5 inches at the turbine end. To provide the most positive protection against oil leakage across the contact face, the seal is designed with the oil at the outer edge of the rotating interface so that any leakage has to oppose the centrifugal force of the rotating members. Two labyrinth seal assemblies are located adjacent to each carbon face seal. High-pressure helium-xenon gas fed between the labyrinth seals provides a pressure differential across the face seal and a purge for oil that might weep past the face seal. Any small amount of oil picked up by the buffer gas is removed in an adsorber bed prior to return to the cycle.

Immediately inboard of each bearing is an impeller machined into the sealplate to act as a scavenge pump for the oil-gas mixture passing through the bearing and seal. The two scavenge impellers operate in series to provide sufficient head to circulate the gas-oil mixture through the lubrication system. Heat exchangers located external to the BRU cool the two-phase oil-gas mixture as it is pumped between bearing compartments.

The separator overhung from the BRU shaft at the compressor end consists of a conical housing assembly containing a woven metallic matrix. The stationary outer housing of the separator is cooled to condense oil vapor carried in the gas. Only gas returned to the powerplant as make-up for leakage through the two face seals passes through the separator. Further purification of the gas is accomplished in an adsorber located external to the BRU. The adsorber consists of a polyurethane prefilter and glass wool.

The following list of design features was incorporated into the rotor support and lubrication system of the BRU.



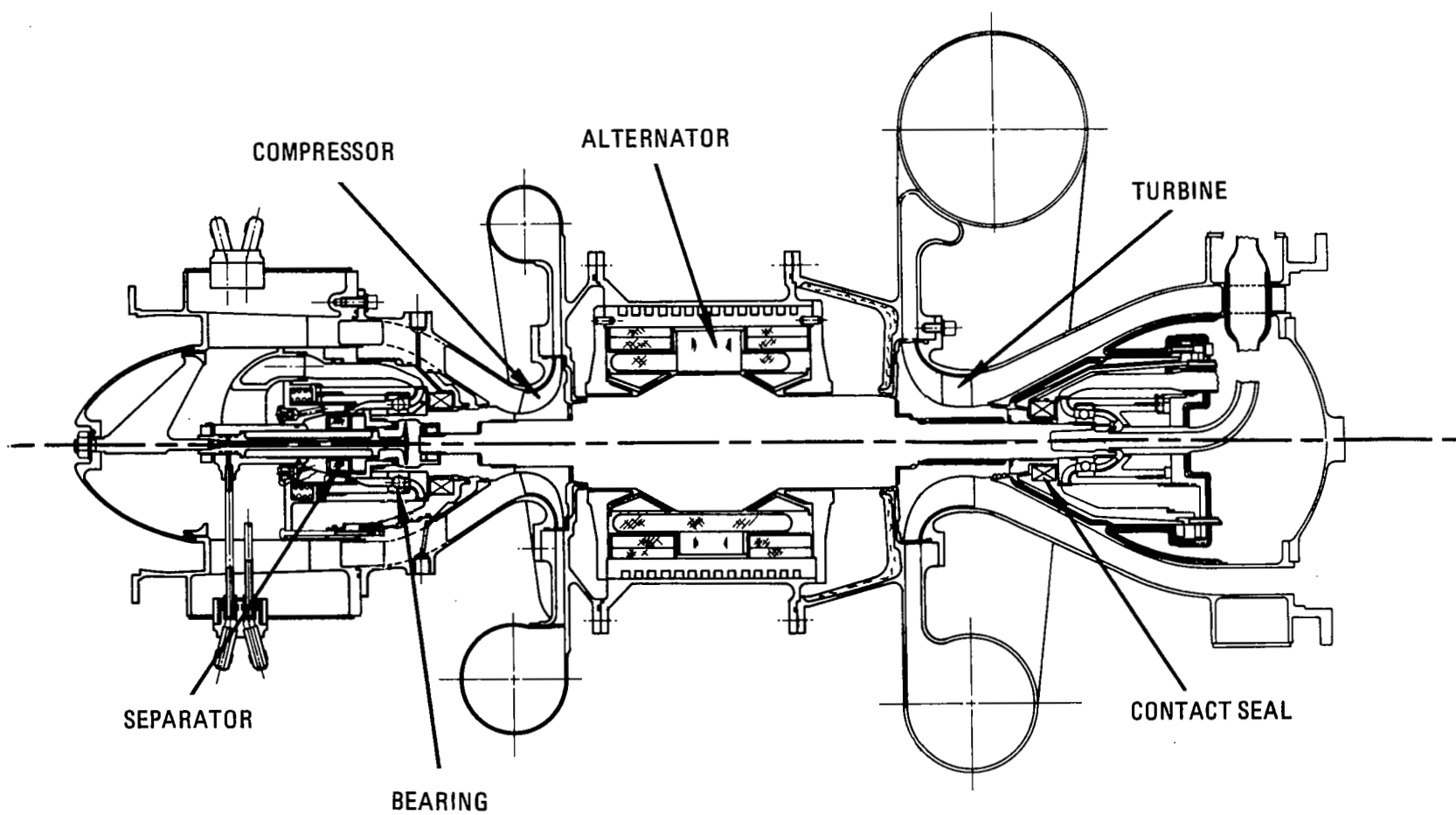


Figure 2 BRU with Rolling-Contact Bearings M-54839

1. Small angular-contact ball bearings with DN values of 0.72 and  $1.26 \times 10^6$  mm-rpm. Such a bearing with a DN of  $1.0 \times 10^6$  mm-rpm was successfully tested at representative conditions for 2500 hours with no measurable wear detected. Tests at speeds up to 60,000 rpm indicated no skidding, as predicted.
2. Small dry-face carbon seals (incorporating a damped-bellows secondary seal) with rubbing velocities of 236 and 322 feet per second. Two such seals running on chrome carbide-coated sealplates with a rubbing velocity of 335 feet per second were successfully tested at representative conditions for 2500 hours with low carbon wear (wear rate was about 1/2 to 1/3 of wear allowance), extremely low gas leakage amounting to less than 2 pounds per year, and complete bellows integrity in both seals, each with an imposed cyclic history of 7.5 billion cycles. Tests at speeds up to 60,000 rpm indicated satisfactory seal operation.
3. A small mechanical gas-oil separator incorporating a fine-mesh structure to separate oil from the gas returned to the powerplant as make-up for seal leakage. The separator designed under Contract NAS3-7635 was successfully tested for 2500 hours and measurements indicated the separation effectiveness ratio\* of about 1,500,000 remained unchanged throughout the endurance test.
4. An oil inventory control system which maintains the oil level in a rotating pool with an immersed stationary scoop connected by piping to an accumulator. When tested, this system demonstrated satisfactory oil flow capacity.
5. A two-phase circulating oil-gas lubrication system using centrifugal impellers in the bearing compartments, to develop the required gas pressure rise for circulating the mixture through the separator, piping, heat exchanger, seals and bearings. Such a lubrication system was successfully demonstrated in multiple orientations to show zero-gravity operating capability, and was operated for 2500 hours with all measured parameters showing maintenance of performance and component temperatures. Multiple start and stop tests also indicated capability for proficient start-and-stop functions in space. Tests at speeds up to 60,000 rpm indicated satisfactory operation. In addition to the testing with argon gas, the system was tested using the BRU helium-xenon gas mixture and krypton gas at the BRU design pressure level and at the low and high off-design pressure levels, with excellent performance results. The test with the He-Xe gas mixture at BRU design pressure level was conducted for 100 hours, and no significant performance degradation or change in component temperatures was evident during the endurance test.
6. An adsorber to remove oil and certain possible oil decomposition products from the cleaned gas which enters from the mechanical separator as the gas flows to the powerplant, to make up for the quantity of gas leaking through the face seals. An adsorber is also used to clean the buffer-zone sweep gas on its return to the powerplant. Four such adsorbers of varying material composition and flow geometry were tested in endurance tests ranging from 1000 to 2500 hours, and accumulated over 6000 hours of successful operation. One of the adsorbers was tested in the pilot system demonstration test, and

---

\*Separation effectiveness ratio is the ratio of the oil entering the separator to the oil leaving the separator in the cleaned gas

performance for the 2500-hour endurance test showed an average oil separation effectiveness ratio of 450. Subsequent improved adsorber designs demonstrated oil separation effectiveness ratios up to 8500. These adsorber performance levels, in conjunction with the mechanical separator performance and face-seal oil leakage rates, indicate a potential of restricting the powerplant oil contamination to less than one gram per year. Studies indicate that this amount of oil contamination is from one to two orders of magnitude less than that which could be deleterious to the columbium-alloy heat receiver being used by the NASA Lewis Research Center in the solar Brayton-cycle system test.

7. A buffer gas zone is located behind each face seal to prevent oil leaking through the face seal from entering the powerplant. This zone consists of two sets of labyrinth seals pressurized with a small fraction of compressor discharge gas at the interface between the two labyrinth seals. Part of the supply gas passes through one set of labyrinth seals to the powerplant. The remaining buffer gas flows toward the face seal and then passes out of the BRU through an adsorber to the compressor gas inlet. The sweep gas removes oil from the buffer zone by entrainment of liquid droplets and by evaporation of oil into the flowing gas. The latter capability was demonstrated in two 2500-hour endurance tests. The low face-seal oil leakage discussed above represents about one percent of the vapor-carrying capacity of the contemplated sweep-gas flow in the BRU.
8. The lubricant used in the design study was 5P4E polyphenyl ether, PWA 524 oil. This lubricant was used throughout the testing conducted under Contract NAS3-7635, and property measurements made after the 2500-hour pilot-system endurance test indicated no significant property changes.

Of particular importance in the integration of the above demonstrated components into the total BRU design were the scavenging, separating and gas purifying, heat rejection, and flow portions of the system. These will be discussed in following sections.

## B. Rolling-Element Bearing Lubrication System Design

### 1. Lubrication System

The lubrication system must provide proper lubrication and cooling of the bearings and seals during development testing, prelaunch checkout, and during operation in a gravity-free space environment without contaminating the cycle gas. In addition, these requirements must be achieved with low power consumption. The lubrication system must also prevent contamination of the cycle gas with the rotor not rotating. During development testing and prelaunch checkout, the system should be capable of operation in a horizontal position or in either vertical orientation.

The requirement that the powerplant be able to operate in various orientations in various gravitational fields with low power losses presents a unique requirement for the oil feed and scavenge design. An oil sump and pump system for a conventional engine is dependent upon gravity and ordinarily is not restrained by power consumption limits. In order to circumvent

these two restraints, systems which depend upon rotational-centrifugal effects to circulate the oil and gas through the system and to separate the oil from the gas are utilized. A combination of face and labyrinth seals is used to separate and restrict the leakage of oil into the cycle gas and the leakage of cycle gas into the lubrication system.

A flow schematic of the lubrication system used in this design is shown in Figure 3. Oil enters the compressor-end bearing at Location 1 in a mist as it passes through the balls and in a liquid state as it passes under the inner race of the bearing, and subsequently as it passes through the sealplate. The oil mist, after experiencing a pressure rise imparted by the impeller vanes machined on the back of the sealplate, mixes with the oil leaving the sealplate. The heated oil-gas mixture passes out of the bearing compartment to a liquid-cooled heat exchanger where the temperature of the mixture is lowered in preparation for introduction into the turbine-end bearing. The mixture passes through the turbine-end bearing compartment shown in Figure 4, is cooled again in a heat exchanger, and is reintroduced into the compressor-end bearing shown in Figure 5. The oil cools the bearings by passing through slots in the inner race, and oil as a mist is carried by gas through the bearing balls to provide lubrication. The oil cools the rotating sealplate after leaving the bearing inner race. Figure 6 is a photograph of the scavenge hardware tested in the previous program and is the same size as that shown for the turbine-end bearing compartment of the BRU. The pressure rise in the gas developed by this sealplate impeller is shown by the test data in Figure 7. The lubrication system is connected in series so that pumping action of the compressor-end sealplate is added to the turbine-end pressure rise to move the gas through the system.

A fraction of the mist as shown in Figure 3 is separated to purify some gas for introduction into the powerplant to make up for face-seal gas leakage. The centrifugal field within the shaft separates most of the oil from the gas as shown in Figure 5. At this point in the lubrication system a small amount of the oil mist flows to the separator. The separator centrifuges oil from the oil mist to the outer periphery of the rotating gauze-like metallic mesh where the separated oil flows along the tapered housing to join the oil mist flowing through the bearing balls. The gas leaving the separator passes through an adsorber column where oil retained in the gas is adsorbed and the cleaned gas is returned to the cycle to make up for seal leakage.

Oil is stored in an accumulator which is connected to a rotating pool of oil inside the BRU shaft by a stationary disc scoop, as shown in Figure 5. The stationary disc is totally immersed in the pool of rotating oil. When the pool depth decreases by a loss of oil inventory, pressure head at the disc oil opening decreases. Therefore, oil flows from the pressurized accumulator into the system. If the oil level rises, the pressure rise forces oil back into the accumulator. The result is a rotating pool with an essentially constant inventory. Because the BRU speed will vary about a nominal speed of 36,000 rpm, the oil level in the rotating pool will vary. The amount of oil depth variation is acceptable. Holes which meter oil flow to the bearing inner race are located at the bottom of the rotating oil pools. The scoop or static disc has a tip radius of approximately 0.5 inch and operates with about 0.1 inch submergence of the disc tip in oil. At these values, the pressure in the pool existing at the static disc inlet is about 78 psia. Since this is the desired oil level in the pool, the accumulator pressure also is designed at 78 psia.

When the BRU is not operating, isolation valves close off the accumulator oil line and the clean gas line from the separator to the adsorber column.

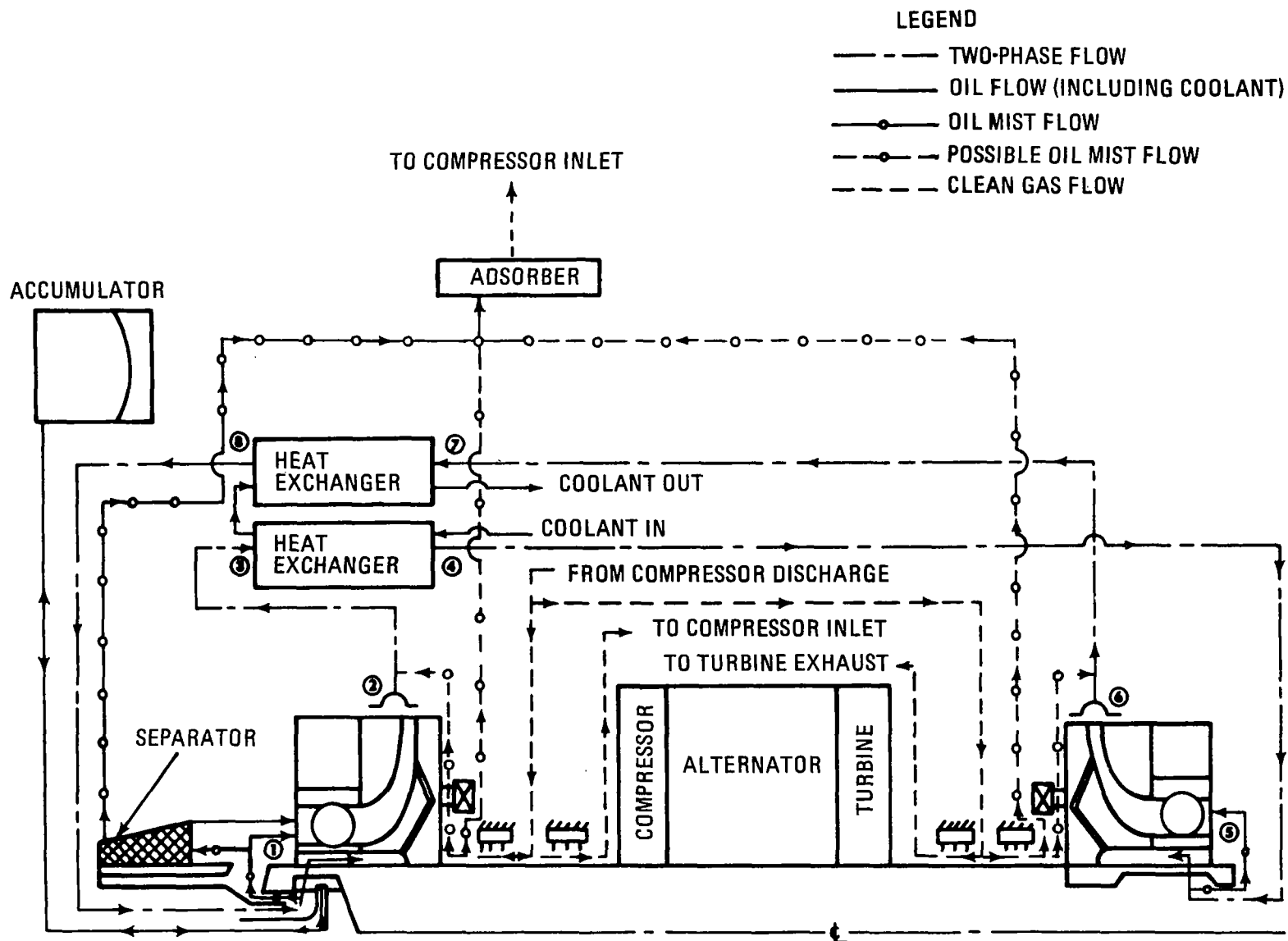


Figure 3 BRU Lubrication System Schematic M-59993

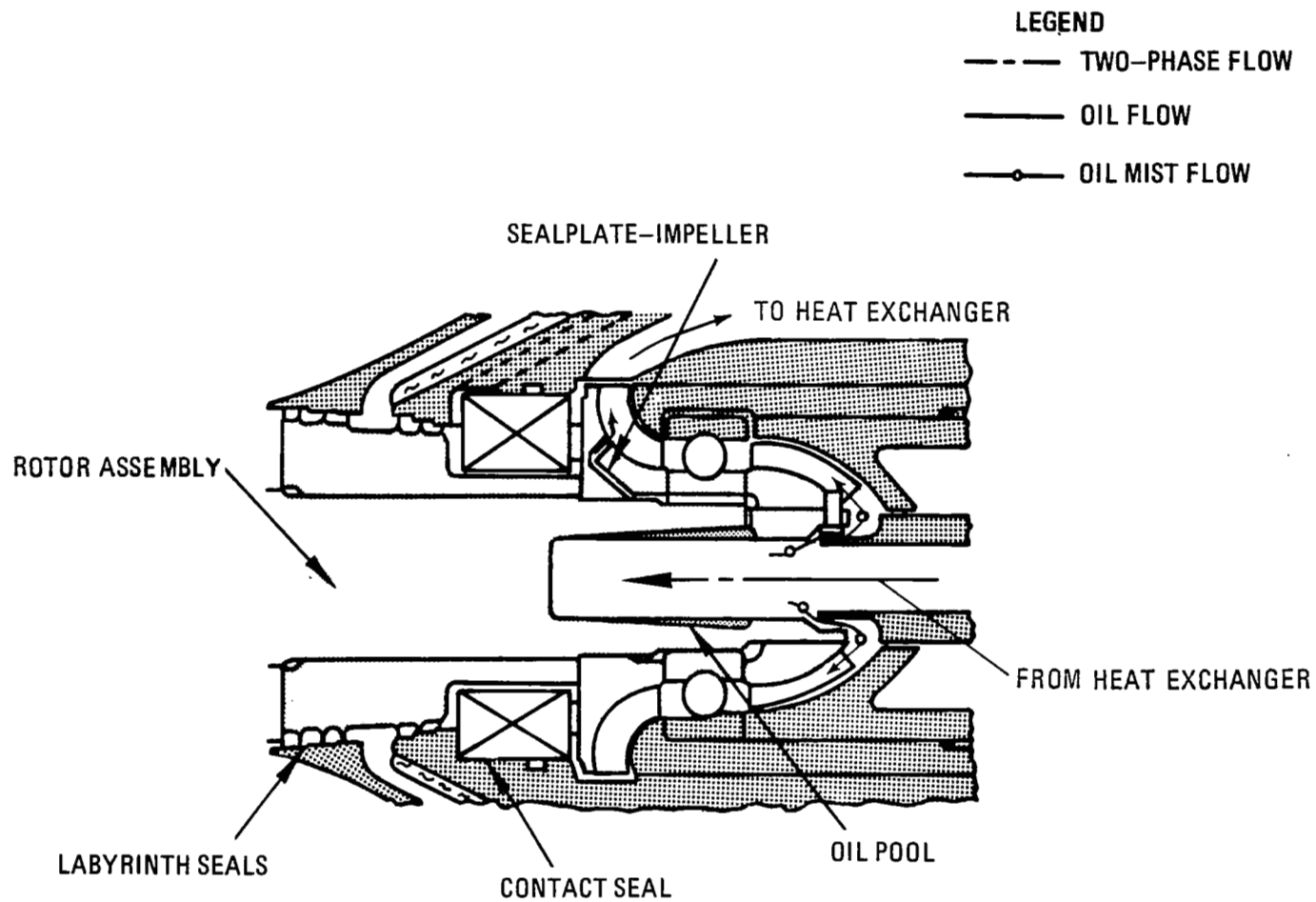


Figure 4 Turbine-End Bearing Compartment M-54840

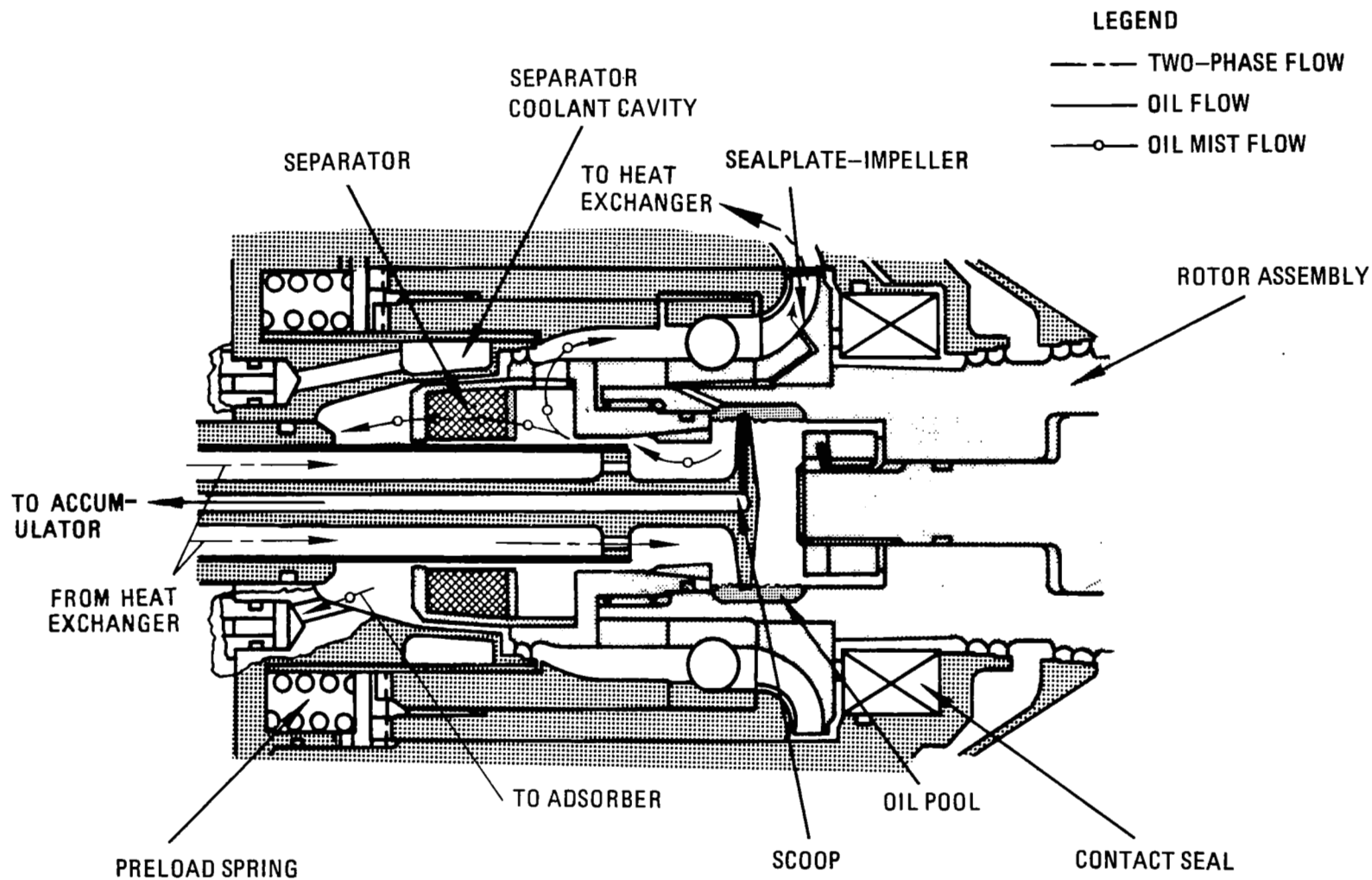


Figure 5 Compressor-End Bearing Compartment M-54841



Figure 6 Scavenge Pump M-43351



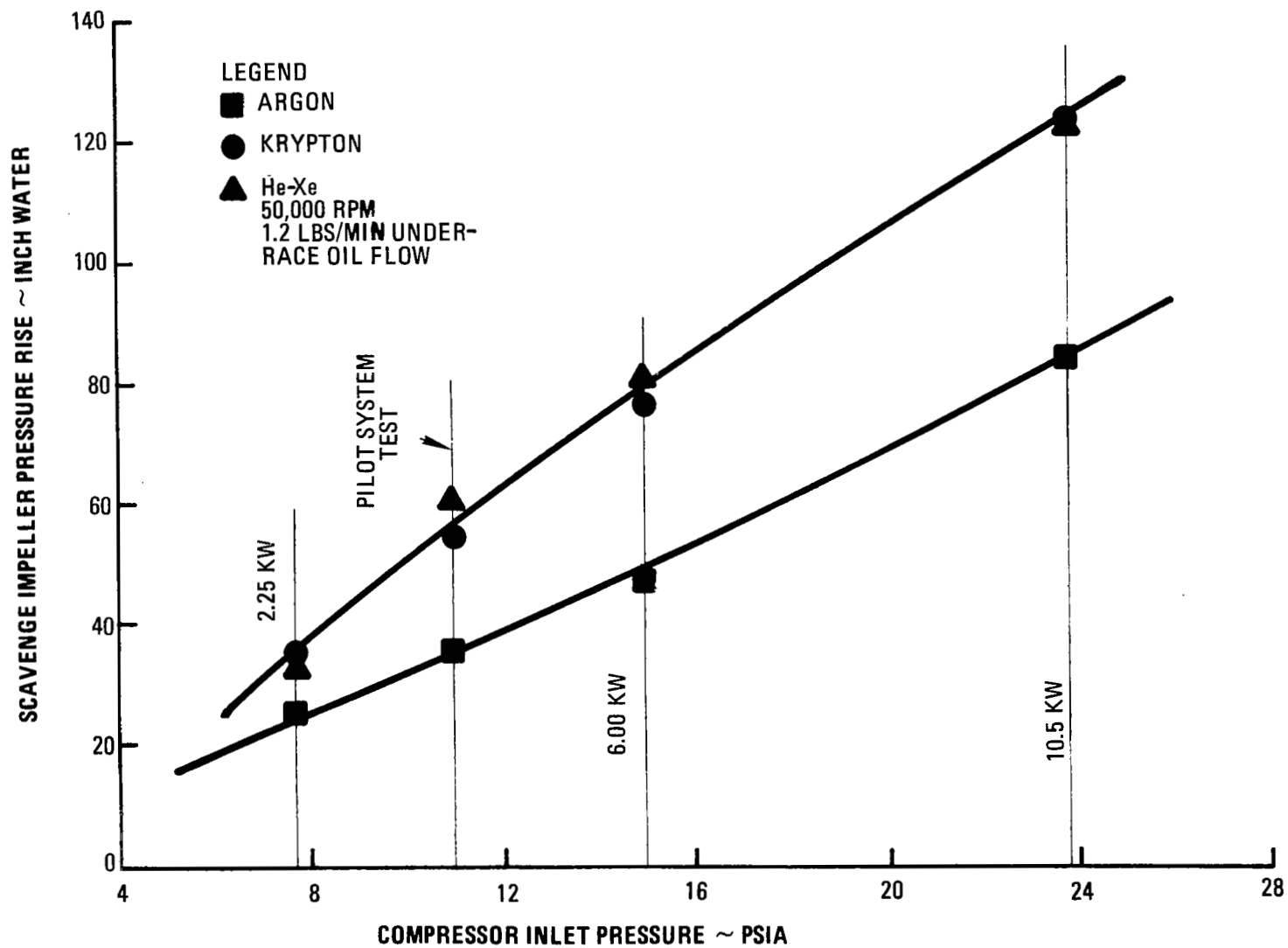


Figure 7 Scavenge Impeller Performance M-49452

Two labyrinth seals are provided on the gas side of the face seals as shown in Figure 3. High-pressure gas is bled from the compressor and fed between these labyrinth seals. Some of this gas leaks back to the main cycle stream and some leaks into the bearing compartment. A small flow of gas is bled from the area just upstream of the face seal to the adsorber. The object of this flow is to carry to the adsorber any oil that weeps past the face seal.

A layout of the BRU indicating external lubrication system ports is shown in Figure 8.

The total power loss predicted for the lubrication system is 1260 watts. A breakdown of these losses is presented in Table 1.

TABLE 1  
Parasitic Power Losses

	Power Loss, watts	
	20 mm Compartment	35 mm Compartment
bearing heat generation	56	185
carbon seal heat generation	274	605
oil pumping power	22	52
gas pumping power	8	18
probe disc drag	-	18
separator drag	-	22
Total loss per compartment	360	900

Total power loss for both bearing compartments = 1260 watts

Predicted flow rates for the lubrication system are indicated in Table 2 for the 6.0 KW design power level and for the two off-design power levels of 2.25 KW and 10.5 KW. Figure 9 is used in conjunction with Table 2 to identify the location of the various points indicated. The gas and oil flow combination of 55 pounds per hour oil flow and 48 pounds per hour gas flow at the design point indicates that the scavenge flow pattern is well within the annular flow region as defined by the prediction system of Ovid Baker and verified in previous testing. The two scavenge pumps in series are adequate to overcome the total line losses resulting from the gas-oil flow combination required to insure annular flow. The previous testing demonstrated that scavenging can be accomplished without annular flow, but all current pressure-loss and heat-transfer correlations assume the existence of annular flow. Therefore, the assumption requiring annular flow results in a conservative design. Figure 10 is a photograph taken during the previous testing program showing both horizontal and vertical two-phase flow.

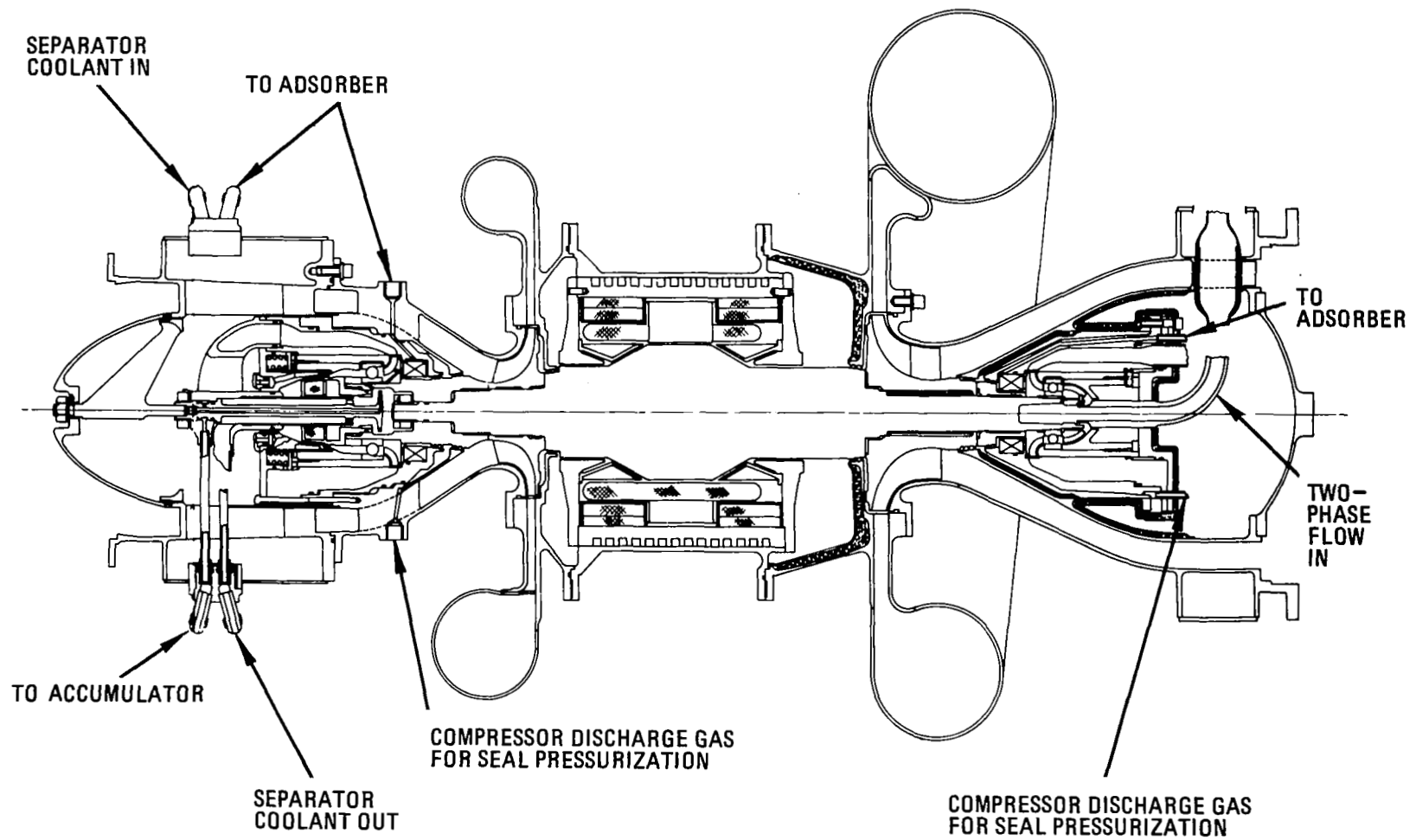


Figure 8 BRU with Rolling-Contact Bearings M-59999

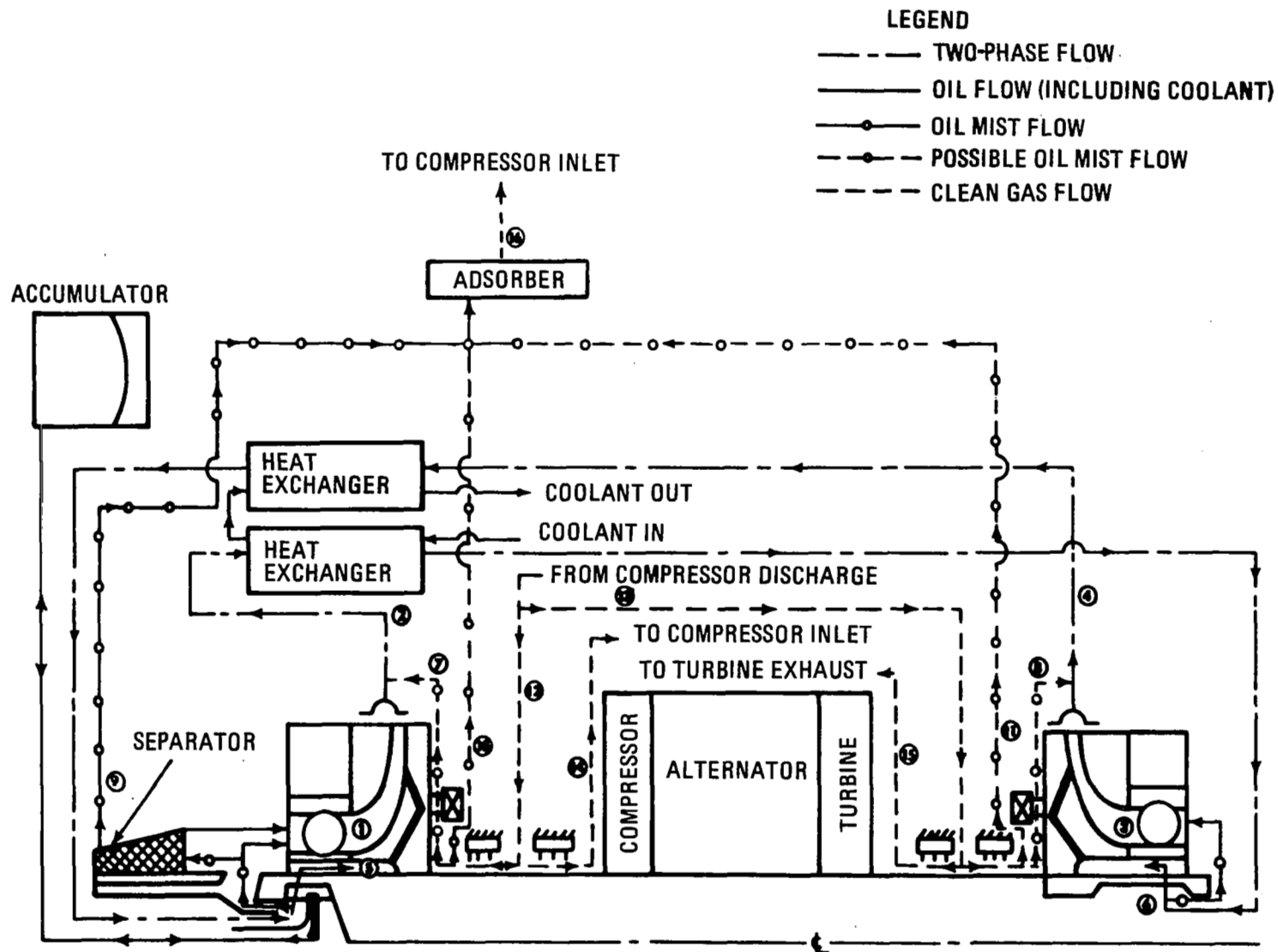
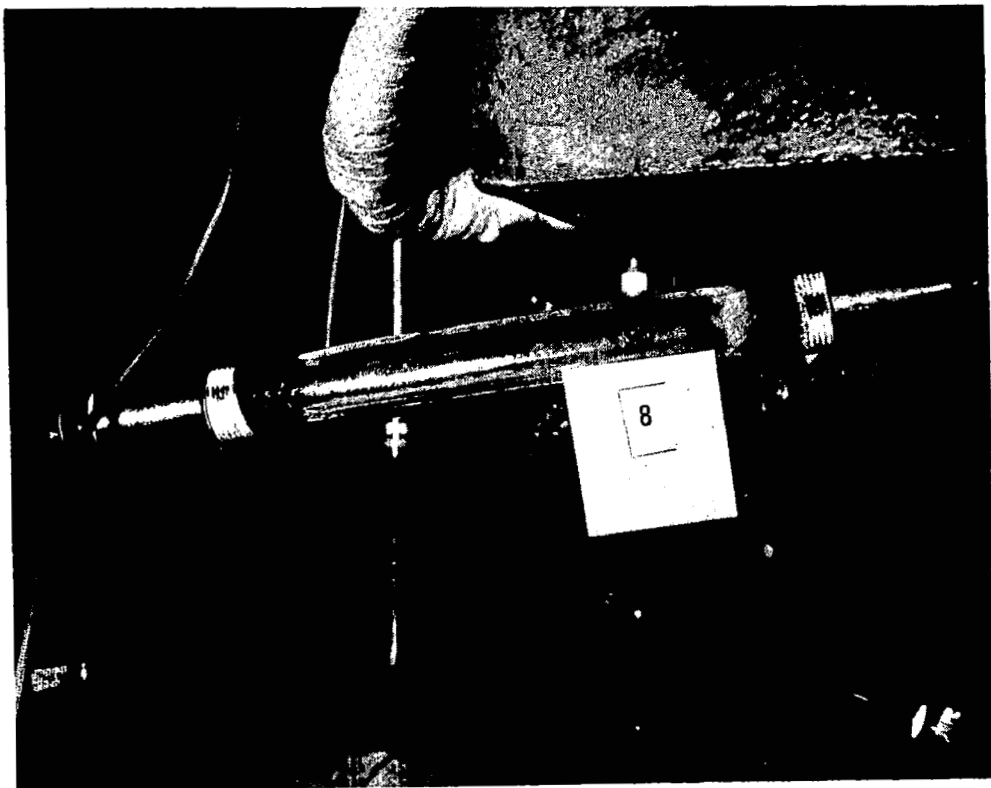


Figure 9 BRU Lubrication System Flow Rates M-61073

## HORIZONTAL 2-PHASE FLOW



## VERTICAL 2-PHASE FLOW



Figure 10 Two-Phase Flow M-44051

TABLE 2

## Lubrication System Flow Rates

Flow Rate Location	Flow Rates, lb/hr		
	Power Level, KW		
	<u>2.25</u>	<u>6.0</u>	<u>10.5</u>
1	20.4/5.50*	48.0/5.50*	98.3/5.50*
2	20.8/55.0	48.9/55.0	99.7/55.0
3	20.8/5.50	48.9/5.50	99.7/5.50
4	21.3/55.0	49.7/55.0	101/55.0
5	0/49.5	0/49.5	0/49.5
6	0/49.5	0/49.5	0/49.5
7	0.45	0.86	1.42
8	0.45	0.86	1.42
9	0.90	1.72	2.82
10	1.37	2.61	4.33
11	1.21	2.31	3.82
12	15.4	29.3	48.5
13	13.8	26.4	43.8
14	13.6	25.8	42.8
15	12.2	23.5	38.5
16	3.48	6.64	11.0

\*Numbers listed as X/Y refer to two-phase regions; X represents gas flow and Y oil flow.

The same lubrication system schematic is repeated in Figure 11, this time keyed to Table 3 which presents lubrication system pressures at the same three power levels. As Table 3 indicates, the pressure rises across the sealplate impellers are 2.25 psi and 0.98 psi for the 35 mm and 20 mm bearing compartments, respectively, at the 6.0 KW design power level. It can also be seen in the table that the pressure drop across the carbon face seal is towards the lubrication system, to prevent leakage of contaminated gas into the powerplant.

TABLE 3

## Lubrication System Pressure Levels

Pressure Location	Pressure Level, psia		
	Power Level, KW		
	<u>2.25</u>	<u>6.0</u>	<u>10.5</u>
1	8.14	14.75	24.26
2	9.41	17.01	27.84

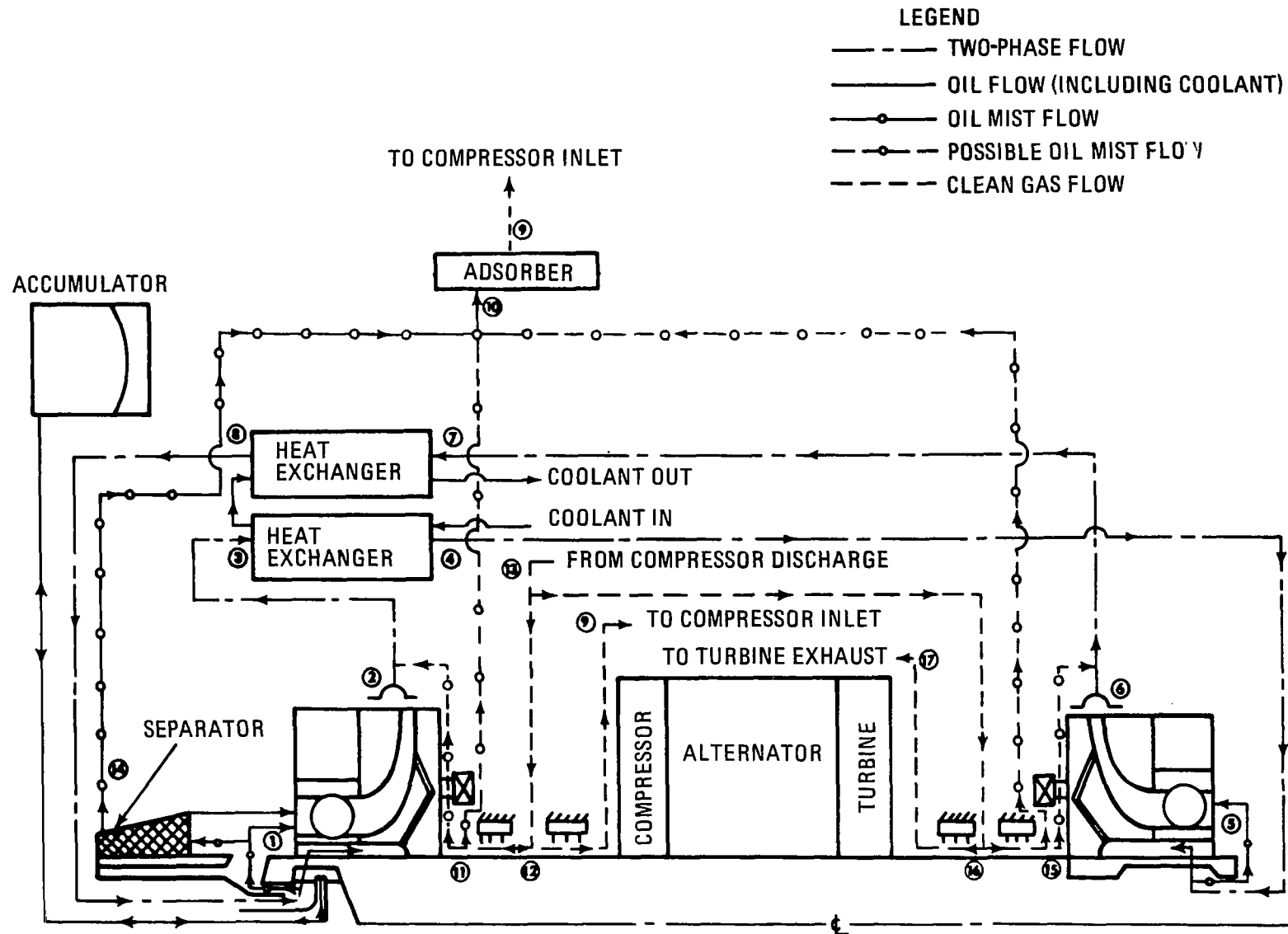


Figure 11 BRU Lubrication System Pressures M-59085

Pressure Location	<u>2.25</u>	<u>6.0</u>	<u>10.5</u>
3	9.30	16.83	27.55
4	8.87	16.11	26.42
5	8.30	15.13	24.90
6	8.88	16.11	26.31
7	8.44	15.21	24.95
8	8.29	14.93	24.50
9	7.60	14.20	23.70
10	8.10	14.70	24.20
11	11.83	22.01	37.75
12	11.97	22.28	38.21
13	14.30	27.00	45.00
14	8.10	14.70	24.20
15	10.53	21.11	33.58
16	10.67	21.37	34.01
17	7.92	14.73	24.67

Note: All external lines are 0.44 inch in inside diameter

A radial clearance of 0.006 inch was used for all labyrinth seals in making the above calculations of flow rate and pressure drop. This results in a total cycle gas bleed flow of about 2 percent for the labyrinth seals shown in Figure 9. Because the rolling-element bearing can support much higher loads for short periods of time than the normal design load, the BRU labyrinth seal clearance can be made initially very small. The BRU then can be operated at design conditions and the labyrinth seals permitted to machine themselves to the required dimensions. After this initial run the BRU would be cleaned and the bearings replaced. This technique would substantially reduce the above-predicted cycle bleed flow.

Buffer-gas oil-vapor transport capability is dependent on the leakage gas flow through the labyrinth seal. Based on the above leakage rates through the labyrinth seals, an estimate of buffer-gas oil-vapor transport capability is presented in Table 4. This value is virtually the same over the range of BRU power levels. The buffer-gas oil-vapor transport capability given in Table 4 should not be construed as the amount of oil that will be transported, but as the maximum amount that can be carried by the buffer gas to the adsorber as a vapor. The gas also can carry an additional quantity of oil by entrainment. The actual amount is dependent upon the carbon face seal oil weepage, which is predicted to be about two orders of magnitude less than the vapor-transport capability of the buffer gas. Seal oil weepage is discussed further in a later section.

TABLE 4

Buffer-Gas Oil-Vapor Transport Capacity-grams/year

compressor-end buffer seal -	
maximum oil-vapor transport	1280
turbine-end buffer seal -	
maximum oil-vapor transport	1260



## 2. Separator

The lubrication system used in this design incorporates an oil-gas separator to clean up the small amount of gas returned to the cycle as make-up for seal leakage. The oil-gas separator indicated in Figure 5 consists of a conical housing assembly attached to the BRU shaft outboard of the compressor-end bearing. This housing contains a woven metallic matrix to improve the effectiveness of the separator. Oil separated in the matrix is pumped along the tapered inside surface of the matrix housing to return to the lubrication system. In addition, the stationary outer housing of the separator is cooled at an average temperature of about 100°F to reduce the gas temperature in the mesh, and to condense oil vapor carried in the gas. The condensed oil droplets formed on the mesh are also centrifuged out of the gas stream. The gas flows to the adsorber. An important feature of the separator is to provide sufficiently low gas velocities to prevent carry-through of the entrained oil or pickup of oil after the oil has been separated. Also, sufficient residence time must be provided to permit cooling of the gas and oil vapor, and subsequent formation of droplets by condensation. High rotative tip speed of the separator is obviously a desirable performance factor.

The separator developed during the previous program was mounted on the outboard end of the 12,000 rpm turboalternator, as shown in Figure 12. This separator was designed to handle all of the gas-oil mixture circulated in the lubrication system. Figure 13 is a photograph of the separator rotating meshes and housing. The separator was tested at speeds up to 14,400 rpm and for a quick transient up to 20,000 rpm. Satisfactory performance of the separator was demonstrated over a range of oil and gas flows shown in Table 5. The 2500-hour endurance test of the separator conducted as part of the pilot-system demonstration indicated that the separator performance remained substantially constant throughout the test at a separation effectiveness ratio of 1,500,000 \*.

TABLE 5

### Separator Performance

mesh density, percent	10
mesh material	woven stainless-steel wire
speed, rpm	12,000
oil in-flow, lb/hr	12-80
argon in-flow, lb/hr	4-12
argon flow to adsorber, lb/hr	1
liquid oil carried by argon to adsorber, gm/yr	110-240
effectiveness	500,000 to 1,500,000

---

\*Separation effectiveness ratio is the ratio of the oil entering the separator to the oil leaving the separator in the cleaned gas

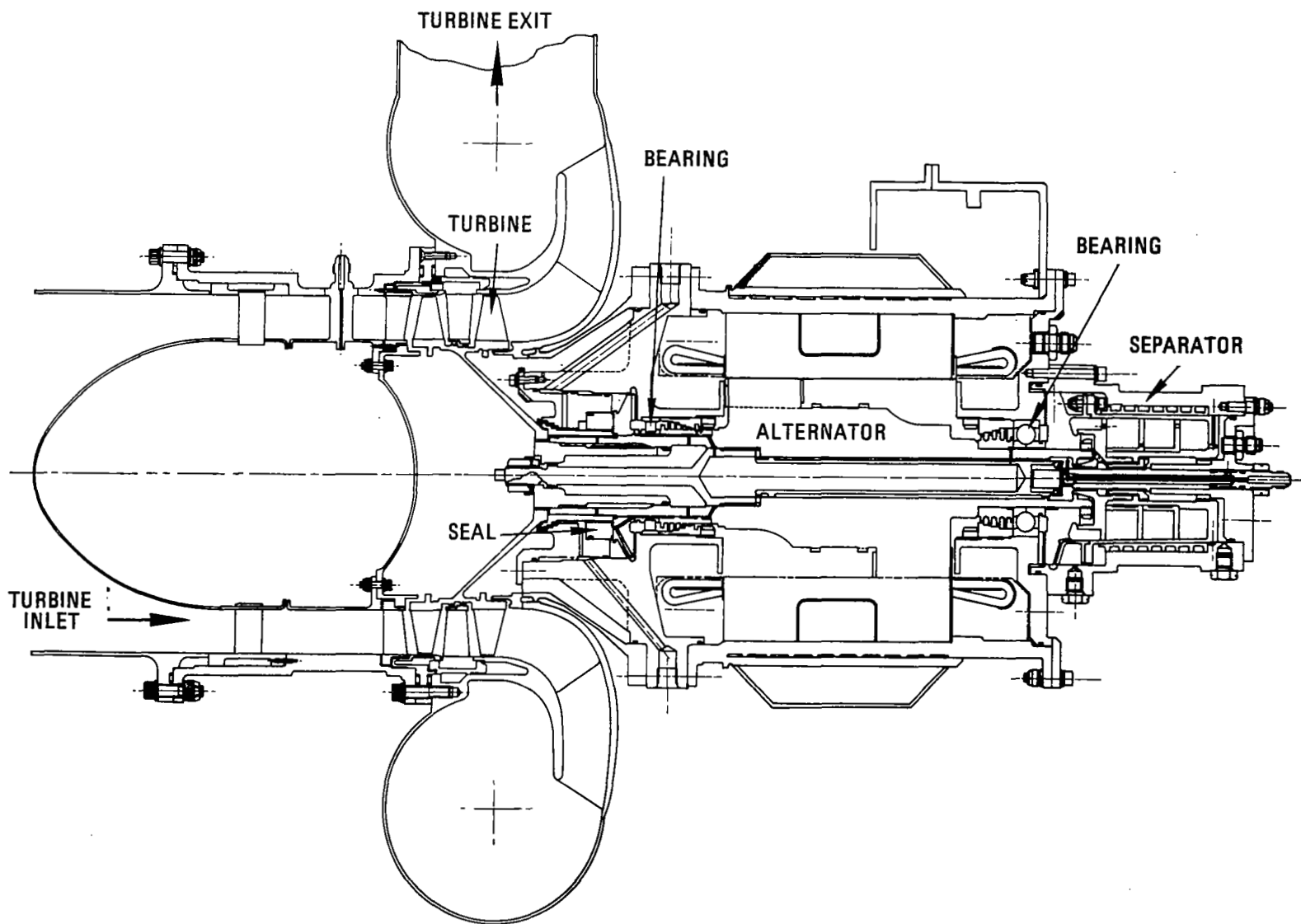


Figure 12 Turboalternator Design M-37972

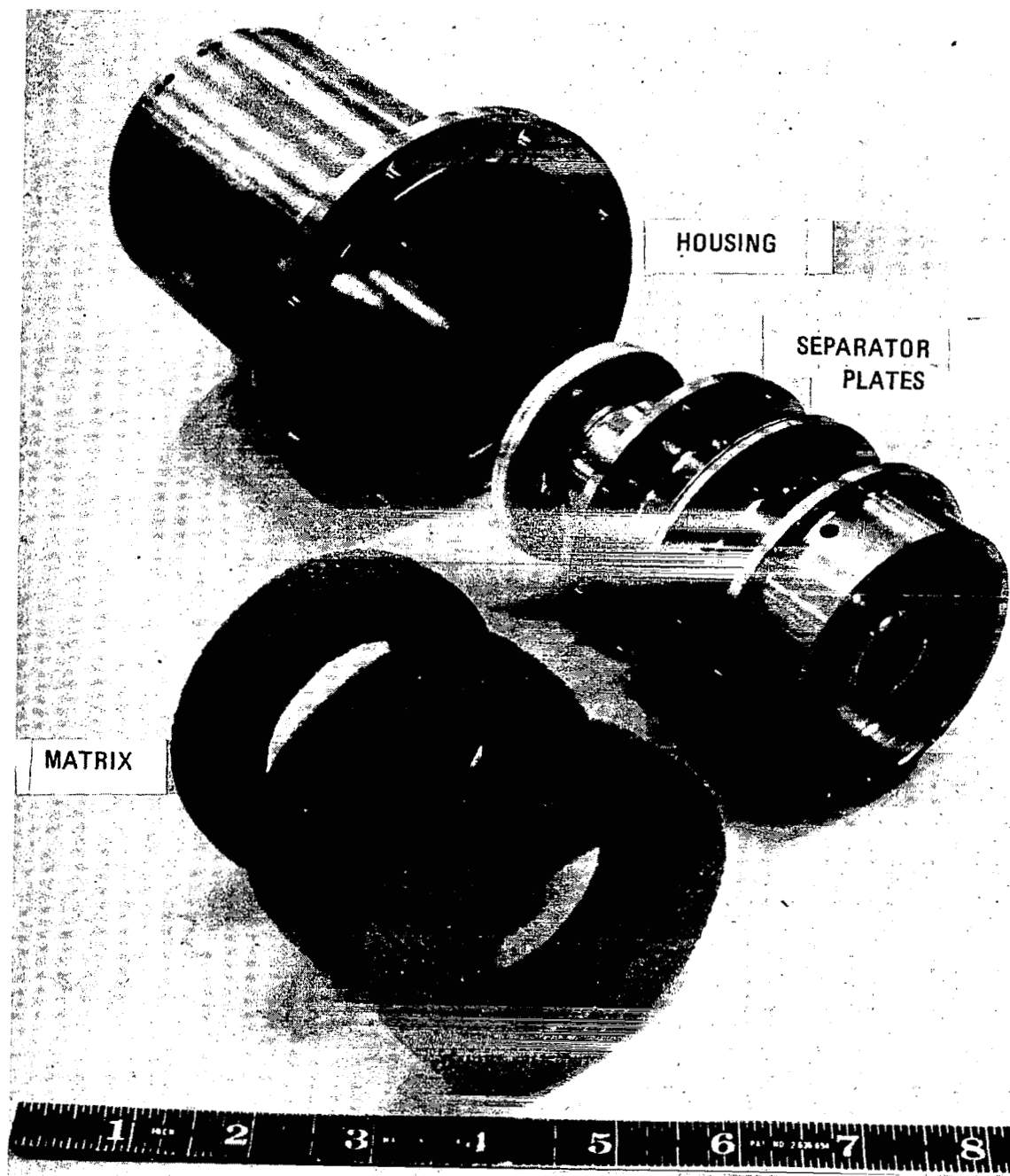


Figure 13 Rotating Parts of Separator M-43350

The separator in the BRU design is considerably smaller than the separator shown in Figure 13. The mesh outside diameter has been reduced from 3 inches to 1½ inches and the overall separator length has been reduced from 2½ inches to ½ inch. Several factors are responsible for this reduction in separator size. The largest single factor is obtained by passing only face-seal gas leakage flow rather than the total lubrication-system gas flow through the separator. The predicted leakage flow is approximately 5 percent of the total flow. Since the measured face seal gas leakage is about three orders of magnitude lower than the predicted leakage, this approach is considered sound. Also two face seals are used in the single-shaft design compared to the three seals used in the two-shaft design. A further factor in the reduction of the required separator flow area is due to the density difference of the argon used previously and the He-Xe mixture used in this study, because of the molecular weight change and the change in compressor inlet pressure from 6.0 psia to 14.2 psia. As a result of these considerations it is possible to reduce the separator cross-sectional area to approximately 1/6 of the area of the previous separator. The BRU separator cross-sectional area is slightly greater than 1/3 that of the previous design, considerably larger than the minimum 1/6 area calculated above. As a result, the gas velocity in the separator mesh is lower in the present design. Also the length of the separator in the BRU provides a gas residence time about 1.4 times greater than the previous design. Rotative tip speed of the BRU separator design is also greater than that of the previous design by about 1.5. These features should improve separator performance in the BRU.

### 3. Heat Exchanger

The preliminary design of a compact tubular counterflow heat exchanger for cooling the lubricant is shown in Figure 14. The oil-gas mixture passes through the heat exchanger as it flows between bearing compartments. The circled numbers on the heat exchanger figure correspond to those on the lubrication system schematic of Figure 3.

### 4. Lubricant Selection

The lubrication system described above is a closed system with sufficient oil inventory to last the projected mission life of over 10,000 hours. The lubricant both cools and lubricates the bearings and seals at both ends of the BRU shaft. In accomplishing this, it is subjected to temperatures from 100°F to 400°F as it flows through the system. In order to conserve the oil and He-Xe inventories and to prevent contamination of the cycle gas, the gas that leaks past the seals into the bearing compartments must be purified and returned to the working cycle. Considering the similarity of these system conditions and requirements to the lubricant test conditions under the previous program, the same oil, PWA 524 remains the preferred lubricant. Property measurements of this oil after 2500 hours of testing under the earlier contract indicated no significant changes. No deleterious effects were apparent

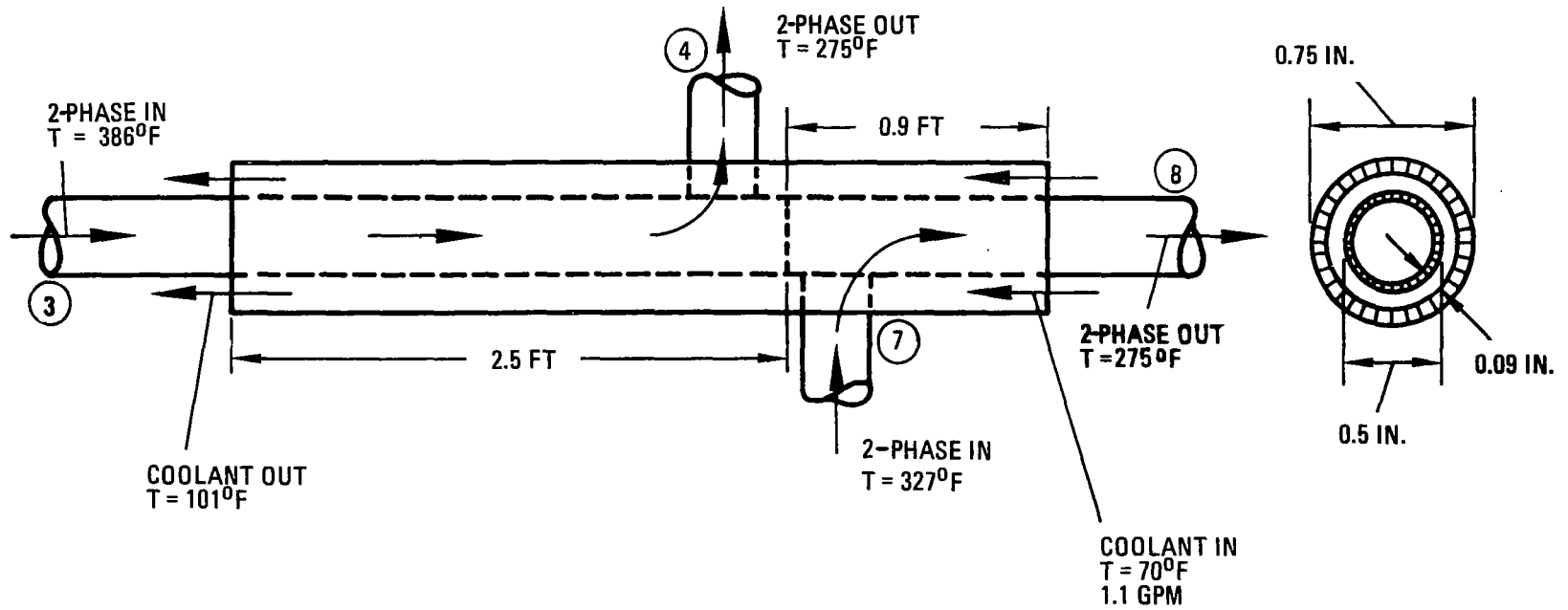


Figure 14 Heat Exchanger Design M-59086

during the two 2500-hour endurance tests and other performance testing. Some deposition of an anti-oxidant additive was evident at certain locations on some components but this additive is not required by the Brayton-cycle application and can be left out of the oil in the future. This oil was selected for the Brayton-cycle turbomachinery for the following reasons:

- 1) High temperature stability,
- 2) Good lubricating qualities,
- 3) Viscosity at temperatures being considered in the bearing compartments compares with that of lighter oils,
- 4) Low vapor pressure at the temperatures being considered for the separator and adsorber, and
- 5) Radiation resistance.

## 5. Adsorber

An adsorber bed is used to further purify the gas being returned to the powerplant main-stream from the separator as make-up for face seal in-leakage. The adsorber also purifies the buffer gas returning to the powerplant. Possible oil decomposition products in the returning gas are also removed in the adsorber. The adsorber designed for this application utilizes the design technology developed under the previous program.

The operating principle of the adsorber is to condense the oil vapor and other condensibles present in the gas and then to subsequently adsorb the oil and possible oil decomposition products. Glass wool and polyurethane have been found in the previous test program to be excellent for oil removal. The removal of oil decomposition products is accomplished with molecular-sieve materials in the form of pellets.

Four adsorbers of different configurations and materials were designed and tested at representative conditions for periods ranging between 1000 and 2500 hours. These designs are shown in Figure 15. The tested performance of these four adsorber designs is summarized in Table 6. Based on the test results of these configurations, the adsorber shown in Figure 16 was designed for the BRU system. The geometry and operating characteristics of this design are listed in Table 7. Molecular-sieve requirements must be determined from power-plant system tests to establish oil decomposition rate. Significant oil decomposition at the temperatures anticipated is not expected.

TABLE 6  
Adsorber Performance Comparison  
(Gas Flow - One Pound Per Hour)

	<u>Pilot System</u>	<u>Mixed Spiral</u>	<u>Glass Spiral</u>	<u>Glass Cylinder</u>
test hours	2500	1000	1500	1000
oil extracted from adsorber assembly, gms ①	59.7	52.9	337.3	24.6

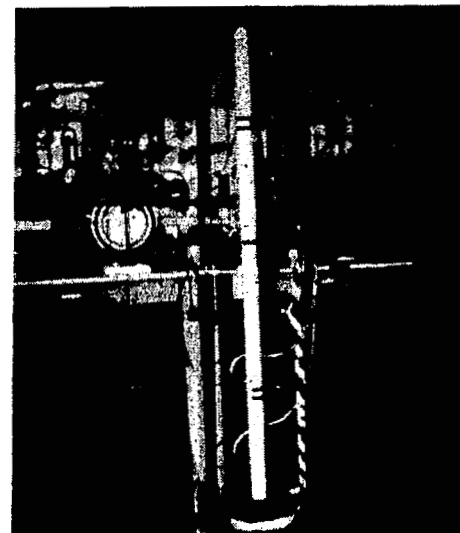
PILOT SYSTEM



MIXED SPIRAL



GLASS CYLINDER



GLASS SPIRAL



Figure 15 Tested Adsorber Configurations M-59929

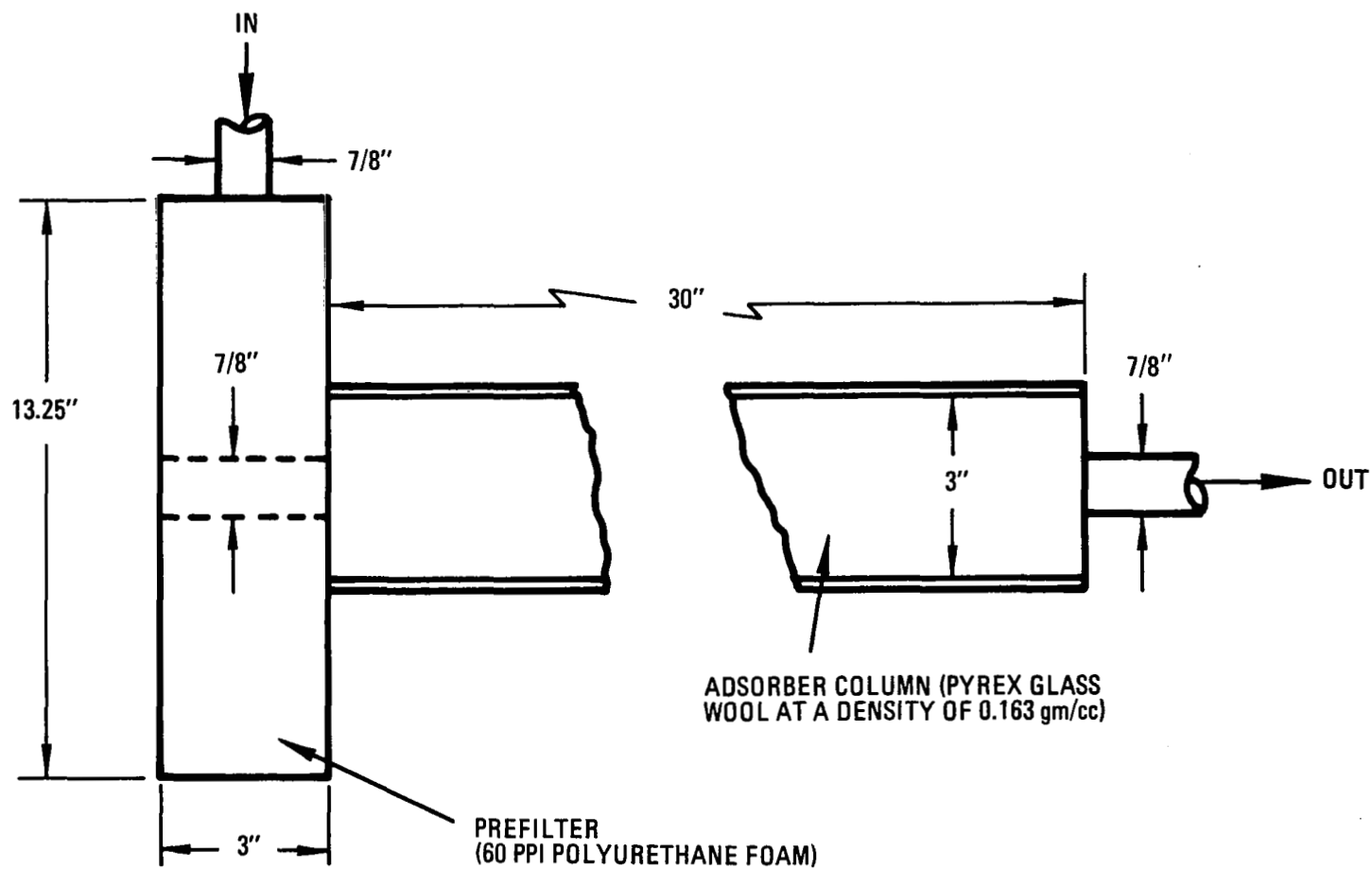


Figure 16 Adsorber Configuration M-61027



	<u>Pilot System</u>	<u>Mixed Spiral</u>	<u>Glass Spiral</u>	<u>Glass Cylinder</u>
oil extracted from monitor columns, gms <span style="float: right;">②</span>	0.1317	0.4249	0.3498	0.0029
efficiency $\frac{①}{① + ②}, \%$	99.780	99.204	99.896	99.988
effectiveness ratio $\frac{① + ②}{②}$	455	126	966	8486
oil collected in adsorber, gms/hr	0.02389	0.05297	0.2249	0.02461
oil leaving adsorber, gms/yr	0.526	4.249	2.33	0.029
<u>monitor column oil</u> cold trap oil	-	-	147/4	29/90

TABLE 7

#### Adsorber Design

adsorber column - pyrex glass wool at density of 0.163 gm/cc  
 prefilter - 60 ppi polyurethane foam  
 adsorption efficiency - 99.780%  
 inlet temperature - 100°F  
 inlet pressure - 14.70 psia  
 flow rates in,  
   gas - 6.64 lb/hr  
   oil - 22.5 gram in 10,000 hours  
 flow rates out,  
   gas - 6.64 lb/hr  
   oil - 0.05 gram in 10,000 hours  
 pressure drop - 0.5 psi

#### C. Bearing Design

The bearings in the BRU were designed to provide a rotor support system capable of supporting the axial and radial loads and of achieving a B<sub>1</sub> failure rate (1.0 percent or lower) for at least 10,000 hours with minimum power consumption. Two ball bearings were incorporated to support the rotor, thrust-loaded against each other by springs to preclude skidding which could occur in a lightly-loaded high-speed application such as this.

The selection of an outboard bearing configuration with a 35 mm bore bearing at the compressor end and a 20 mm bore bearing at the turbine end, as shown in Figure 2, was the result of the study of a number of alternate BRU configurations which are described in the

Appendix of this report. At the BRU design speed of 36,000 rpm, the bearing DN (the linear speed of a bearing is usually defined as the product of the bore diameter, D, in millimeters and the shaft rotational speed, N, in rpm) is  $1.26 \times 10^6$  mm-rpm for the 35 mm bearing and  $0.72 \times 10^6$  mm-rpm for the 20 mm bearing.

The selection of bearing size and geometry depends on three major factors, fatigue life, friction losses, and skidding tendencies. In designing for long fatigue life, large bearings are normally selected. Fatigue life is usually improved with tight race-curvatures, and, in the case of pure thrust loading, high design contact angle. Unfortunately the skidding tendencies are increased by these factors as well. Also, large sizes, large contact angles and tight curvatures result in high levels of heat generation. Thus, the bearing design is a compromise between long fatigue life on the one hand and low skidding characteristics and frictional power loss on the other.

Studies were conducted using digital computer techniques to evaluate the tradeoffs between bearing life, skidding margin and geometry. Power consumption, lubrication, installation, fabrication, and metallurgical factors were also considered. The life of bearings of various design was examined at the design speed of the BRU (36,000 rpm) with a combined radial and thrust load.

As a result of the alternate BRU study, the minimum bearing bore of 35 mm was determined where oil inventory controls (separator and static disc) are incorporated. Bearing diameters below 35 mm do not permit sufficiently large flow passages through the separator. The use of a single separator rather than two separators permits the use of a 20 mm size bearing in the turbine-end compartment with accompanying reduction in parasitic power. A minimum bearing bore of 20 mm was determined for the turbine-end compartment because cross-sectional area available in the BRU shaft under the bearing for oil-gas flow passages becomes marginal below this diameter. Power losses due to bearing heat generation at 36,000 rpm are 56 watts for the 20 mm bearing and 185 watts for the 35 mm bearing.

Bearing performance tests conducted under the previous program on a 20 mm bearing such as shown in Figure 17, indicated satisfactory power consumption and temperatures for a wide range of oil and gas flow rates. This data is shown in Figure 18. The relatively small change in temperature for the orders of magnitude changes in oil flow through the bearing balls shows that the bearing has tolerance to wide changes in lubricant flow. Figure 19 indicates no skidding, as predicted up to 60,000 rpm. A bearing was endurance tested at 50,000 rpm for 2500 hours at representative conditions, and no measurable wear or distress was discernible during inspection. Several start-stop cycles were also imposed on the bearing during the endurance test and performance remained unchanged throughout the test.

Figure 20 shows the direction of the preload, radial and aerodynamic thrust loads. As shown in the figure, the system is preloaded by means of springs on the outer race of the 35 mm bore bearing. With the aerodynamic thrust load in the direction shown, the load on the 20 mm bore bearing is decreased and the load on the 35 mm bore bearing will remain constant unless the thrust load exceeds the preload. In order to keep the bearings from skidding during anticipated operating conditions, a preload of 100 lbs was selected.

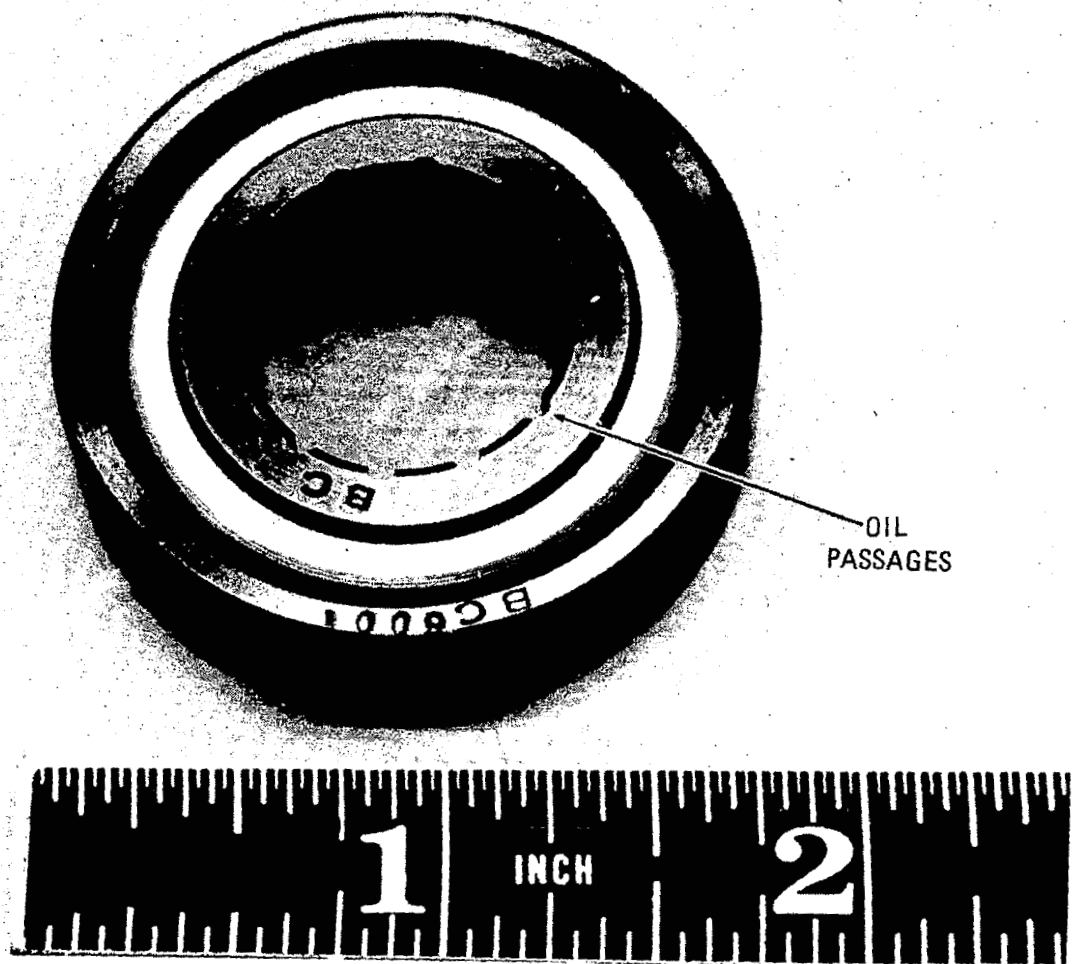


Figure 17 20 mm Angular-Contact Ball Bearing M-49740

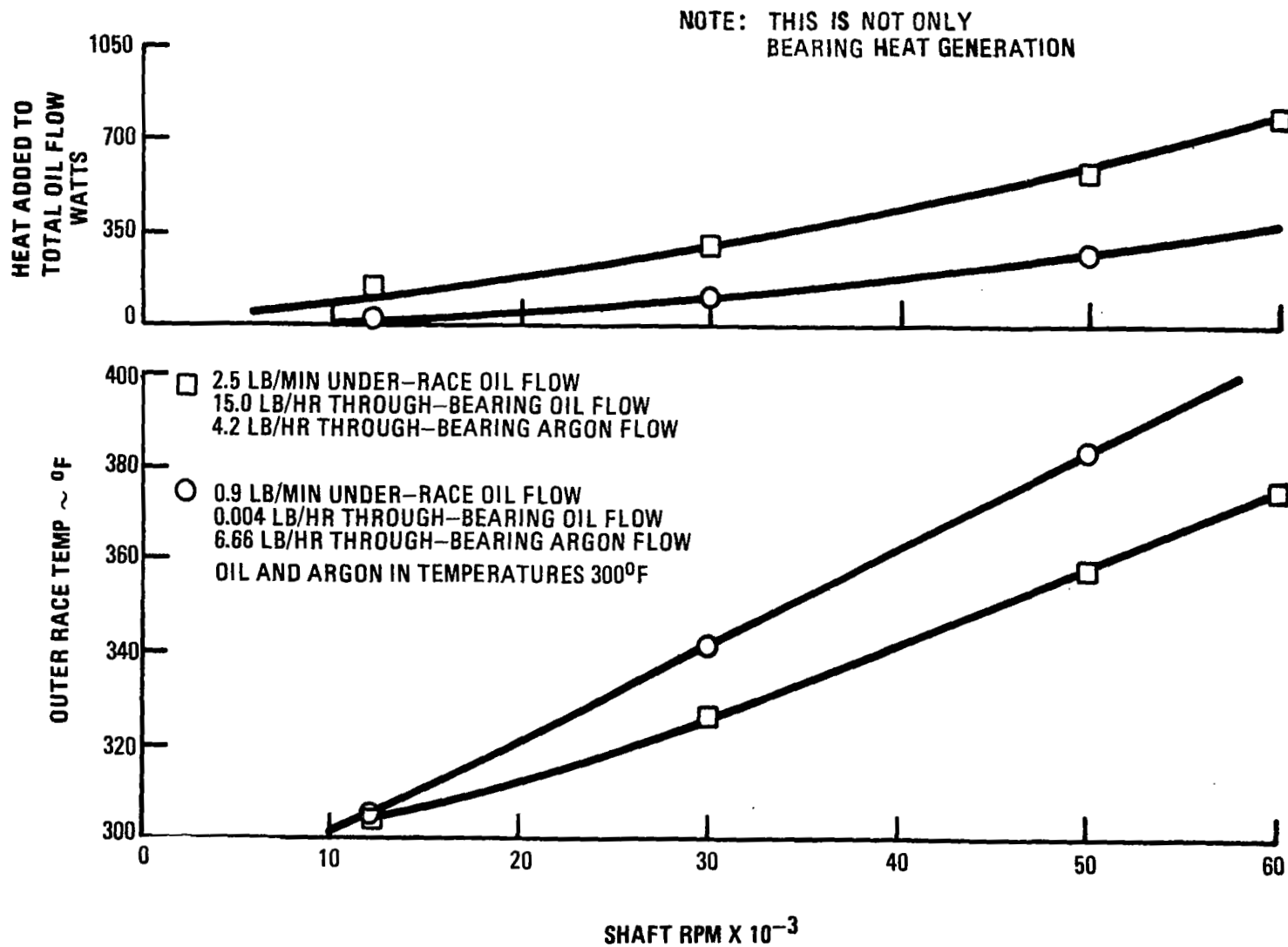


Figure 18 Bearing Performance M-43322

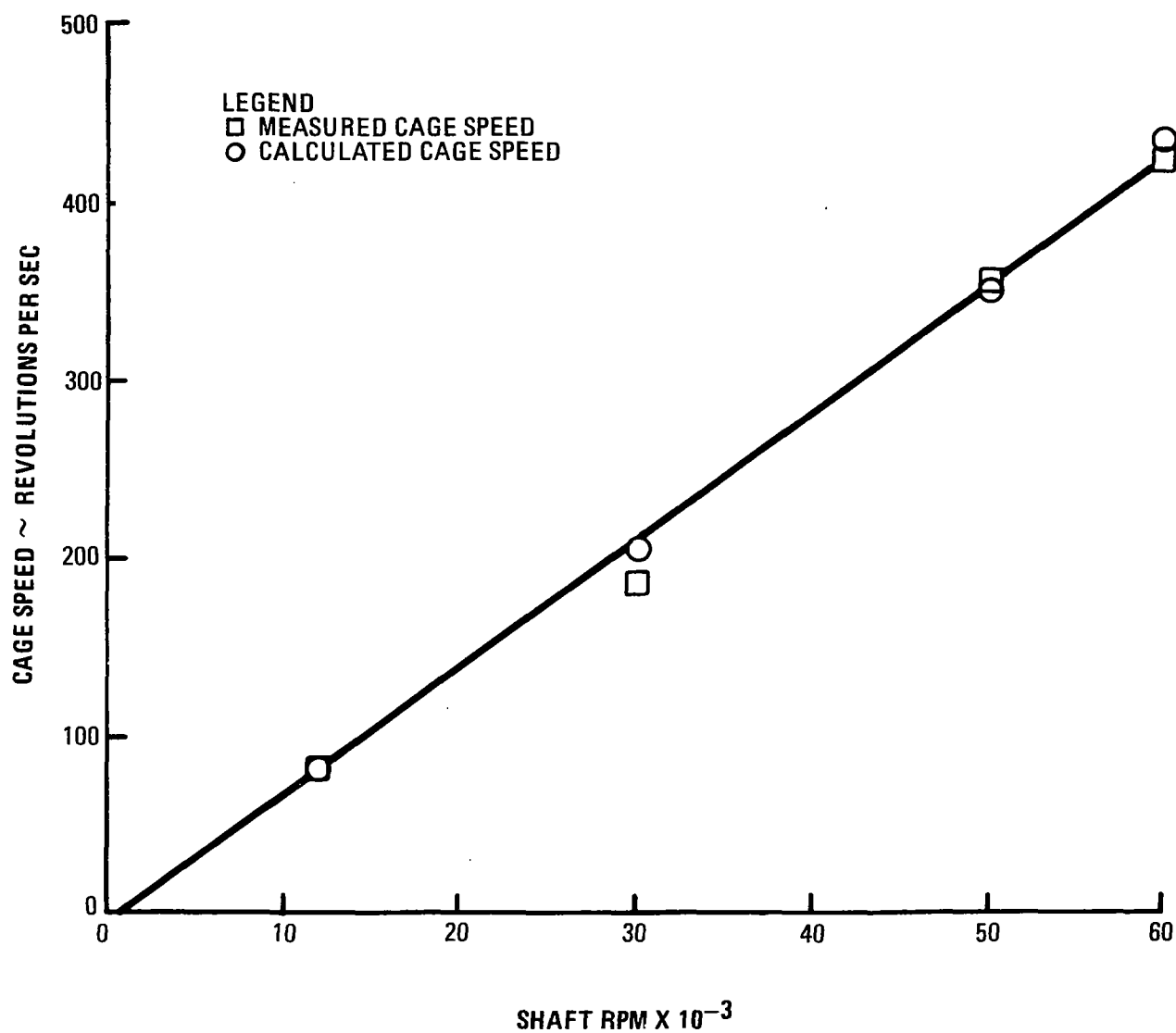


Figure 19 Bearing Cage Speeds M-49739

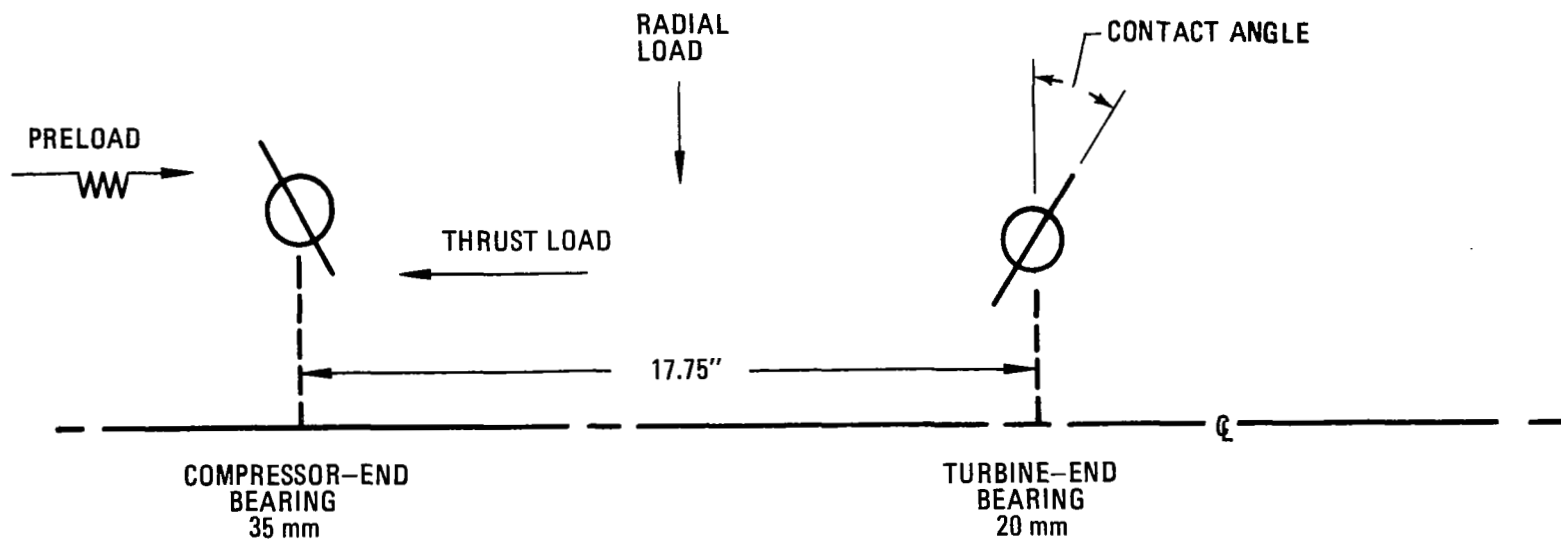


Figure 20 Bearing Load Diagram M-61032

The bearing study was performed at the design conditions of 36,000 rpm with a 22-pound radial load and a thrust load of 18 pounds towards the compressor end. Bearing  $B_1$  lives (99 percent survival) are presented in Table 8 for three power levels. The estimated life of the 20 mm bearing changes at each power level because only this bearing is affected by the change in aerodynamic thrust associated with each power level.

**TABLE 8**  
**Bearing  $B_1$  Lifetime**

<u>Power Level, KW</u>	<u><math>B_1</math> Lifetime, hours</u>	
	<u>35 mm Bearing</u>	<u>20 mm Bearing</u>
2.25	13,400	19,400
6.0	13,400	25,700
10.5	13,400	40,100

Figure 21 presents the variation of bearing life with radial load. As the figure shows, both the 35 mm and 20 mm bearings could withstand a large radial load (or radial unbalance) of 85 pounds and still maintain  $B_1$  lifetimes of 10,000 hours.

These bearings are also designed to operate for extended periods of time during development testing. As Figure 21 indicates, operation in a horizontal position will cause no difficulty, since the bearings can tolerate substantial radial loads at  $B_1$  lifetimes in excess of 10,000 hours. With the shaft operating in a vertical position with the 35 mm bearing on top,  $B_1$  lifetimes of 13,400 are estimated for both the 35 mm and 20 mm bore bearings. With the 20 mm bearing on top,  $B_1$  life for the 35 mm bearing remains at 13,400 hours and the 20 mm bearing  $B_1$  life increases to 60,800 hours.

Bearing race temperatures were determined at the 6.0 KW design condition with the following results:

	<u>35 mm Bearing</u>	<u>20 mm Bearing</u>
outer race temperature, °F	361	301
inner race temperature, °F	340	295
$\Delta T$ oil, °F	23.6	7.2

As these values indicate, the race temperatures are well within the 400°F maximum and 40°F  $\Delta T$  maximum specified. No significant change in these temperatures is anticipated for the other power levels.

To illustrate the effect of survival probability criterion on bearing lifetime,  $B_{10}$  lifetimes were calculated. At the 6.0 KW design power level the  $B_{10}$  (90 percent survival) life of the 35 mm bore bearing is 58,400 hours and for the 20 mm bore bearing  $B_{10}$  life is 112,000 hours.

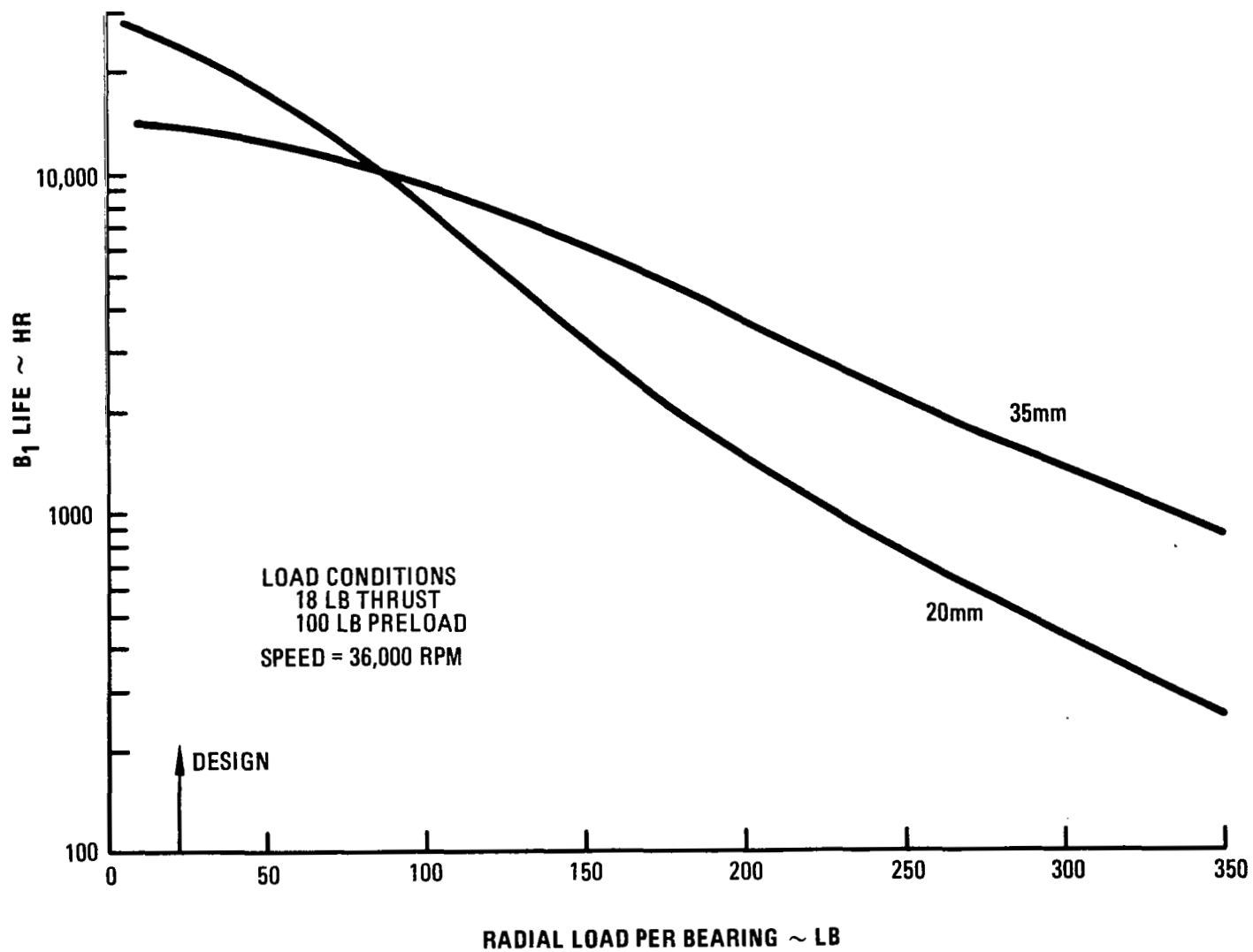


Figure 21 BRU Bearing Life M-61030



The materials of construction of the selected bearings are the same as those used in the previous program. In that program, as in the present one, the bearing design objective was to provide maximum fatigue life consistent with low power consumption and the absence of skidding. Traditionally SAE 52100 steel has been the standard bearing material. Developments such as vacuum melting of SAE 52100 have considerably improved bearing fatigue life. Current aircraft turbine engines require better properties than SAE 52100 offers, and considerable experience has been accumulated with better bearing materials.

Consumable-electrode vacuum-melted M-50 tool steel has demonstrated superior fatigue life and is currently being specified for many of these high performance applications. Because of this favorable experience M-50 tool steel was specified for the BRU bearings.

The bearing life estimates included modifications to the usual AFBMA calculations based on experience in high-speed applications. These modifications accounted for the detrimental effect of centrifugal force on the balls, and the advantageous effects of increased resistance to fatigue and narrower distribution of failure lives, which is characteristic of the vacuum-melted M-50 steel bearings.

Experience has shown that for high-speed long-life applications such as the Brayton cycle, the ball retainer designs must be of one-piece fully-machined construction to achieve high strength and fine balance. An inner-race riding retainer was selected because of the extensive experience with this configuration, the better bearing tolerance for short interruptions of oil flow, and the ability of the inner-race oil cooling to remove the heat generated in the retainer-race bearing area. Since a one-piece retainer was selected, the only bearing configurations that could be used were the counterbore type or the split inner-ring type. The risk in the split inner-ring configuration is that the ball-race contact ellipse may extend to the chamfer at the split on the inner race. If this were to occur, the stresses in the contact zone would be significantly increased and the bearing life would be reduced accordingly. While the calculations indicate that the ball would not ride on the chamfer at the split, some transient radial load might produce such a condition. Therefore, the counterbore configuration employing a solid inner ring was selected.

In summary, the bearings selected for the BRU are a 35 mm bore at the compressor end and a 20 mm bore at the turbine end. Both are extra-light series ball bearings constructed of M-50 steel with one-piece cages. The design requirements of the selected bearings appear in Tables 9 and 10.

**TABLE 9**  
**Requirements for Compressor-End Bearing**

bearing type	angular-contact ball bearing with counterbore outer race
operating conditions	axial load = 100 pounds rotating unbalance load = 22 pounds at 36,000 rpm
oiling system	mist lubrication axial cooling slots on bore of inner ring
heat generation	185 watts
bearing size	35 mm bore diameter 62 mm outer diameter 14 mm wide
internal geometry	15 balls of 11/32 inch diameter 1.905 inch pitch diameter 18-degree nominal mounted contact angle at operating fits and clearances

**TABLE 10**  
**Requirements for Turbine-End Bearing**

bearing type	angular-contact ball bearing with counterbore outer race
operating conditions	axial load = 82 pounds rotating unbalance radial load = 22 pounds at 36,000 rpm
oiling system	mist lubrication axial cooling slots on bore of inner ring
heat generation	56 watts
bearing size	20 mm bore diameter 45 mm outer diameter 12 mm wide
internal geometry	10 balls of 5/16 inch diameter 1.275 inch pitch diameter 18-degree nominal mounted contact angle at operating fits and clearances

#### D. Seal Design

The basic sealing concept for both bearing compartments consists of two labyrinth seal assemblies adjacent to a face seal. High-pressure He-Xe gas fed between the labyrinth seals provides a pressure differential across the face seal and a purge for oil that might weep past the seal.

This pressure differential aids in containing the oil within the lubrication system. This feature also provides a buffer zone between the cycle gas and the bearing and seal cavities, to reduce cycle gas contamination. A system was provided to recover, clean up and reuse the bleed gas, as well as the gas which leaked past the seals.

The primary consideration in designing face seals for this application was to minimize oil leakage, gas leakage and power consumption, consistent with Brayton-cycle power system durability and reliability for long-term operation. A further requirement of the seal design was to restrict oil leakage from the bearing compartment at shutdown. The seal used provides a positive contact seal at shutdown, effectively sealing the lubricating system from the cycle working fluid for startup and inactive periods.

The seal design geometry and materials of construction are the same as those successfully utilized in the previous program. These seals are of the dry-face rubbing-contact type similar to that shown in Figure 22. Predicted gas leakage is about 0.9 pound per hour for each seal. This value is about three orders of magnitude higher than expected in the BRU, based on gas leakage measurement made in the previous program. Estimated heat generation rates for this design are 605 watts and 274 watts for the 35 mm and 20 mm bearing compartments, respectively.

Seal diameter was made as small as possible to achieve the lowest power consumption and leakage with greatest durability. The design of the carbon face seal at the 20 mm turbine-end bearing is essentially the same as that designed and tested under the previous program and shown in Figure 22. The design of the 35 mm compressor-end seal is substantially the same as that of the smaller seal, with a difference only in the diameter of the seal itself. Two seals of this type were endurance tested in the previous program for 2,500 hours at 50,000 rpm and at representative conditions. During the testing both seals experienced several start-stop cycles. As shown in Figure 23, gas leakage measurements indicate an average rate of less than 0.0002 pound of gas (argon) per hour. The short-duration spikes of higher gas leakage are probably due to a piece of debris temporarily separating the seal rubbing surfaces. Figure 24 presents seal power consumption as a function of speed. A helium leak check of the bellows and the post-test inspections of both seals indicated bellows integrity. Oil weepage accumulated past the face of the seal was about 2.7 grams after 2,500 hours.

The selection of design parameters for a rubbing-contact face seal begins with the choice of seal diameter and interface contact load and pressure. At the 35 mm bearing end, a mean face seal diameter of 2.0 inches was chosen resulting in a mean rubbing velocity of 322 ft/sec. Similarly, a mean rubbing velocity of 236 ft/sec results from a selected mean face seal diameter of 1.5 inches at the 20 mm bearing end of the BRU. To provide the most positive protection against oil leakage across the contact face, the choice was made to have the oil at the outer edge of the rotating interface so that any leakage had to oppose the centrifugal force of the rotating members.

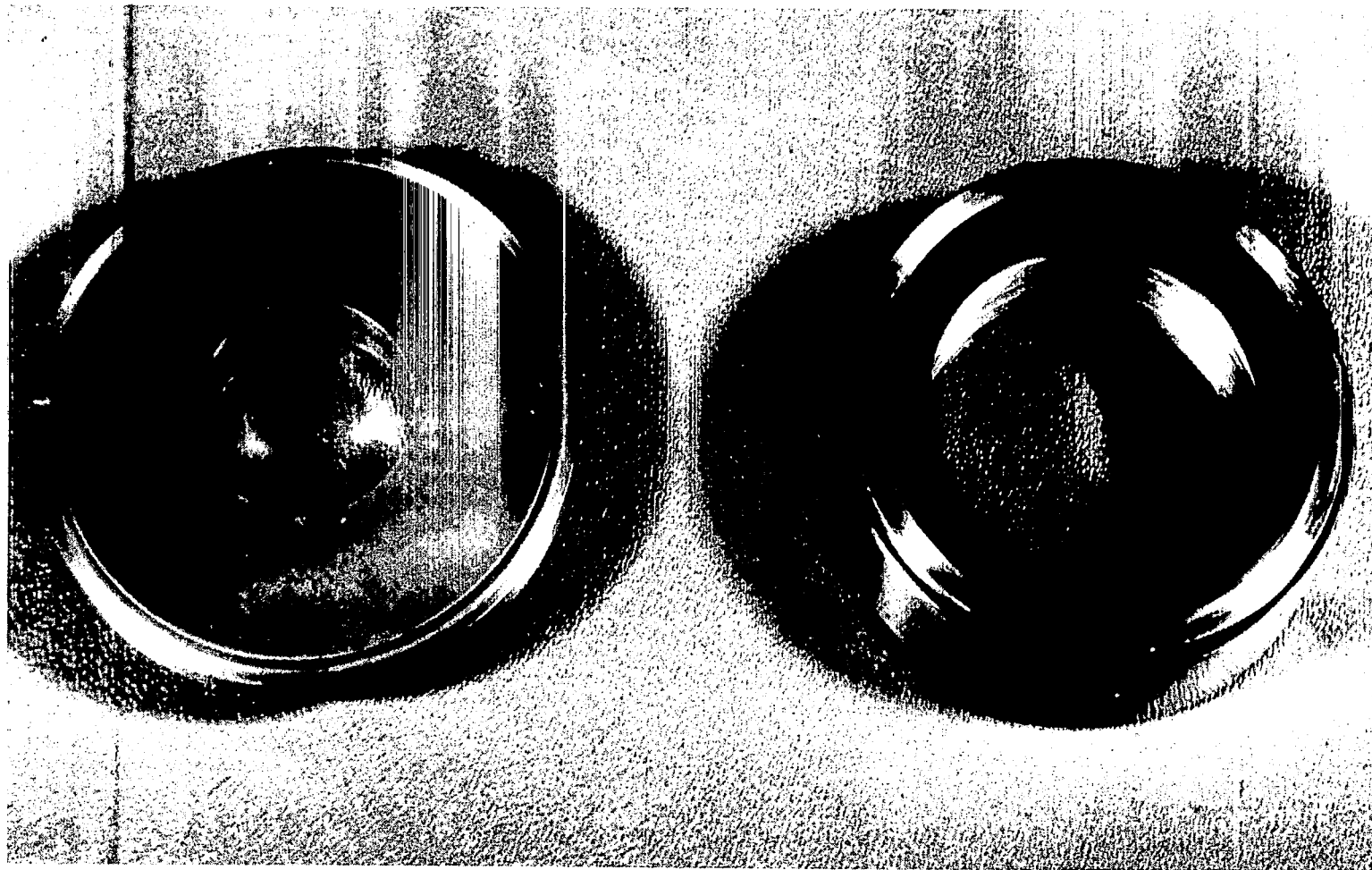


Figure 22 Dry-Face Seal and Sealplate M-44047

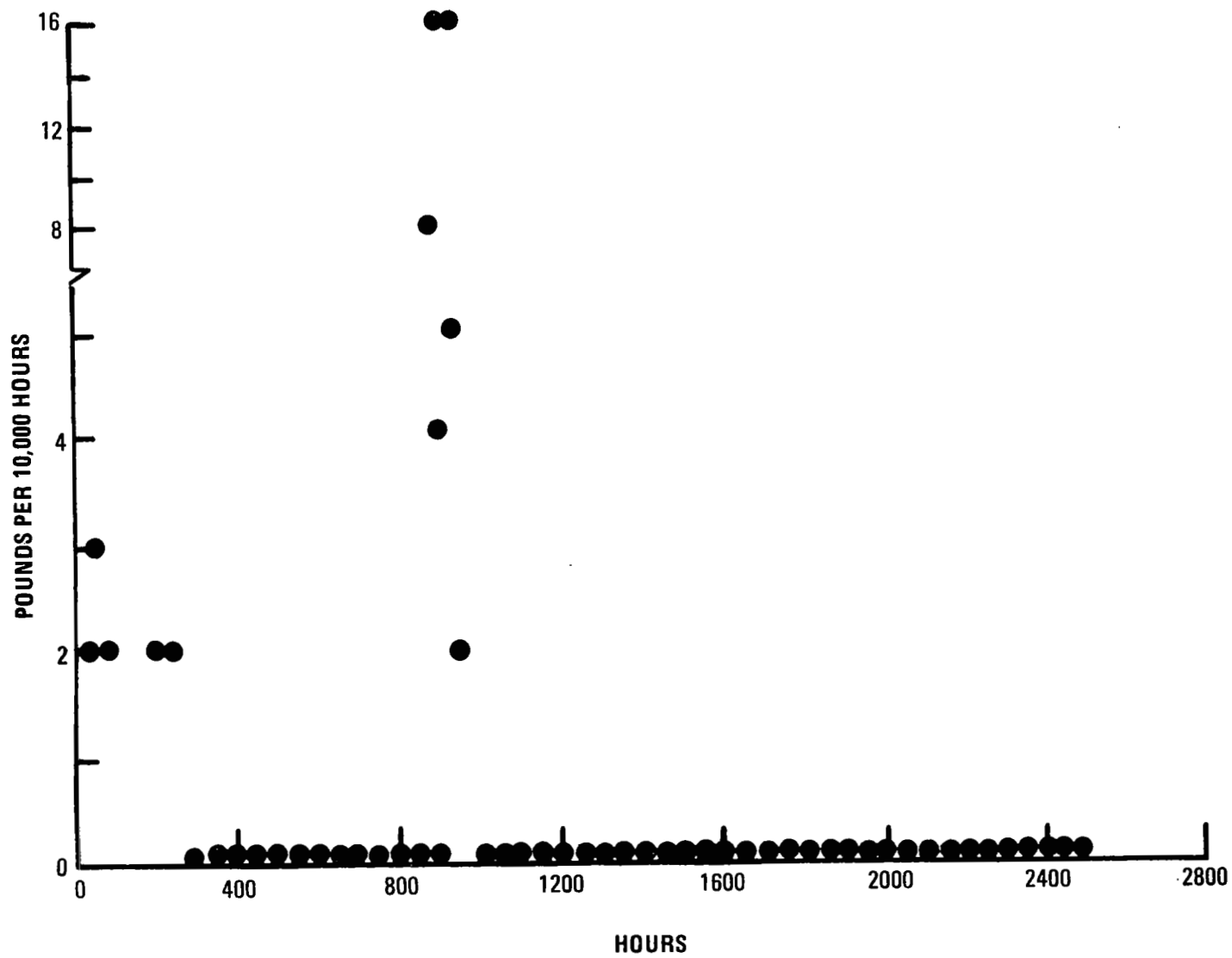


Figure 23 Carbon Face Seal Gas Leakage M-49779

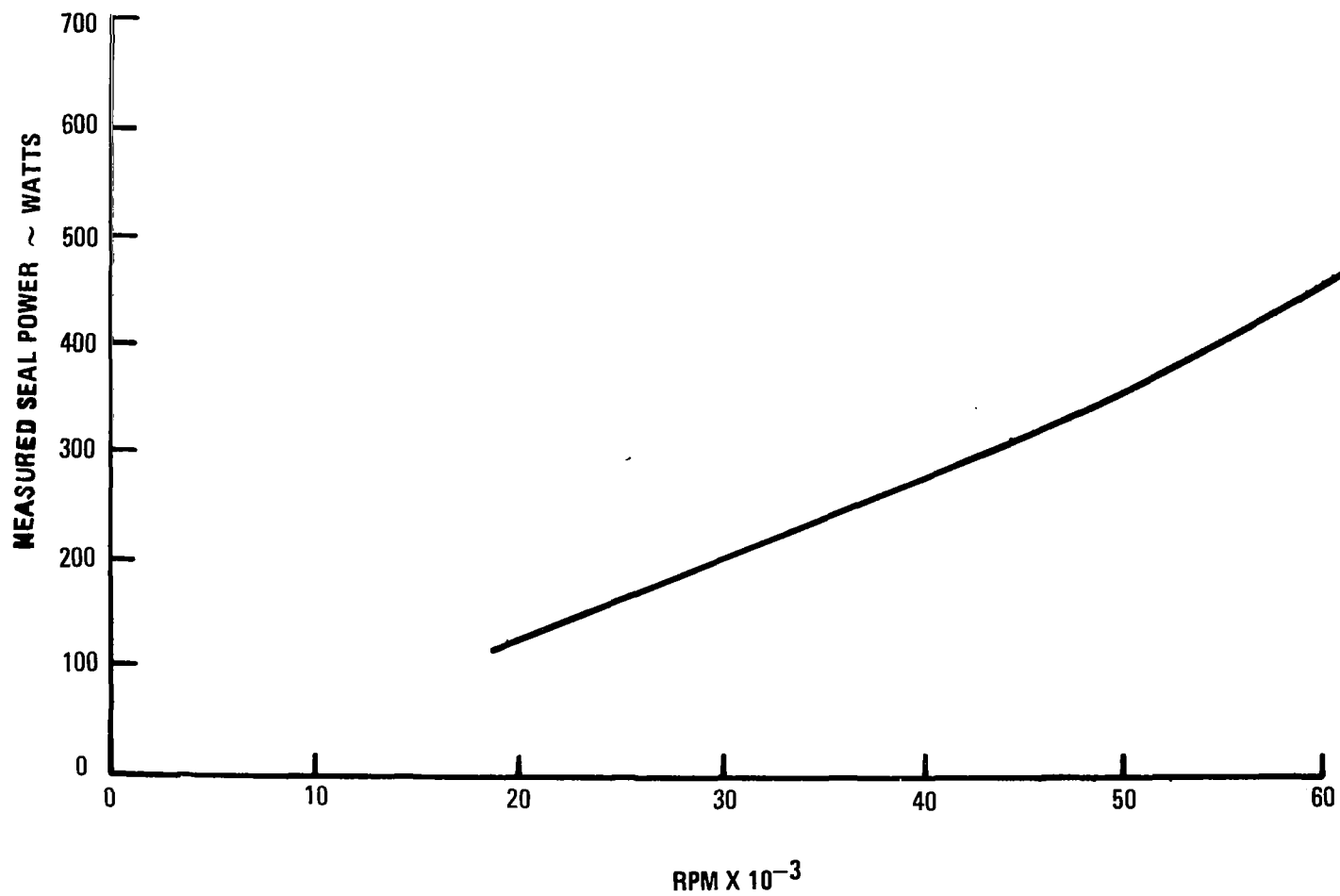


Figure 24 Carbon Face Seal Power Consumption M-44073  
(Seal in 20 mm Bearing Compartment)

The choice of seal materials for this design is the same as in the previous program. Current engine applications demonstrate excellent performance with sealplates of AMS-5613 hardened to a Rockwell C of 30-38, with a hard-faced coating of chrome carbide bearing against CDJ-83 carbon. Both the sealplate and carbon ring flatness and surface finish are held to close tolerances.

With a wear allowance of 0.030 inch designed on the carbon ring, seal life for the BRU is predicted in the range of 16,000 to 36,000 hours, based on the data shown on Figure 25 obtained during the previous program on two seals. The wear rate was probably higher in the seal tested in the pilot system test because this test had 28 shutdowns and restarts, while the seal test rig was subjected to only 12 such cycles. These shutdowns were generally caused by commercial electrical power outages and rig safety interlock actuation. Because seal carbon wear is accelerated when the seal is subjected to transient operating conditions, seal life in the BRU may be more than the above-predicted values if the number of transient cycles in the BRU is less than those experienced in the above tests.

#### E. Oil Contamination of Power System

The lubrication system of the BRU is isolated from the powerplant working cycle by the use of face seals backed up by a labyrinth seal buffer zone. The buffer zone is located between the face seal and the working cycle, and is pressurized with compressor discharge gas to maintain the gas pressure outside of the face seal higher than the pressure in the lubrication system. In this manner, face-seal gas leakage is into the bearing compartment, thus preventing contaminated gas from leaking out. However, to maintain gas inventory in the powerplant, clean gas must be added to the powerplant cycle as make-up for the gas leaking into the bearing compartments. If the lubrication system pressure is maintained at the lower pressure by venting gas overboard, then a high-pressure tank of gas must be used to supply make-up gas to the powerplant working cycle. If the face-seal leakage rate in the BRU did not significantly exceed the measured amounts shown on Figure 23 then a gas tank of about 100 pounds weight would be ample. However, to increase reliability of the system, a gas clean-up system was designed into the BRU. This system purifies gas in the lubrication system and supplies this gas to the powerplant cycle. Therefore any oil that can be introduced into the powerplant cycle must either be in the gas leaving the clean-up system or it must leak past the buffer zone.

Oil leaking into the buffer zone through the face seal is anticipated to be about the same level measured in the previous program. Thus about 11 grams of oil is expected to weep past the face seal in 10,000 hours. Based on the estimate of buffer gas flow shown in Figure 9, the buffer gas will transport this oil weepage as a vapor to an adsorber where the oil in the gas will be reduced at least by the factor of 455 measured in the previous program. Therefore, it is estimated that about 0.04 gram of oil will enter the power system as a result of weepage past the two BRU face seals in 10,000 hours.

Oil carried into the powerplant cycle in the gas discharged through the cleanup system is a function of the amount of gas make-up and the performance of the separator and adsorber.

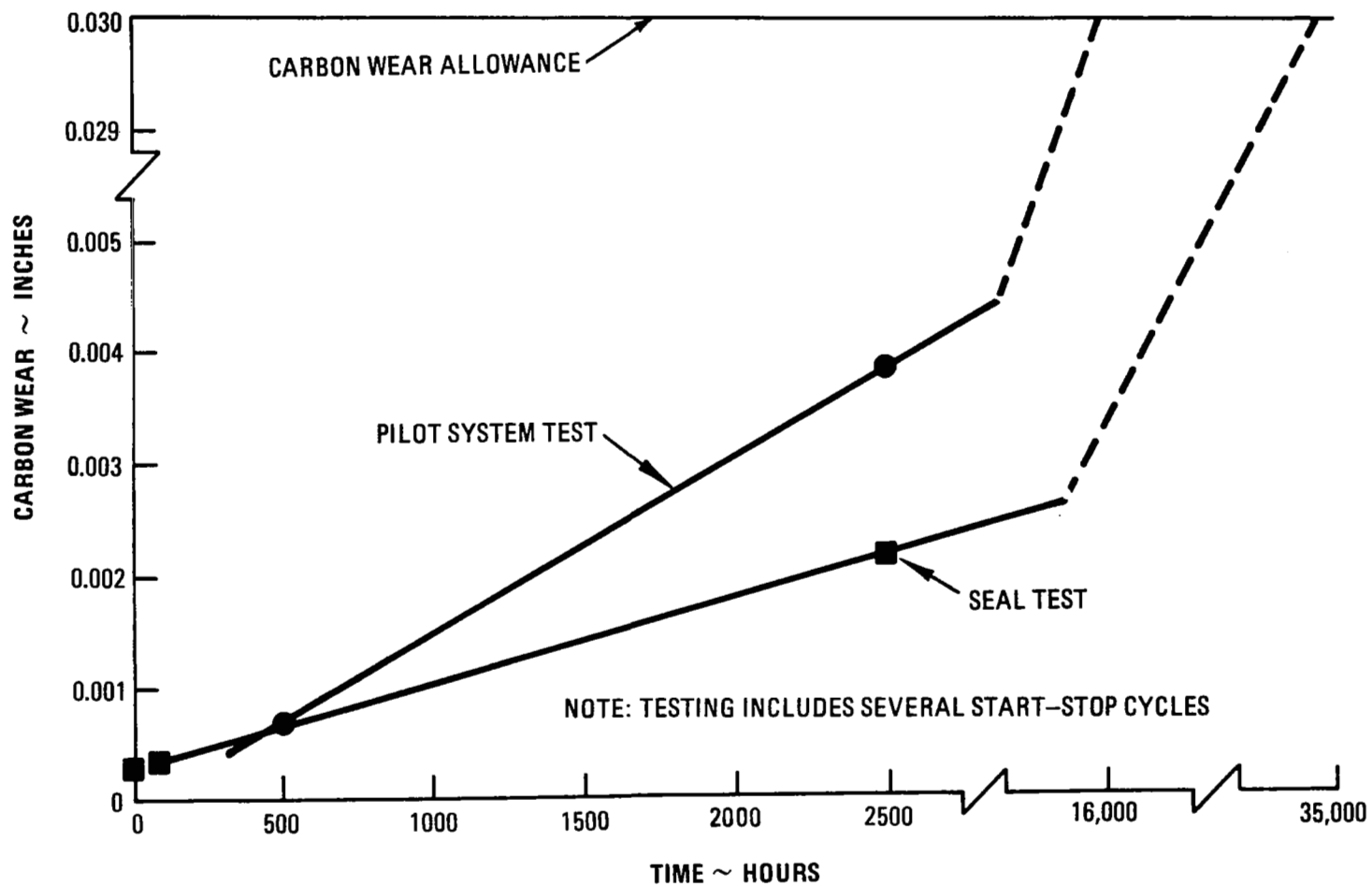


Figure 25 Seal Wear M-49226



The gas entering the separator is estimated to contain about 0.12 pound of oil per pound of gas. Using the separator effectiveness of the previously-tested separator and adsorber bed, the oil content of the gas is reduced to 0.078 microgram of oil per pound of gas. Based on the predicted total face-seal gas leakage of 1.7 pounds per hour, it is estimated that about 0.013 gram of oil will enter the powerplant cycle from the cleanup system in 10,000 hours. However, if the face seals perform as well as measured in the previous program and the seal leakage is three orders of magnitude lower than predicted, then the oil entering the powerplant through the cleanup system will be proportionately lower than estimated above. Also, if the BRU separator performance is improved by the features discussed previously, the oil contamination level will be reduced.

Adding the estimated oil contamination introduced by the buffer gas to that introduced by the make-up gas, the total oil contamination is about 0.05 gram of oil in 10,000 hours.

Using the design data in Table 11 for the columbium-alloy heat receiver of a solar-heated Brayton-cycle system, which was provided by the NASA, this oil contamination level is at least two orders of magnitude lower than allowable limits, based on the surface formation of columbium carbide.

TABLE 11  
Solar Heat Receiver Design

material	Cb-1Zr
weight, pounds	187
surface area, in <sup>2</sup>	7000

#### F. Temperature Maps

Predicted thermal maps of the BRU at a steady-state 6.0 KW design power level are indicated in Figures 26 and 27. The temperature patterns shown are well within reasonable limits for the selected materials and anticipated operating conditions. Temperature limits specified consist of a 400°F maximum bearing outer race temperature and a maximum inner-to-outer race temperature difference of 40°F. The thermal maps indicate that these conditions are met in both bearing compartments. Another significant thermal area is the gas-oil separator and its adjacent cooling passages. The predicted temperature distribution in this area, which is vital to the proper operation of the lubrication system, is shown in Figure 26. The figure shows the stationary outer housing of the separator which is cooled at about 100°F to reduce the gas temperature in the mesh, and condense the oil vapor carried in the gas.

The proximity of the alternator housing to the turbine inlet area in this configuration required detailed attention. Using the alternator heat generation rates and distribution provided by NASA, a satisfactory temperature distribution was obtained in the area between the alternator and turbine by incorporating a Min-K type insulation.

The BRU on rolling-element bearings employs many of the same components operating in the same environment at the same stress levels as in the gas-bearing configuration.

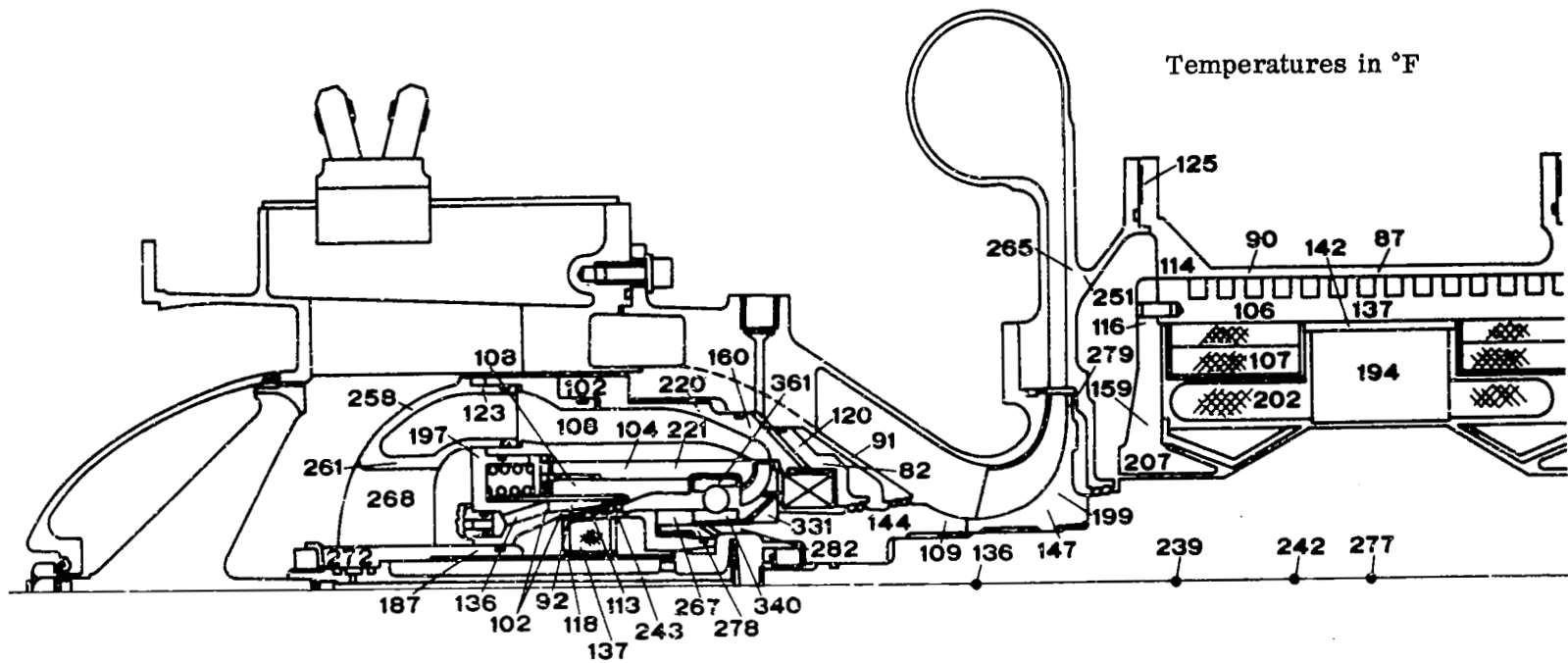


Figure 26 Thermal Map of Compressor End (6 KW) M-61029

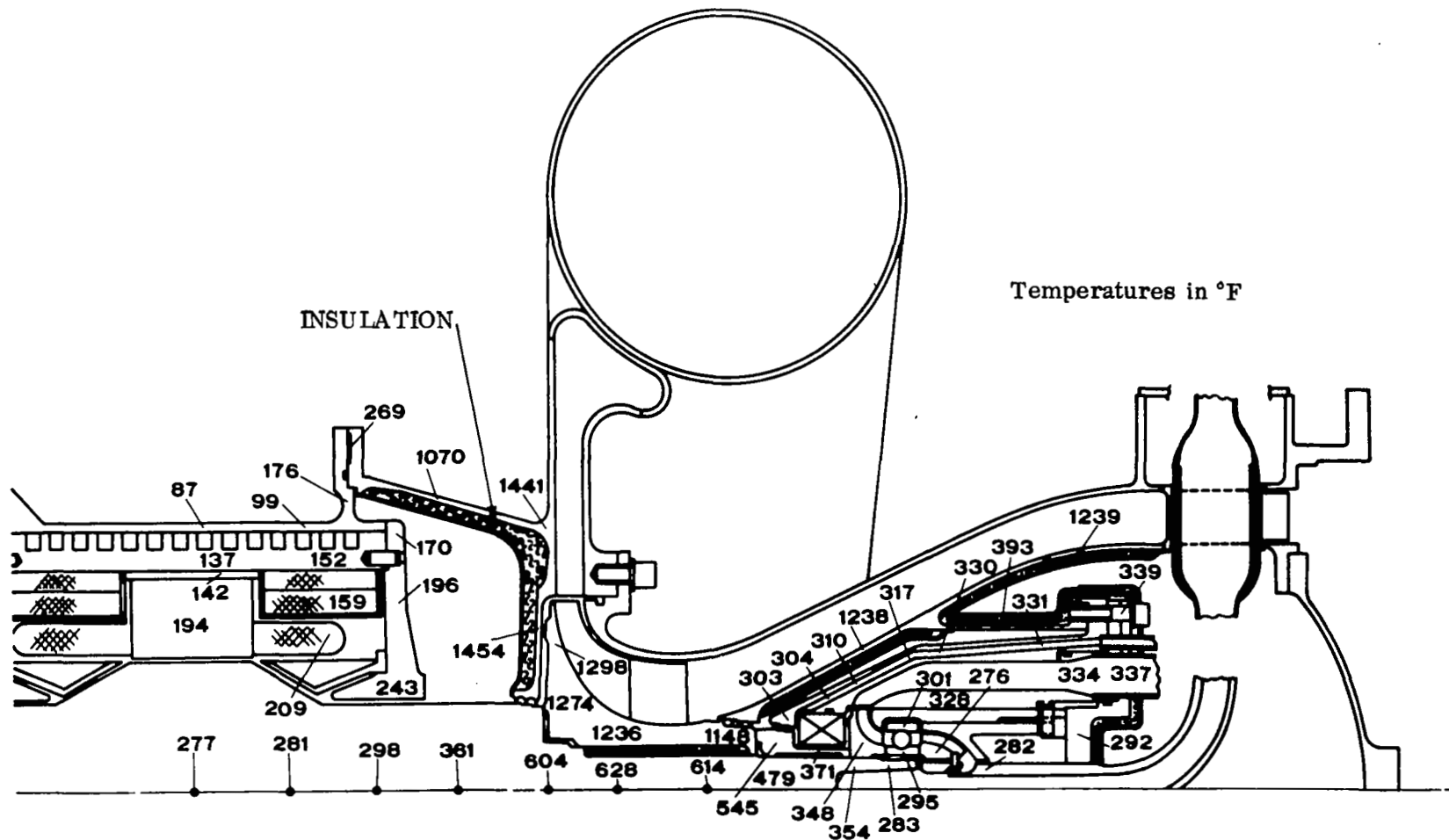


Figure 27 Thermal Map of Turbine End (6 KW) M-61028

No significant modifications were made to the aerodynamics of the compressor or turbine or to the electrical design of the alternator. However, some mechanical modifications were necessary to reasonably incorporate the rolling-element bearings and associated equipment. The compressor wheel remains virtually unchanged from the gas-bearing version, however the hub of the turbine wheel was modified to permit the use of a 20 mm bore bearing, and to incorporate a thermal dam area under the turbine.

#### G. Critical Speed Analysis

Evaluation of critical speeds for the rotor-support system was determined as a function of rotor-support springrate. The springrate for the design configuration was estimated to be 300,000 pounds per inch. The first critical speed is a rigid-body conical mode which occurs at about 18,000 rpm. The second critical speed is a rigid-body translatory mode at approximately 47,000 rpm, and the third critical speed, which is the bent-shaft mode, occurs above 96,000 rpm. None of these critical speeds occurs in the range of the operating speed (including the 20 percent over-speed design condition) or in the range of the equivalent electrical speed for this machine. Figures 28 and 29 illustrate the distribution of mass and the distribution of polar moment of inertia for the rotor system. The total weight of the rotor assembly is 22 pounds and the total polar moment of inertia is 0.087 in-lb-sec<sup>2</sup>.

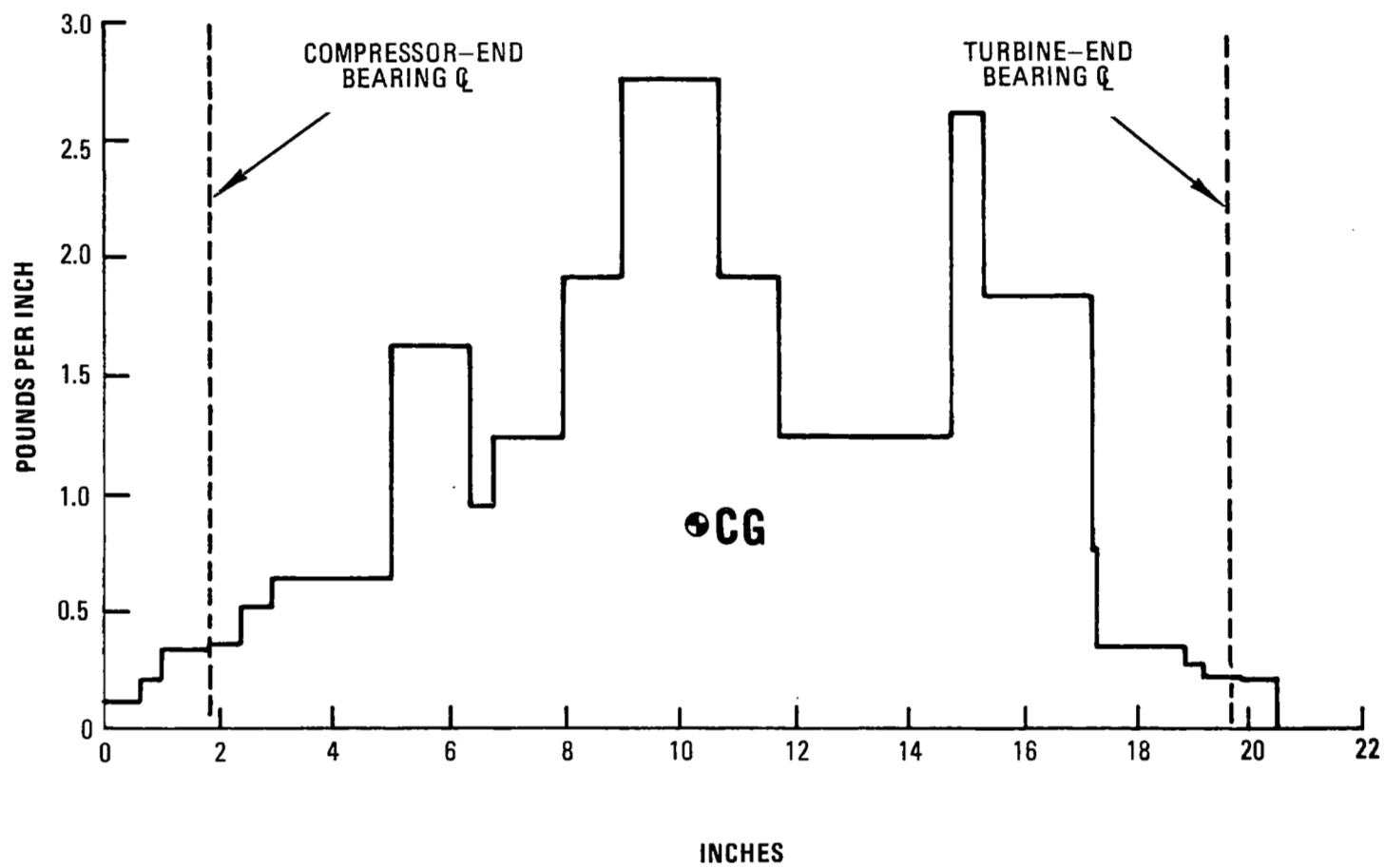


Figure 28 Mass Distribution of Rotor Assembly M-59974

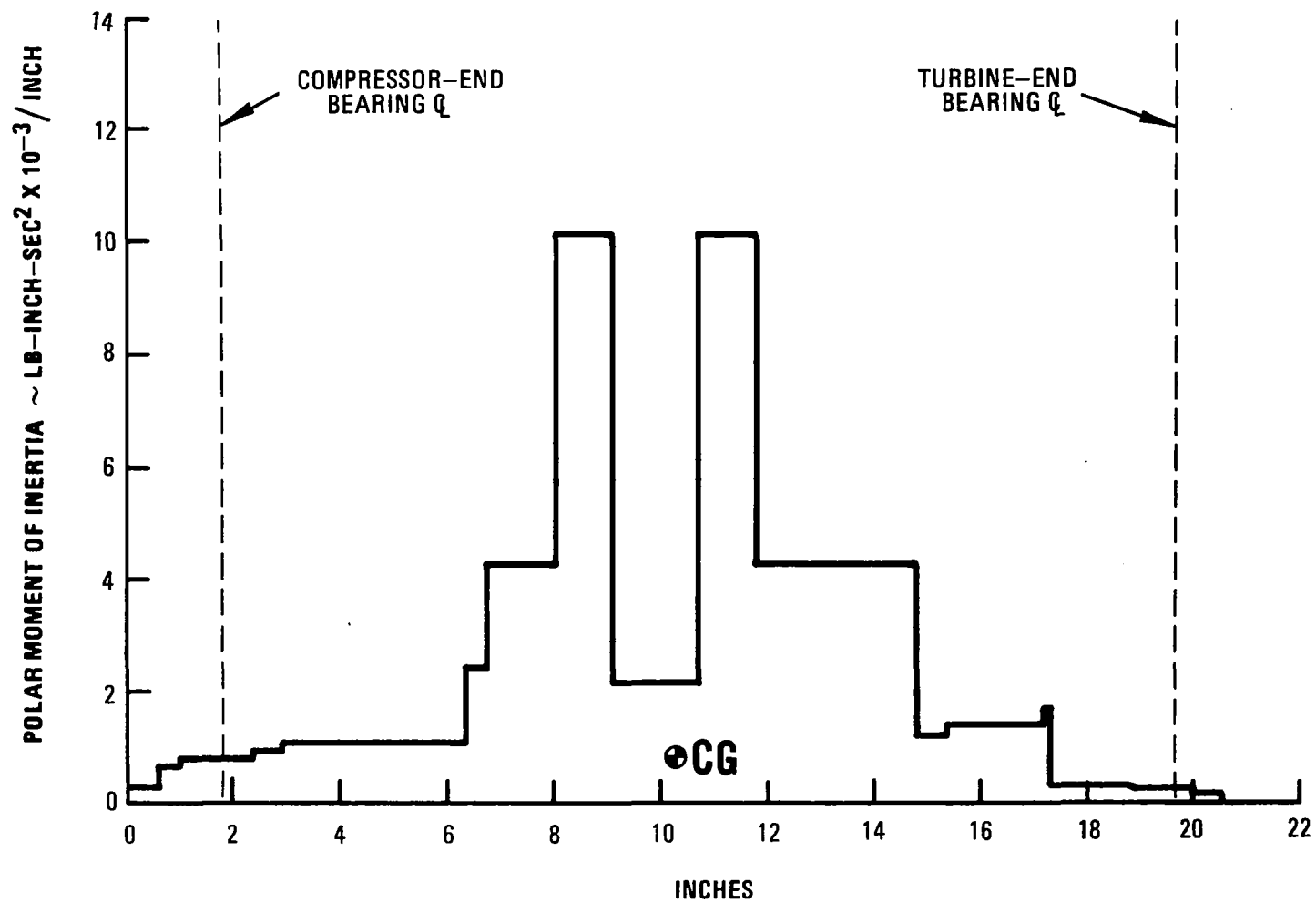


Figure 29 Distribution of Polar Moment of Inertia of Rotor Assembly M-61050



## APPENDIX

### Alternate Configurations of Brayton Rotating Unit

#### Summary

This appendix contains a description of the alternate BRU configurations analyzed during the design study. The inboard bearing configuration which is similar to the gas-bearing BRU design was first considered. The configurations with one inboard and one outboard bearing compartment were then investigated. Finally the outboard bearing configurations which resulted in the reference design selection were studied. Emphasis was placed on arrangements incorporating a high-speed separator on the BRU shaft; however both inboard and outboard bearing designs with no separator were studied.

As a result of the inboard bearing study it was concluded that the minimum parasitic power loss for a design with an integral separator would be approximately 10.5 KW. This would be a design with two 70 mm bore bearings. For a BRU design with no integral separator the parasitic power loss would be about 2.5 KW for a 40-40 mm bearing configuration. Critical speed values were acceptable for the inboard designs, but seal rubbing speeds were in excess of 350 ft/sec and DN values were well over  $1.5 \times 10^6$  mm-rpm for designs including an integral separator.

Configurations with one inboard and one outboard bearing compartment resulted in reduced parasitic power loss relative to the inboard bearing configurations. However, the former configuration lacked the potential to reduce parasitic power loss to the levels that could be obtained for the outboard configuration.

A minimum bearing bore of 20 mm was determined for outboard designs with no integral separator. Cross-sectional area of the BRU shaft for oil-gas flow passages becomes marginal below 20 mm bore. Outboard type configurations with an integral separator were attempted with bearings down to 30 mm bore. At this diameter, oil pool depth is marginal, gas flow area across the oil pool is limited, and mechanical assembly of the oil-gas passages and static disc is marginal. As a result, minimum bore for an outboard bearing compartment with an integral separator was set at 35 mm. Total parasitic power loss for a 35-20 mm single-separator configuration is then about 1260 watts. This is the reference design selected for detailed study. Total parasitic power loss for a BRU without an integral separator is about 760 watts with 20 mm bearings.

#### A. Gas-Bearing BRU Design Summary

The Brayton Rotating Unit consists basically of a turbine, a four-pole radial-gap alternator and radial-flow compressor mounted on a common shaft, rotating at 36,000 rpm, and supported on gas-lubricated journal and thrust bearings. The complete unit includes a flight-type housing, insulation, coolant provisions, turbine and compressor ducting, and mounting brackets.



A layout of the Brayton Rotating Unit is shown in Figure 30. The rotating group arrangement consists of a modified Lundell alternator rotor, straddle-mounted between gas journal bearings with the radial-flow turbine wheel overhung at one end of the shaft, and the radial-flow compressor wheel and rotating component of the gas thrust bearing overhung at the other end. Figures 31, 32, and 33 illustrate the general geometry of the turbine and compressor wheels and the alternator. Three curvic couplings, 1.75 inches in diameter, are used to locate and couple the components of the rotating group. A tie-bolt running through the center of the rotating group provides the load to hold the components together. A pair of orthogonal proximity probes are located at each journal bearing for monitoring shaft motions. Four speed pickups are located near the compressor journal.

The gas journal bearings are of the three-segment pivoted-pad type incorporating both hydrodynamic and hydrostatic capabilities. Each of the three pads in each journal bearing is mounted on a lapped ball-socket pivot through which the hydrostatic gas supply is fed. A single hydrostatic orifice-pad arrangement, located on the pivot axis of each pad, provides journal bearing lift-off capabilities. One of the three pads at each journal bearing is flexibly mounted on a beam-type spring having a spring rate of approximately 2,000 pounds per inch. The remaining two mounts at each journal bearing are rigidly fixed. A proximity probe positioned behind the flexible mount provides for monitoring of the journal bearing loads during operation of the BRU. Pairs of proximity probes are available for monitoring the leading-edge motions of two pads at each journal bearing.

The gas thrust bearing configuration utilized is the stepped-sector design. The thrust bearing assembly is a double-acting configuration with the two thrust stators mounted face-to-face and separated by a gauged spacer. The spacer, in addition to maintaining flatness and parallelism between the two stator surfaces, establishes the running clearances on the inoperative side of the bearing. Both sides of the thrust bearing have hydrodynamic as well as hydrostatic capabilities. Three proximity probes mounted on the normal thrust stator and one on the reverse thrust stator are available for measuring thrust bearing operating film thickness and thrust load.

The entire thrust bearing assembly is mounted on a gimbal assembly to provide for alignment of the stationary thrust bearing assembly surfaces with the rotor surfaces. The gimbal design incorporates elastic pivots. The pair of pivots in each axis are coplanar and located midway between the two thrust bearing surfaces. A pair of proximity probes are available for monitoring gimbal motions with respect to the reference frame of the unit.

The alternator-stator assembly with its end plates is the nucleus to which all structural ties are made. The compressor and turbine journal bearing carriers are fabricated integrally with the alternator end plates, one on each plate. The stator assembly contains the instrumentation receptacle housing, the alternator power receptacles and all coolant and hydrostatic gas supply fittings. In addition, it contains the BRU mounting brackets and the flanges to which the compressor and turbine scrolls are attached.

In the design of the shaft, thermal shunts fabricated from copper are located beneath the compressor and turbine journals and extend into that portion of the shaft rotating beneath the alternator secondary flux paths. These shunts serve to reduce the axial temperature gradient across the journal, thereby minimizing the coning and crowning of the journal surface.

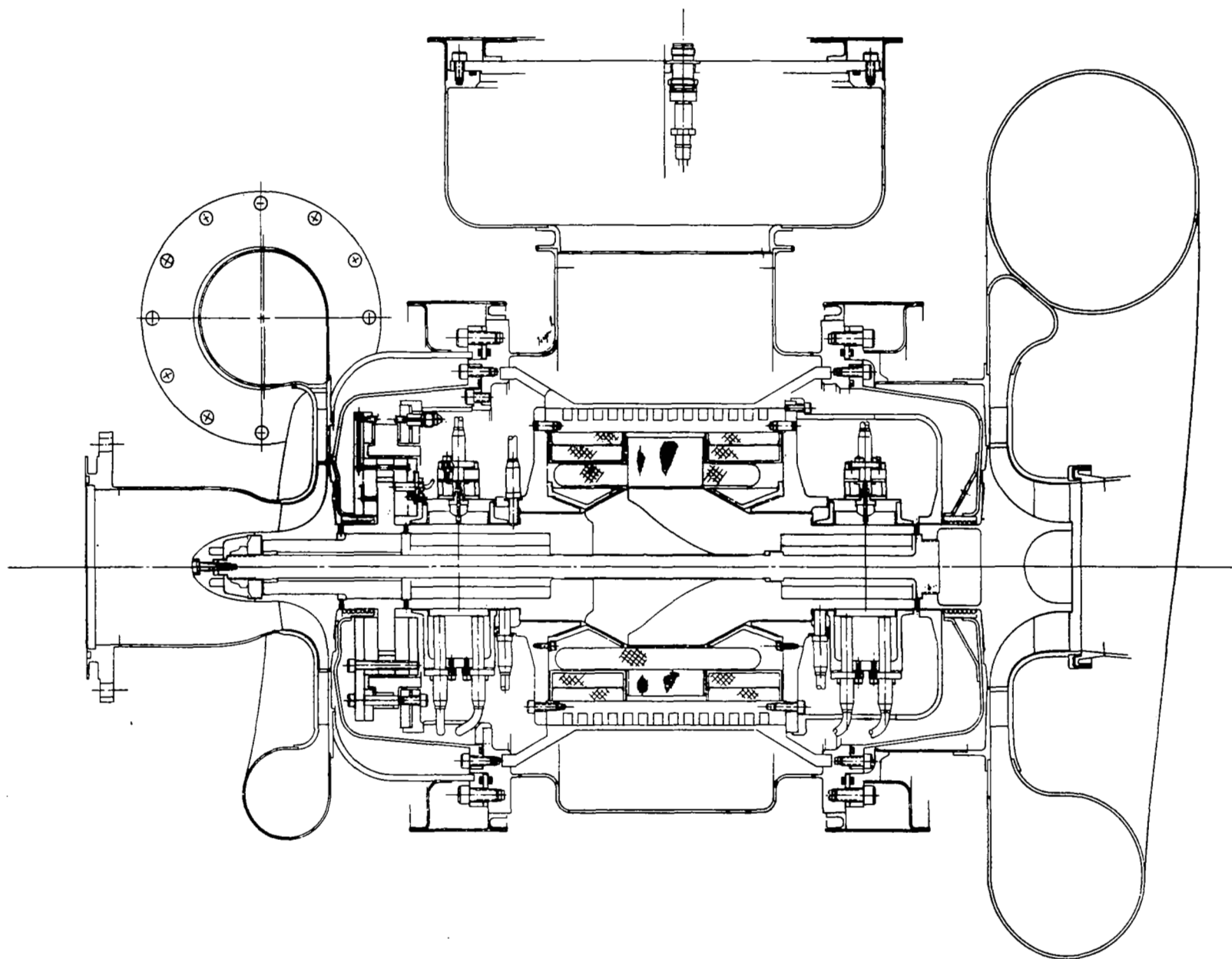


Figure 30 Gas Bearing BRU

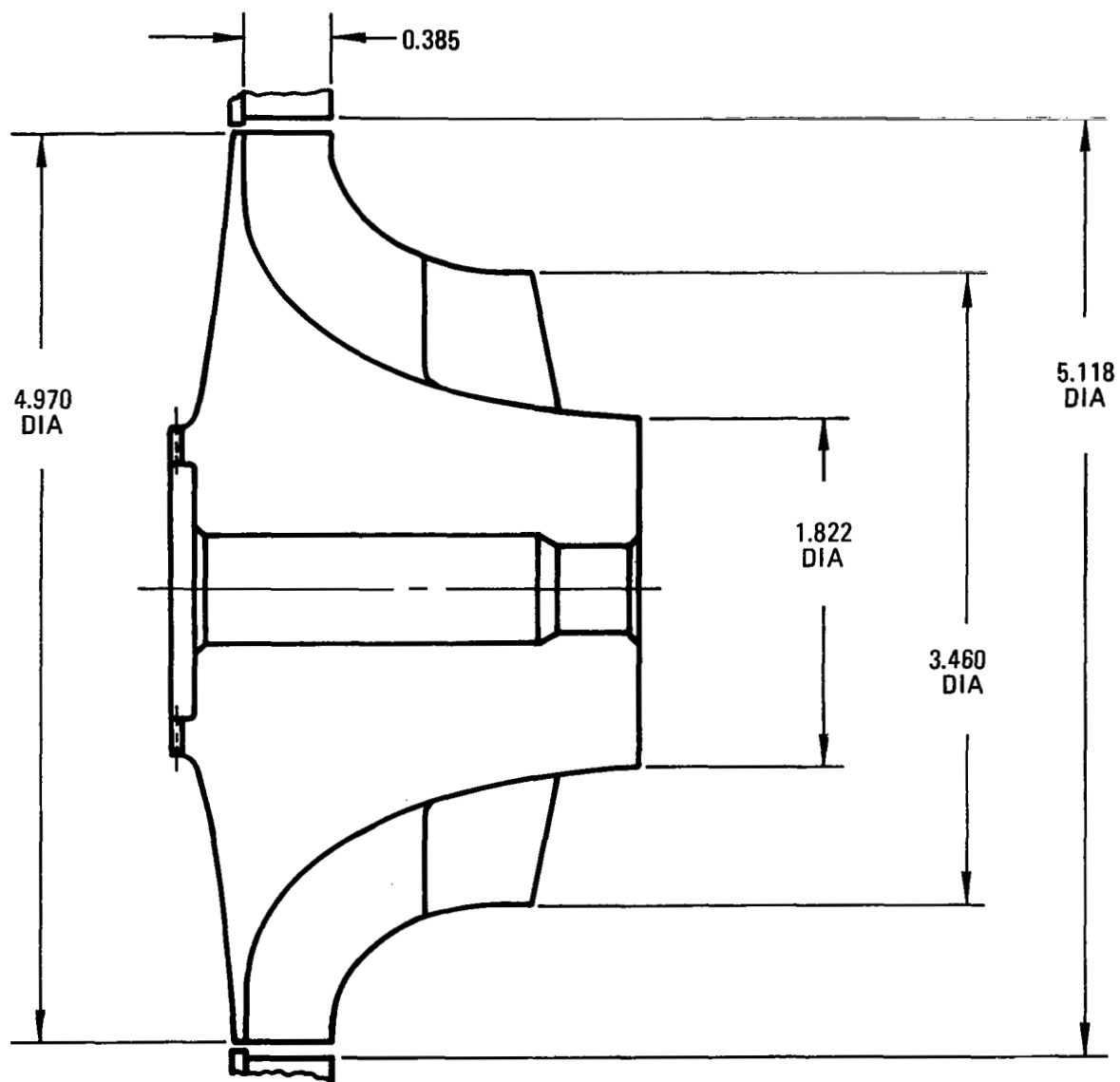


Figure 31 BRU Turbine Wheel

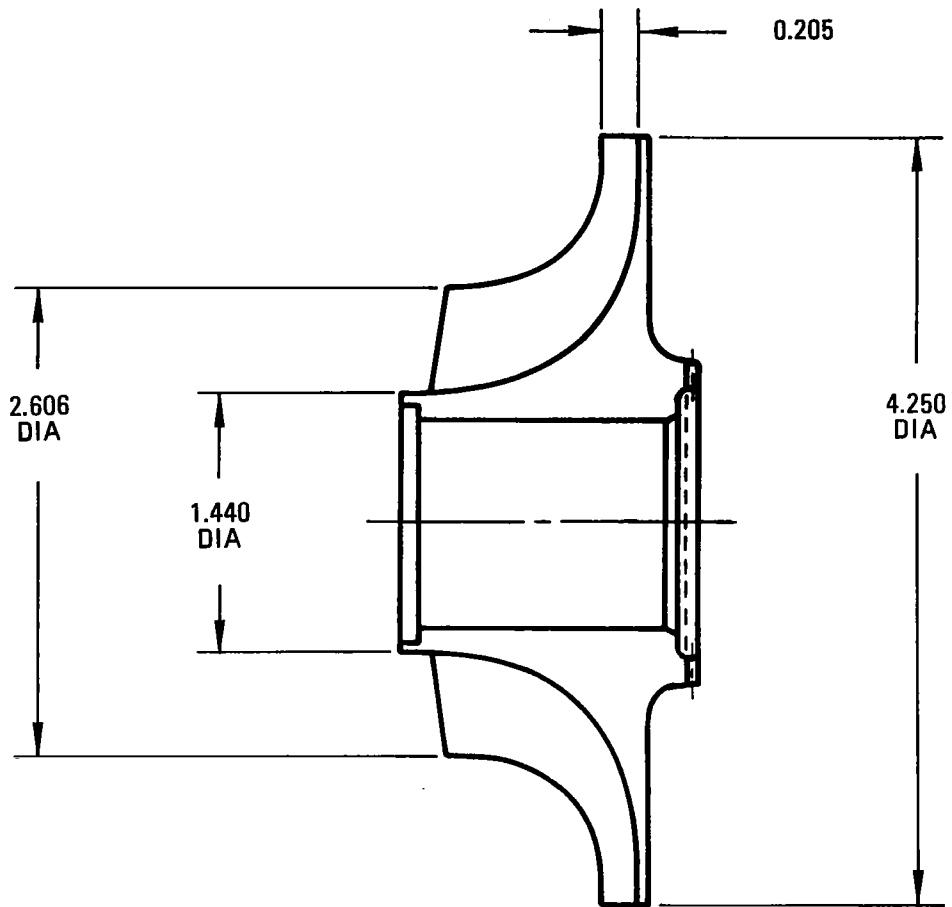


Figure 32 BRU Compressor Wheel

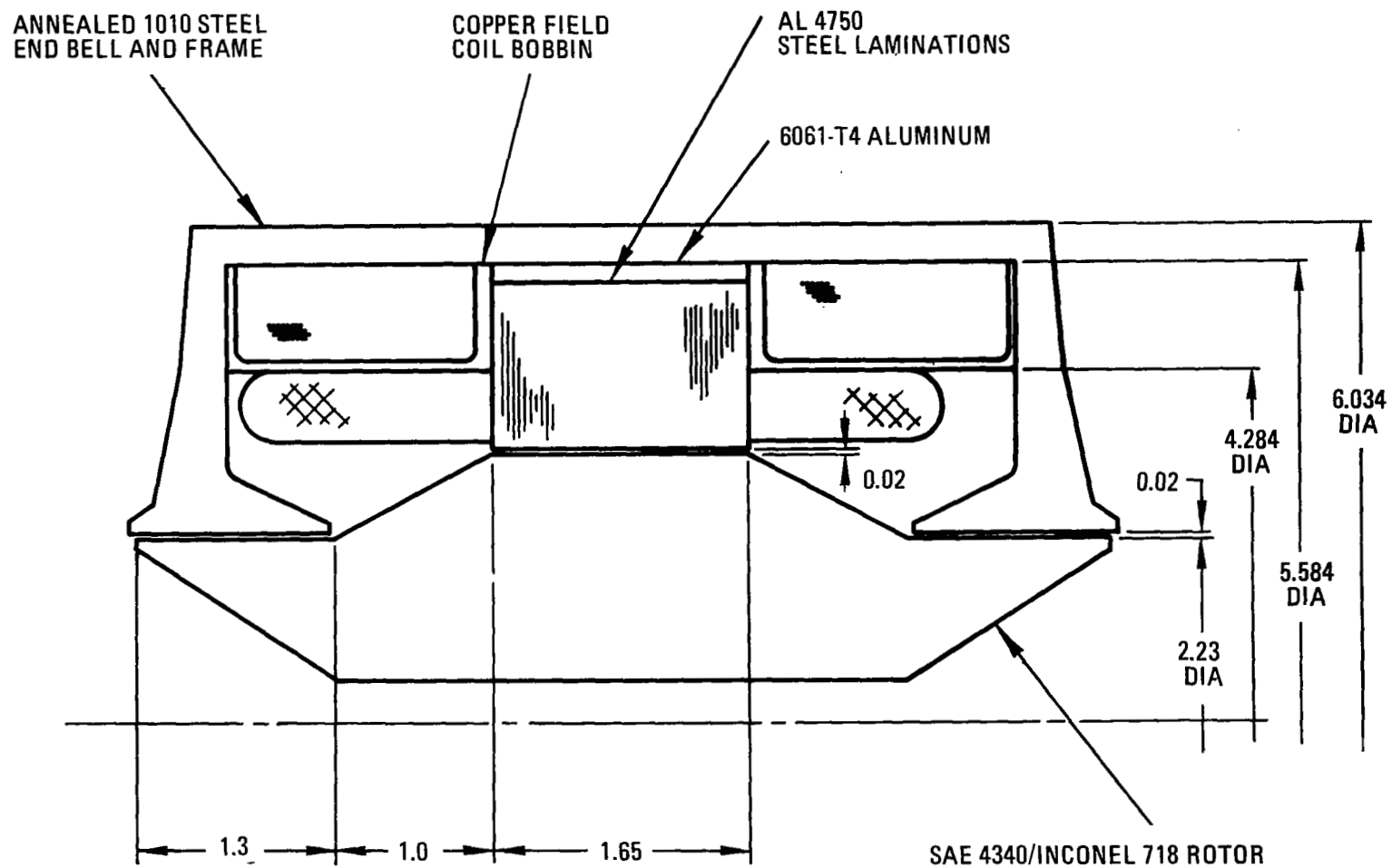


Figure 33 BRU Alternator

In addition, the shunts provide a high conductance path for friction heat generated at the journal bearings to find its way to the cooler secondary flux gap, where it is convected across the gap into the alternator end plate.

A copper thermal shunt is also provided between the thrust-bearing rotor and the compressor wheel. Friction and windage heat generated at the thrust bearings is conducted down the thrust rotor, through the shunt and into the compressor wheel, where it is convected into the compressor through-flow.

The liquid-coolant heat exchanger utilized for cooling the BRU consists of a double helix machined into the outer frame assembly of the alternator stator. The coolant passage cross-sectional dimensions are 0.20 inch wide by 0.25 inch deep and the thread lead is 0.667 inch. Each helical passage is independently supplied with coolant to provide the required coolant system redundancy. The coolant specified for use is Dow Corning 200 which is blended to yield a viscosity of 2.0 centistokes at 77°R. Estimated pressure drop, at the recommended coolant flow rate of 0.12 pound per second, is 7.5 psia.

Thermal isolation is utilized between the journal bearing carriers and their attachment points to the alternator stator end plates. This permits control of the temperature levels of the carriers with little or no influence felt from the relatively cool stator end plates. The journal bearing carriers are heated by convection from areas of the rotating group in close proximity to their respective carriers. This permits the temperature of each bearing carrier to follow the temperature of its journal and thus gross bearing load changes due to relative expansion between the journal and the carrier are reduced to a level that can be easily accommodated by the flexible mount of each bearing.

Labyrinth seals located at either end of the rotating group and mounted on the wheel backshrouds are provided for minimizing leakage of the bearing cavity pressurization gas into the system flow. Running clearances of 0.004 inch at the compressor end and 0.005 inch at the turbine end limit the leakage to 2 percent of the system flow at all power levels. Leakage make-up is provided by bleeding filtered system gas from the compressor scroll discharge duct into the bearing cavity.

Hermetic seal flanges are provided at the compressor and turbine scroll duct attachment points as well as on the BRU outer jacket. Those on the compressor scroll and BRU outer jacket will also accept elastomer o-rings for convenience during system checkout and short-duration running.

A table of general design specifications which applies to both the gas-bearing design and to the oil-lubricated rolling-element bearing design is shown in Table 12.

**TABLE 12**  
**BRU Design Requirements**

type of rotating unit	single shaft
cycle working gas	helium-xenon mixture having molecular weight of krypton (83.8)
net useful power output range	2.25 to 10.5 KWe, inclusive, at a load power factor of 0.85, lagging
<b>Turbine</b>	
total-to-total pressure ratio	1.748
inlet total temperature, °R	2060
<b>Compressor</b>	
type	radial-flow
total-to-total pressure ratio	1.90
inlet total temperature, °R	539
<b>Alternator</b>	
type	radial gap, 4-pole
rotative speed, rpm	36,000
frequency, cps	1200
power factor	0.75 (alternator)
cooling fluid	Dow-Corning 200 (viscosity 2.0 C.S. at 77°F)
supply temperature, °R	530
supply pressure, psia (max)	300
speed capability, % design	0 to 120
environmental conditions	NASA Spec. 1224-1 and 1224-2
<b>radiation environment</b>	
neutron flux	$< 10^{11}$ neut. per $\text{cm}^2$
integrated gamma dose	$< 10^4$ rads. in 5 years

## B. Alternate BRU Configuration Studies

In the course of conducting this design study of a BRU on rolling-contact bearings, various alternate configurations were studied. The general design philosophy throughout this study was to maintain the aerodynamics of the compressor and turbine and the design of the alternator as provided by the NASA. At several points in the study, designs were investigated with a modification to the original compressor to improve design characteristics of certain BRU configurations. However, none of these excursions was necessary for the final design.

In the preliminary design study several major analyses had to be performed because of changes in bearing location and bearing characteristics from the gas-bearing BRU. This included the analysis of rotor critical speeds, the analysis of local bending and of turbine and compressor rotor coupling, and the examination of bearing stack compressions. Heat generation by bearings and seals, coupled with heat transfer into or out of the bearing cavities, were important considerations.

Typical practice in turbomachinery design would be to use a ball bearing and a roller bearing to support the shaft, with each bearing located inboard of the compressor and turbine rotors, respectively, and with the alternator supported between the bearings. Small lightly-loaded ball and roller bearings can skid when operated at high speed. One method of preventing skidding is to apply load to the bearings. Therefore, two ball bearings were studied for the BRU, mounted with a spring force loading one against the other in thrust. Although an inboard bearing location is identical to the gas-bearing version of the BRU, some difficulty is present in the use of oil-lubricated bearings in this location. Locating the bearings inboard of the turbine and compressor rotors prevents introducing the lubricant down the shaft centerline from the end of the shaft, as was done in the turbine-compressor bearing compartment tested in Contract NAS3-7635. An alternate method was used to introduce oil into the shaft for cooling the bearing under the inner race, as well as for cooling the face seal. Figure 34 shows a BRU with inboard bearing compartments in which oil is introduced into the shaft from the periphery as compared to the concept used in the turbine-compressor. Stationary nozzles direct the gas-oil mixture under the rotating shaft scoop slot. The lubricant then flows down the outwardly-tapered channels in the shaft to the inner race of the bearing, and then to the sealplate. Because of the small size of the shaft used in the BRU, the shaft neck-down at the nozzle locations controls the bent-shaft critical speed of the BRU rotor. Therefore, the bearing and face seal are larger than the minimum size possible by the radial size of the shaft oil entrance scoop slot. The larger bearing and face seal required for the inboard bearing concept increases power loss, bearing DN and seal rubbing velocity. Smaller bearings and face seals located outboard of the BRU compressor and turbine were examined in addition to the inboard concept in later configurations. In addition, concepts using an outboard bearing at the compressor end and an inboard bearing at the turbine end were also considered. This arrangement and others of this general approach permit introduction of oil at the end of the shaft and also remove the turbine end bearing from the high-temperature environment. How-



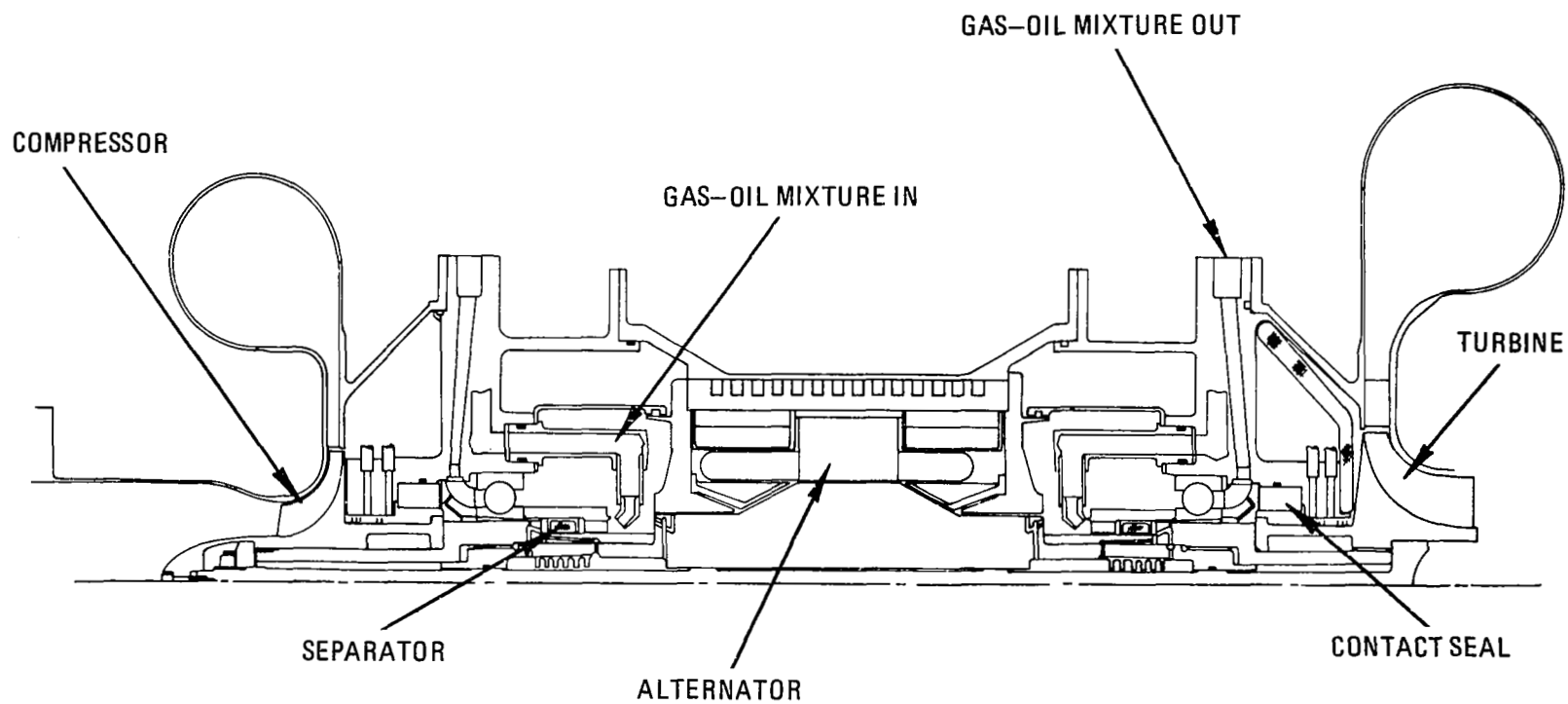


Figure 34 BRU with Rolling-Contact Bearings M-59075

ever, a larger bearing and face seal are required at the turbine-end location to maintain shaft rigidity.

Analysis of the BRU scavenge design and interconnecting piping was performed to size components, estimate power loss, estimate pumping head rise requirements and establish oil and gas flow rates for proper bearing and seal cooling. Computer programs for these analyses of two-phase flow have been substantiated by the multi-gas, multi-pressure level, multi-speed testing of the lubrication system.

Possible oil contamination of the working fluid is a major consideration for longtime operation of a closed-loop Brayton cycle. To minimize oil contamination, it was deemed necessary to maintain a positive pressure drop across the bearing compartment seals to assure that any gas leakage will result in leakage of cycle gas into the bearing compartment, rather than out-leakage of impure gas. Hence, a scheme to maintain working-cycle gas inventory is required.

Two basic concepts for meeting this requirement were studied:

- 1) Exhaust the gas leakage overboard and replenish the system with gas from a make-up supply, as well as any oil that is carried overboard with the gas.
- 2) Design a cleanup system to separate the oil from the leakage gas and return the purified gas to the mainstream of the system.

Considerations of the first concept based on the results of the 2500-hour endurance test on the dry-face carbon seal, indicate that He-Xe make-up required for a 10,000-hour mission would amount to approximately eight pounds of gas. If multiple restart capability were desired, additional gas supply would be required to refill the powerplant and to account for any other loss of gas from the powerplant during start and steady-state operation. An estimate of the weight of a gas make-up system for a range of He-Xe leakage rates is given in Figure 35. A total system weight of 100 pounds is estimated for 0.008 pound per hour of make-up gas, which is a leakage rate 10 times greater than measured for the seals. The quantity of oil make-up for the oil entrained in the gas leaking out of the lubrication system through the face seals, would be a negligible fraction of the oil stored in the accumulator.

This concept was studied for application in the BRU but a serious question arises as to the dependability of the powerplant. If a seal should leak excessively due to a bellows leak or separation of the rubbing surface, the gas inventory of the system could be discharged out of the system and result in loss of the power system. The second concept consisting of a cleanup system has been designed to purify an amount of seal leakage 1000 times greater than the measured seal leakage. This provides a substantial margin of dependability to the power system not possible with the first concept. Therefore, the second concept using a cleanup system was emphasized in the preliminary design study of the BRU.

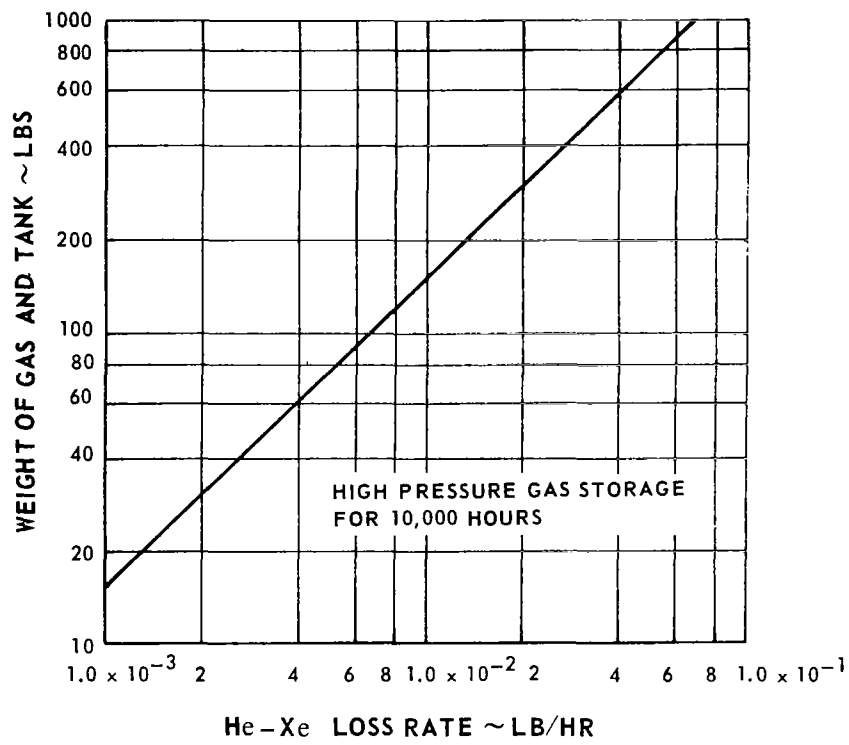


Figure 35 Gas Make-up Weight

As discussed earlier, the design study of the BRU proceeded from the consideration of the inboard bearing configuration which is similar to the gas-bearing BRU design, to configurations with one inboard and one outboard bearing, and finally to outboard bearing designs. The first of the inboard bearing configurations is shown in Figure 34. The oil-gas mixture enters the shaft after leaving a number of stationary nozzles. After entering the shaft slots, the mixture is accelerated up to shaft speed and the oil is thrown to the outer surface of the slot passages, flows through slots bypassing the fine-mesh separator to the inner race of the bearing, and through the sealplate. The gas flows through the mesh separator and radially inwards to the bore of the shaft, where further separation takes place. The gas leaves the shaft through radial holes at the ends of the alternator rotor. Most of the gas flows through the balls of the bearing and is pumped out of the bearing compartment by the rotating impeller. A small fraction of the gas flows through the alternator and then leaves the alternator as it flows to the adsorber.

This initial design incorporated bearings of 50 mm bore, resulting in a DN of  $1.83 \times 10^6$  mm-rpm. Although this value of DN is greater than the desired  $1.5 \times 10^6$  mm-rpm, this rotor configuration was analyzed for critical speed. Two rigid-body critical speeds are predicted in the range of 22,000 to 27,000 rpm and the first bent-shaft critical speed about 42,000 rpm. The low bent-shaft critical speed is due predominantly to the necked-down shaft diameter at the oil-gas mixture inlet nozzle location. The above value of the bent-shaft critical speed is unsatisfactory due to its proximity to the 36,000 rpm operating speed.

Table 13 shows the rotor dynamic behavior of the inboard-bearing configuration as a function of bearing diameter and changes in compressor wheel material and shaft stiffness locally between the compressor wheel and bearing. This information indicates that the inboard-bearing configuration with a separator requires a bearing of at least 50 mm diameter for adequate rotor stiffness.

TABLE 13

Rotor Dynamic Characteristics of  
Inboard-Bearing Configuration

<u>Bearing Diameter, mm</u>	<u>Bearing DN, mm-rpm x 10<sup>-6</sup></u>	<u>Rigid-Body Critical Speed Range, rpm</u>	<u>Bent-Shaft Critical Speed, rpm</u>
40	1.44	19,000 - 24,000	26,000
45	1.62	23,000 - 28,000	41,000
45	1.62	23,000 - 28,000	44,000*
50	1.83	22,000 - 27,000	42,000
50	1.83	23,000 - 28,000	45,000**

\* Titanium compressor wheel

\*\* Titanium compressor wheel and stiffened shaft

A configuration incorporating bearings of 70 mm bore and an oil-inventory control scoop is shown in Figure 36. The increased bearing diameter was necessary to provide space for the oil-inventory scoop. Critical speed analysis indicated two rigid-body critical speeds in the range of 30,000 to 35,000 rpm, and the first bent-shaft critical speed at about 56,000 rpm. This design, like the previous 50 mm design, lacks provision for separator cooling and has a bearing B<sub>1</sub> life of less than 10,000 hours.

The design shown in Figure 37 is an attempt to lower parasitic power consumption by moving the inventory control scoop inward compared to the design shown in Figure 36 and to permit the use of a 50 mm bore bearing. The bearing DN for the 50 mm bore is  $1.83 \times 10^6$  mm-rpm and the seal rubbing speed is 440 ft/sec. The two rigid-body critical speeds for this configuration fall within a range of 25,000 to 30,000 rpm.

In an effort to alleviate the critical-speed problems associated with the above design, and to add separator cooling provisions, the 70 mm bearing configuration shown in Figure 38 was studied. Analysis of this rotor arrangement indicated that two rigid-body critical speeds will occur in the range of 30,000 to 35,000 rpm, with the first bent-shaft critical speed at about 55,000 rpm. Although the bent-shaft critical speed was acceptable, provisions to lower the rigid-body critical speeds would be required.

A flow schematic of the oil-gas flow system applicable to the inboard-bearing system is shown in Figure 39. The oil-gas mixture is introduced into the shaft through a number of stationary nozzles. An initial separation occurs as the mixture accelerates to shaft speed, and oil is thrown to the wall of the rotating shaft undercut. As shown in Figure 39, this oil flows to the inner bearing race and then through the sealplate. Most of the oil mist from the initial two-phase mixture flows directly to the balls of the bearing and is then pumped out of the bearing compartment by the rotating impeller incorporated in the sealplate. The remaining oil mist flows to the separator where the oil is separated and sent to the inner race. The oil mist leaving the separator exit flows through the alternator and then to the adsorber for purification. Total oil and gas flow rates for this 70 mm system are 225 pounds per hour and 80 pounds per hour, respectively, at an oil inlet temperature of 300°F.

The flow schematic, Figure 39, also indicates the flow of buffer gas through the two labyrinth seals and behind each face seal. The gas flow to each bearing compartment from the compressor diffuser exit is divided, with one part flowing to the face-seal area and the remainder returning directly to the powerplant.

Figure 40 shows the stationary nozzles and the oil scoops incorporated in the BRU design shown in Figure 38. In an effort to minimize wake turbulence in the rotating oil pool, the oil scoops in this design operate on static rather than total pressure as they did in Contract NAS3-7635. Also the scoops are located in a disc to further reduce turbulence in the vicinity of the scoop inlet.

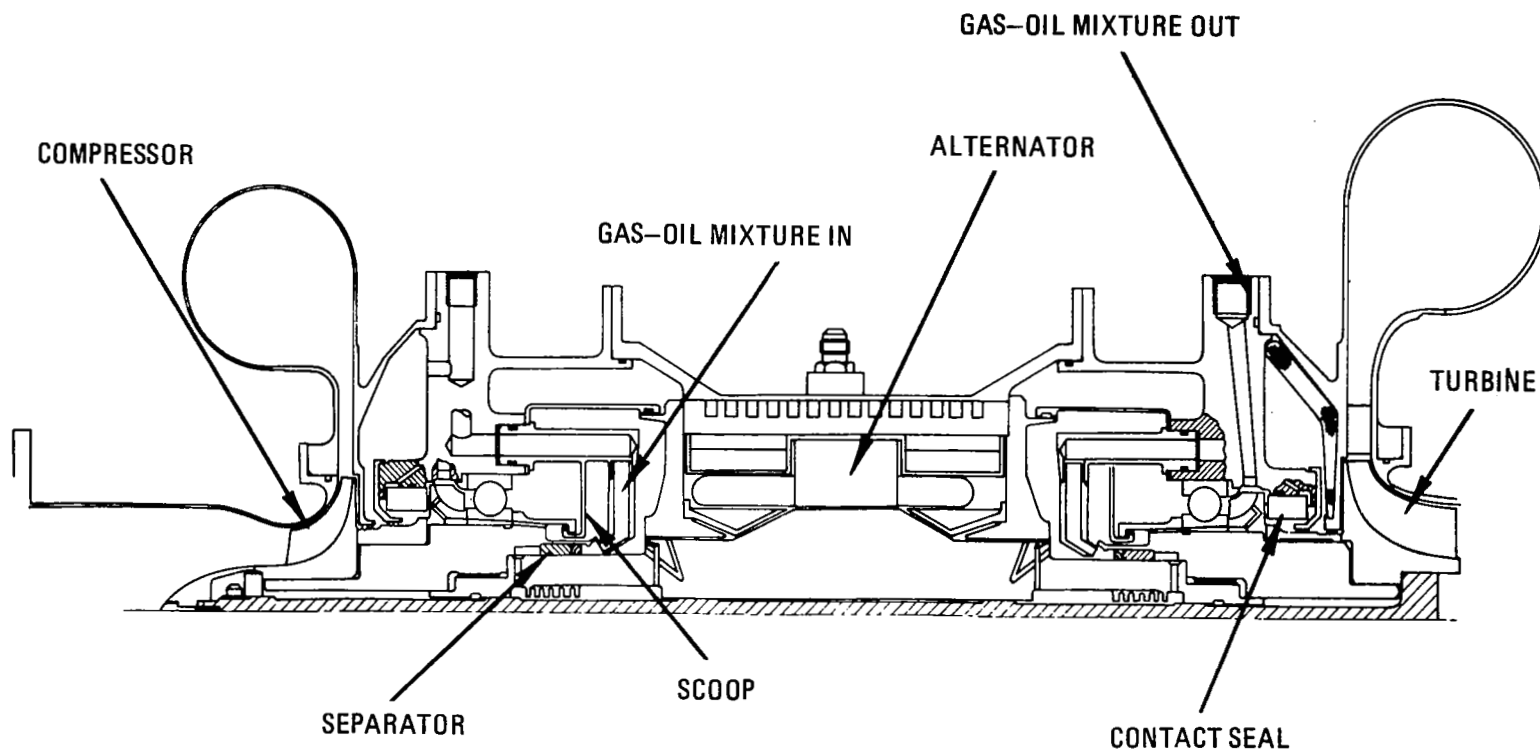


Figure 36 BRU with Rolling-Contact Bearings M-59076

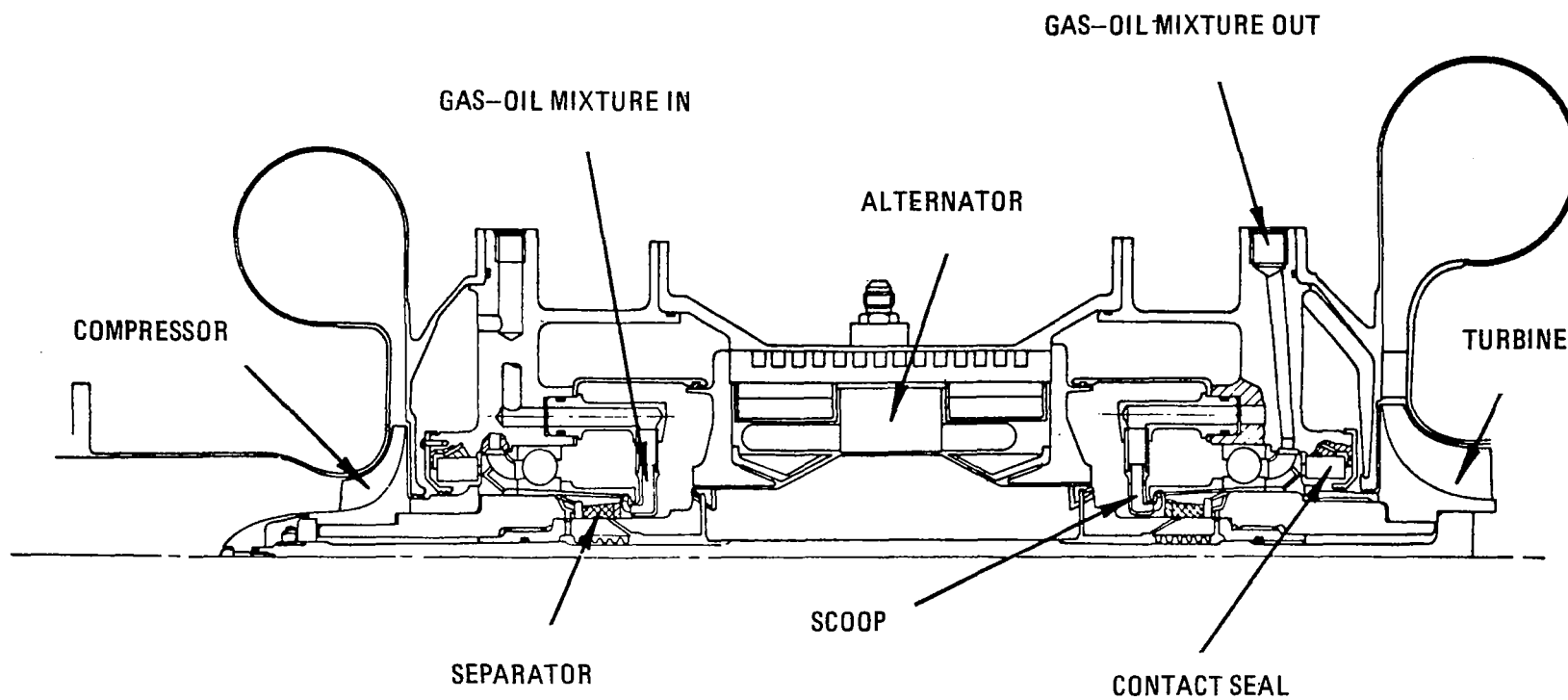


Figure 37 BRU with Rolling-Contact Bearings M-59077

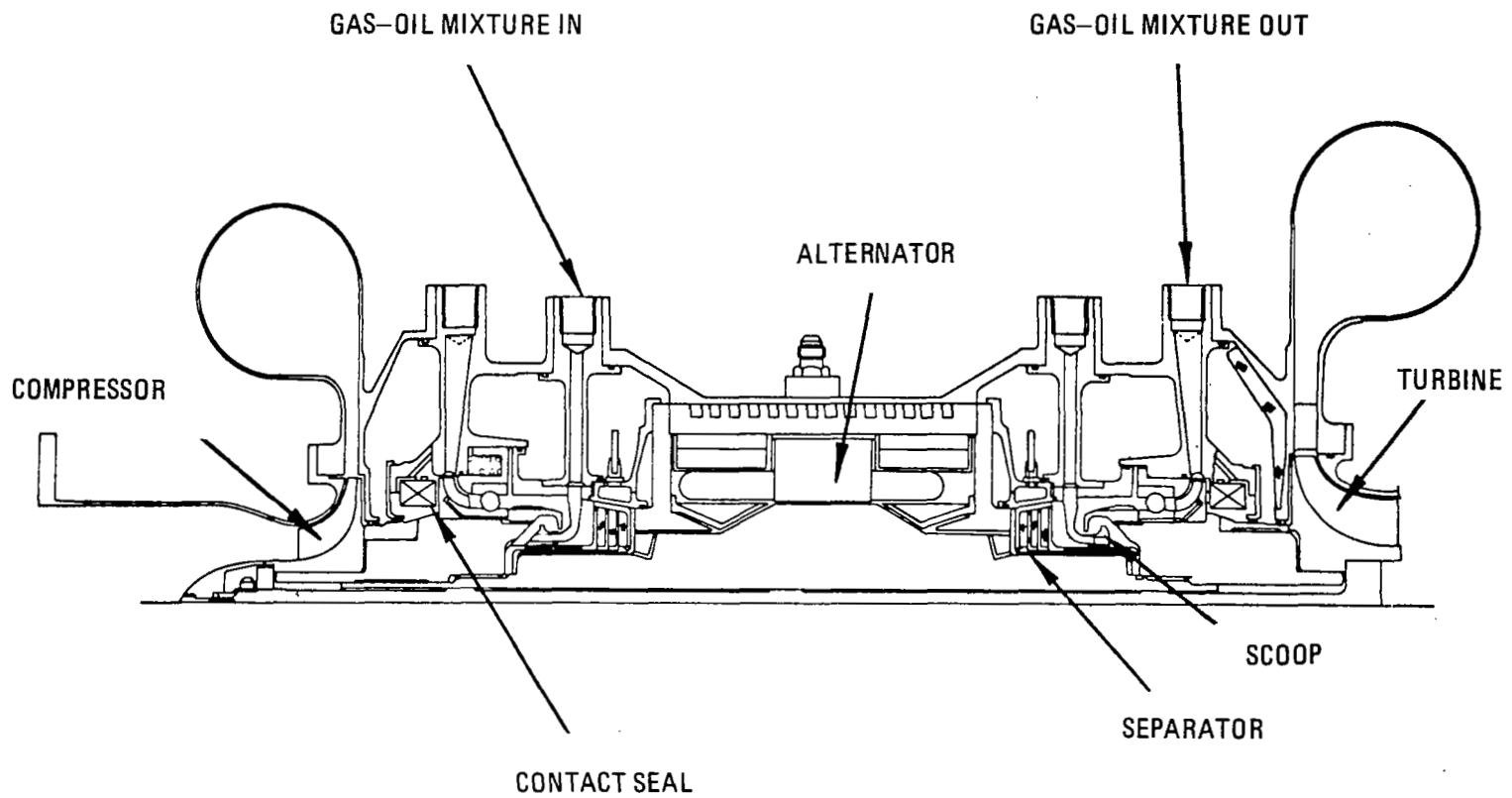


Figure 38 BRU with Rolling-Contact Bearings M-47534



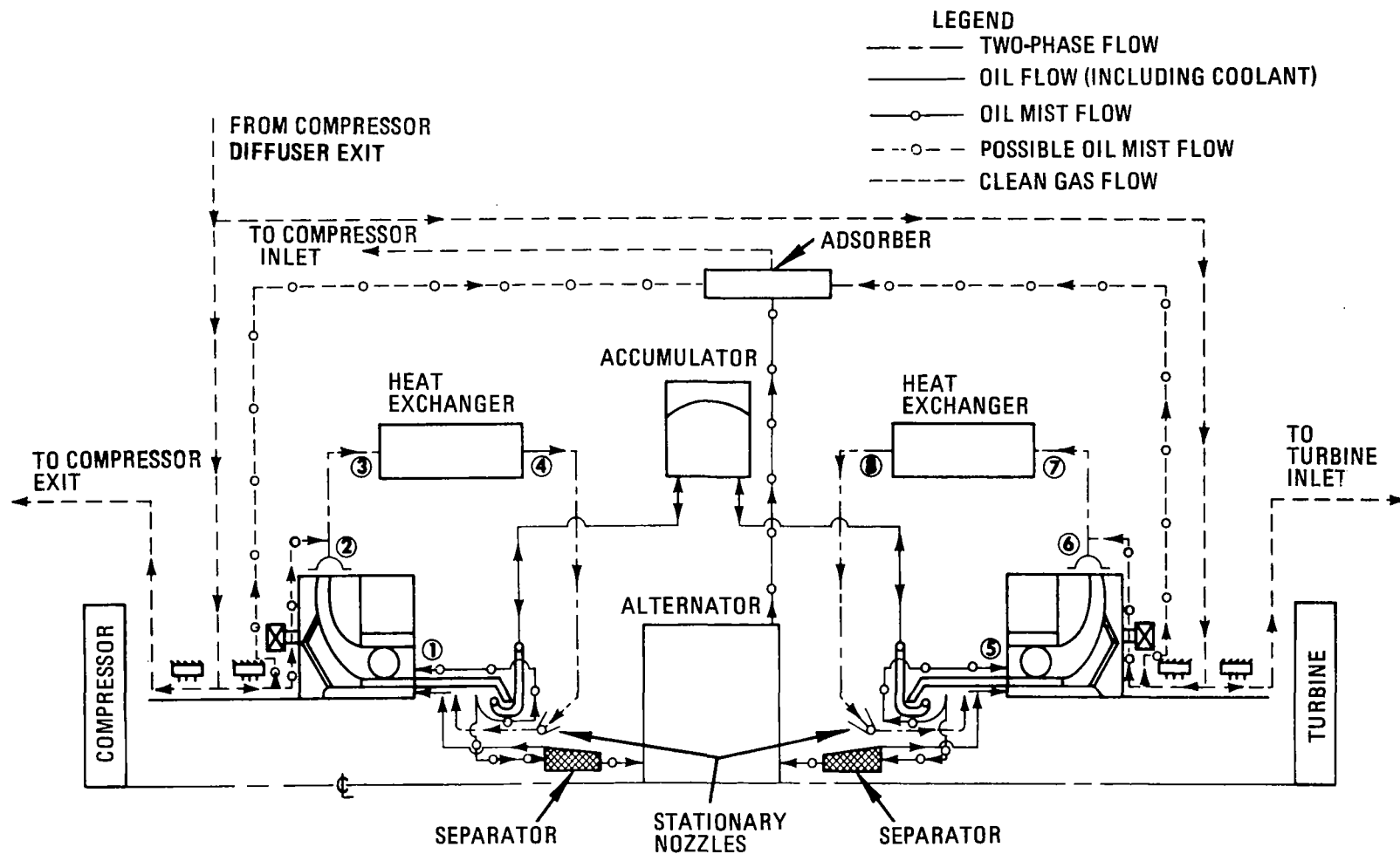
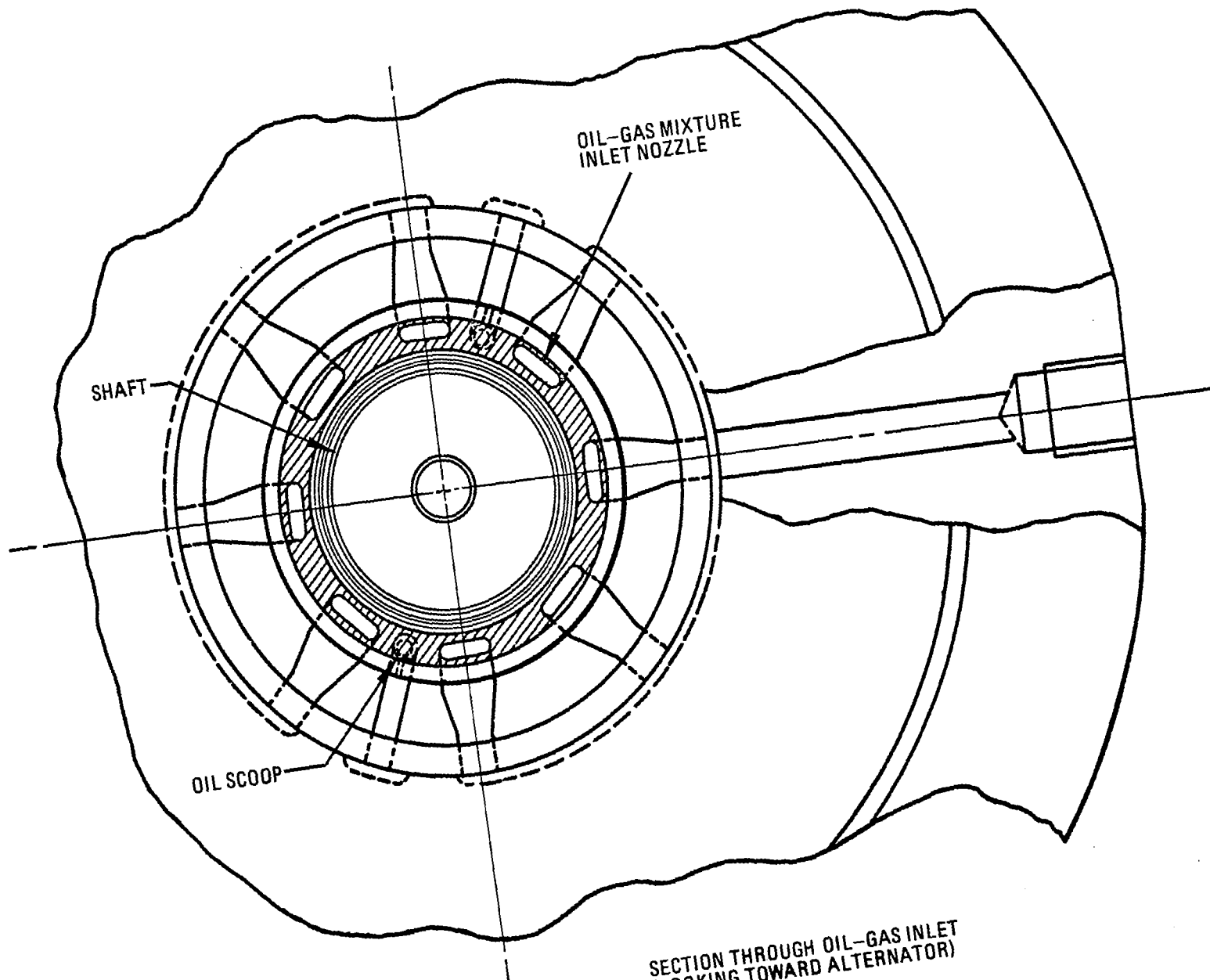


Figure 39 BRU Lubrication System Schematic - Inboard Bearings M-59330



Total parasitic power loss for the 70 mm configuration shown in Figure 38 including separators, bearings, seals, scoops and scavenge pumps, is estimated to be 10,500 watts. Although this power loss is excessive, and although the seal rubbing speed (540 ft/sec) and the bearing DN ( $2.52 \times 10^6$  mm-rpm) are high, it is felt that this design is representative of the inboard-bearing configuration of the BRU incorporating a separator on the shaft.

The inboard-bearing configuration with no separator on the shaft is shown in Figure 41. This BRU design could be operated entirely without a separator, or could use a separately-driven separator. Introduction and removal of the oil-gas mixture and the sweep gas are similar to those of the previous designs. With the omission of the separator, the oil scoop and the accumulator, Figure 39 can be used to describe the lubrication system in this configuration. Removal of the separator and scoop permits the use of a bearing bore of 40 mm diameter and a shaft 2 inches shorter, which results in two rigid-body critical speeds in the range of 25,000 to 30,000 rpm. The first bent-shaft critical speed occurs at about 47,000 rpm. The effect of varying bearing size on rotor dynamic behavior is shown in Table 14. The 40 mm bearing is the smallest diameter considered because it results in marginally-acceptable critical speeds. Parasitic power loss for this version is about 2500 watts. Bearing DN is  $1.44 \times 10^6$  mm-rpm for the 40 mm bore, and bearing  $B_1$  life is predicted to be about 10,000 hours. Due to the lower heat generation rates, the oil flow rate for this design is 75 pounds per hour and the gas flow rate is 20 pounds per hour. Seal rubbing speed for this design is 330 ft/sec.

TABLE 14  
Rotor Dynamic Characteristics  
Inboard-Bearing Configuration (No Separator on Shaft)

<u>Bearing Diameter, mm</u>	<u>Bearing DN, mm-rpm x 10<sup>-6</sup></u>	<u>Rigid-Body Critical Speed Range, rpm</u>	<u>Bent-Shaft Critical Speed, rpm</u>
55	1.97	29,000 - 34,000	82,000
50	1.80	28,000 - 33,000	73,000
45	1.62	27,000 - 32,000	61,000
43	1.55	26,000 - 31,000	55,000
40	1.44	25,000 - 30,000	47,000

The evaluation of inboard-bearing configurations was completed at this point and it was concluded that this configuration would have a parasitic power loss of at least 2500 watts and marginal bearing lifetimes for this application. Efforts were then started to evaluate BRU configurations with one inboard-bearing compartment and one outboard-bearing compartment, to lower parasitic power loss and to facilitate separator integration. The first of these configurations analyzed consisted of placing the bearings on each side of the alternator and overhanging the turbine and compressor on one end of the shaft and the separator from the other end of the shaft, as shown in Figure 42. Potential advantages of this arrangement are simplified separator cooling due to location, simplified oil-gas mixture entrance and exit through the cool shaft end, and a single face seal. The lubrication system differs somewhat in that the oil mist passes from the separator into the alternator, through the bearings and then through the scavenge pumps back to the cooler and separator. Oil flows from the

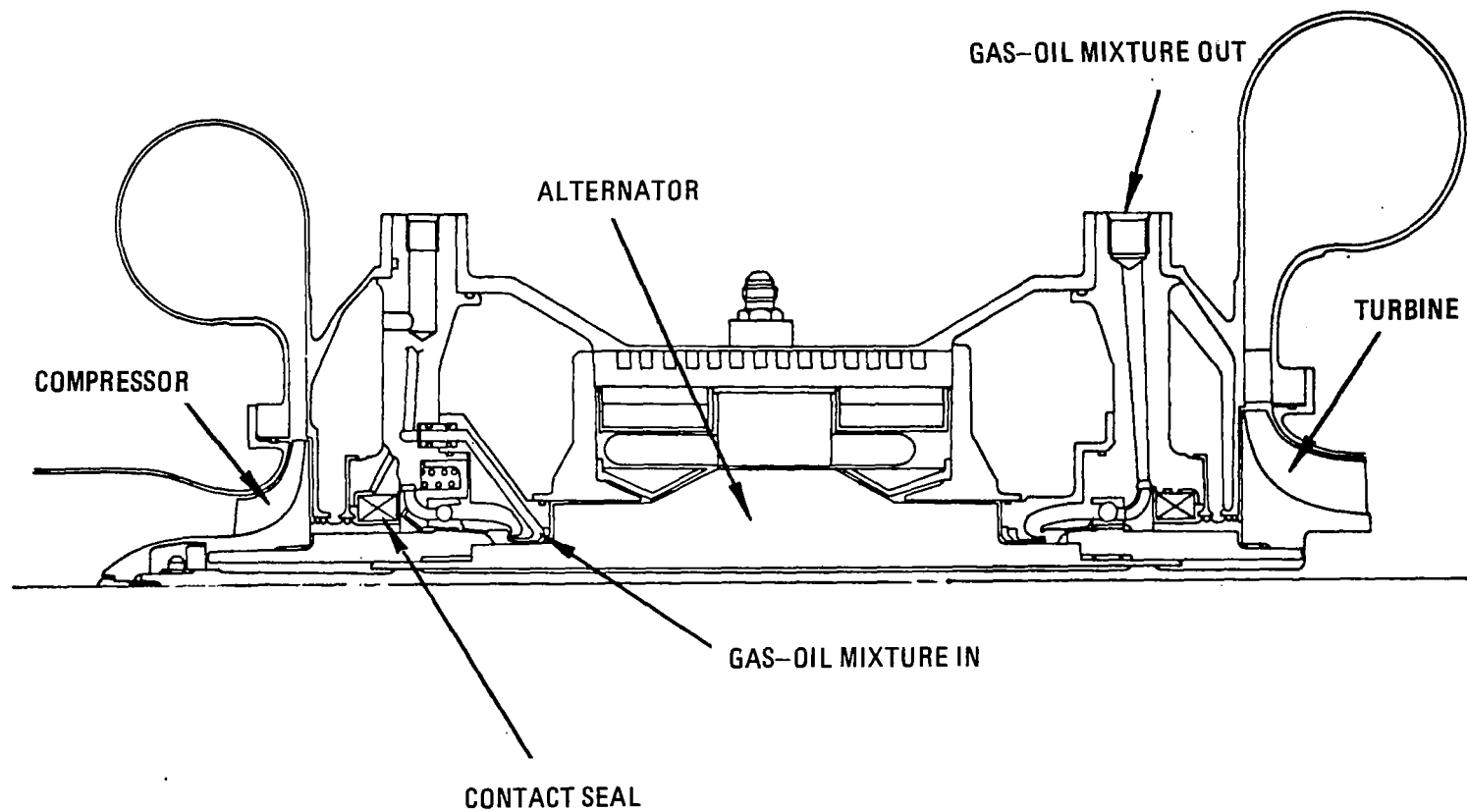


Figure 41 BRU with Rolling-Contact Bearings M-47533

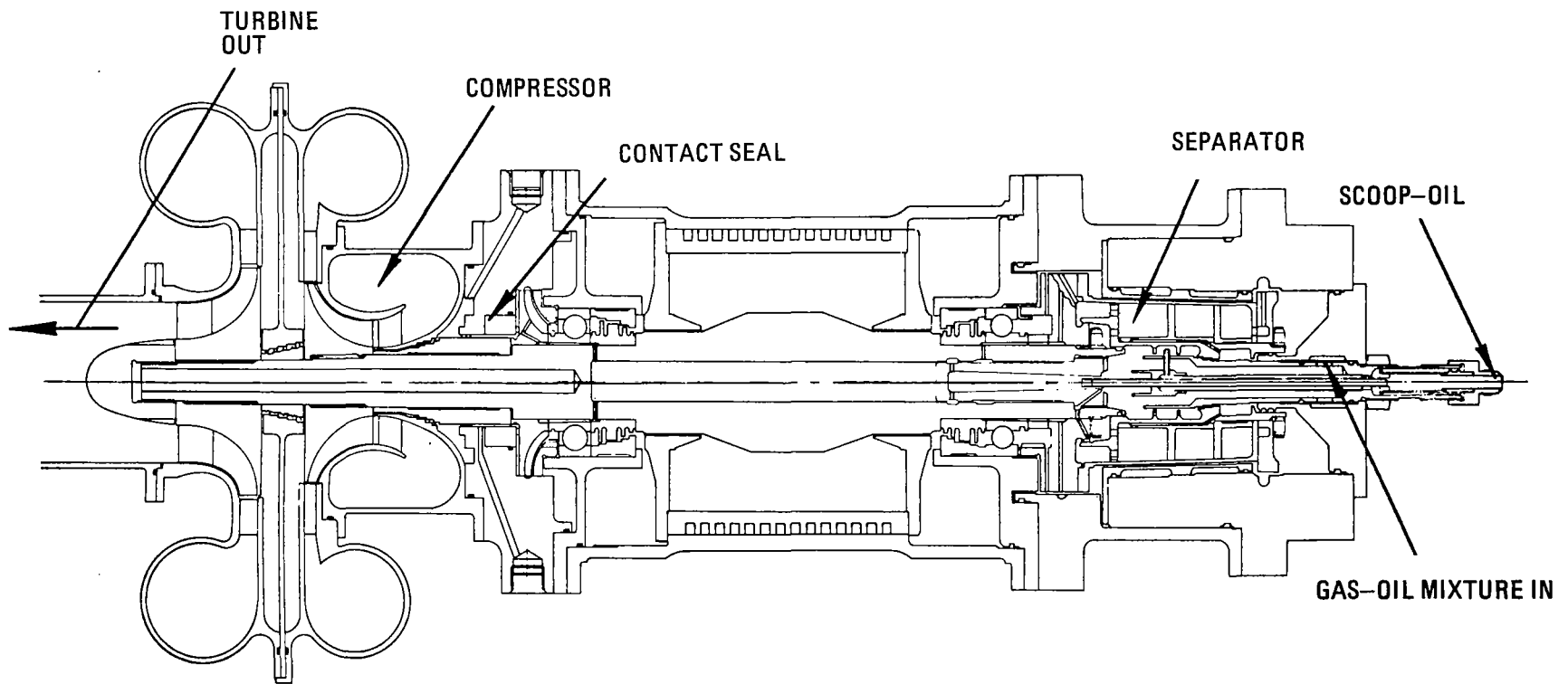


Figure 42 BRU with Rolling-Contact Bearings M-51655

separator and then through the bore of the shaft to the bearing inner races. After the oil cools the bearings and the one sealplate, it mixes with the oil mist from the bearing and is pumped out to the cooler and separator by the scavenge pumps in each bearing compartment. This design is shown with 40 mm bearings at both ends with a DN of  $1.44 \times 10^6$  mm-rpm and a seal speed of 330 ft/sec. Rigid-body critical speeds at about 9,700 and 26,000 rpm were reasonable but the bent-shaft critical at about 29,000 rpm essentially eliminated this design unless larger bearings were used with attendant increased parasitic power loss.

The configuration consisting of one inboard-bearing compartment and one outboard-bearing compartment shown in Figure 43 is similar to Figure 42 above. However, this design has only the turbine wheel overhung rather than the turbine and compressor wheels. Component arrangement is as follows: separator, outboard bearing compartment, compressor, alternator, inboard bearing compartment, and turbine. On bearings of 40 mm bore, the critical speed values were reasonable with rigid-body critical speeds in the range of 19,000 to 24,000 rpm, and a bent-shaft critical speed about 60,000 rpm. Bearing DN for this configuration was  $1.44 \times 10^6$  mm-rpm and seal rubbing speed 330 ft/sec. The oil and gas flow path to the inboard-bearing compartment is down the shaft bore after the oil has been passed through a cooler. An advantage of this arrangement is that the oil does not have to pass under the hot turbine area. The placement of the bearing compartments with respect to the turbine and compressor in this configuration resulted in the requirement for two labyrinth seals (one at each bearing compartment) as compared to only one at the inboard-bearing compartment when both the turbine and compressor were overhung. Further design study on this type of arrangement (inboard-outboard bearing compartments) was terminated because the inboard bearing compartment limits reduction of parasite power loss by reducing bearing size.

The initial design studies of BRU configurations incorporating two outboard bearing compartments concentrated on separator design and integration. These early outboard BRU designs used 40 mm bore bearings at each end with resulting seal rubbing speeds of 330 ft/sec, bearing DN values of  $1.44 \times 10^6$  mm-rpm, and bearing  $B_1$  lifetimes of about 10,000 hours. The initial selection of 40 mm bore bearings was determined by experience with the earlier BRU designs.

The first outboard bearing configuration shown in Figure 44 uses a single separator. The oil-gas mixture enters the separator and flows down the bore to a point just past the scoop where most of the oil is slung out into the scoop pool. About half of the gas continues flowing down the shaft bore towards the turbine end bearing. The oil which flowed to the scoop pool area passes through the inner race of the compressor-end bearing and then through the sealplate. The oil mist flows past the scoop pool area, through the separator to further remove oil, and then through the bearing balls. The oil mist exits from the balls into the scavenge impeller where it mixes with the heated oil stream and passes out to a cooler for recirculation. Oil from the scoop is pumped out the separator, through a cooler, and reintroduced to the center of the shaft at the compressor end, to flow down the bore to the turbine-end bearing along with half of the gas flow originally introduced to the shaft. Flow through the balls, race and sealplate at the turbine end is similar to the compressor-end flow. Table 15 indicates that the second rigid-body critical speed is within the 20 percent overspeed value of 43,200 rpm, at a rotor-support springrate of 250,000 lb/in.

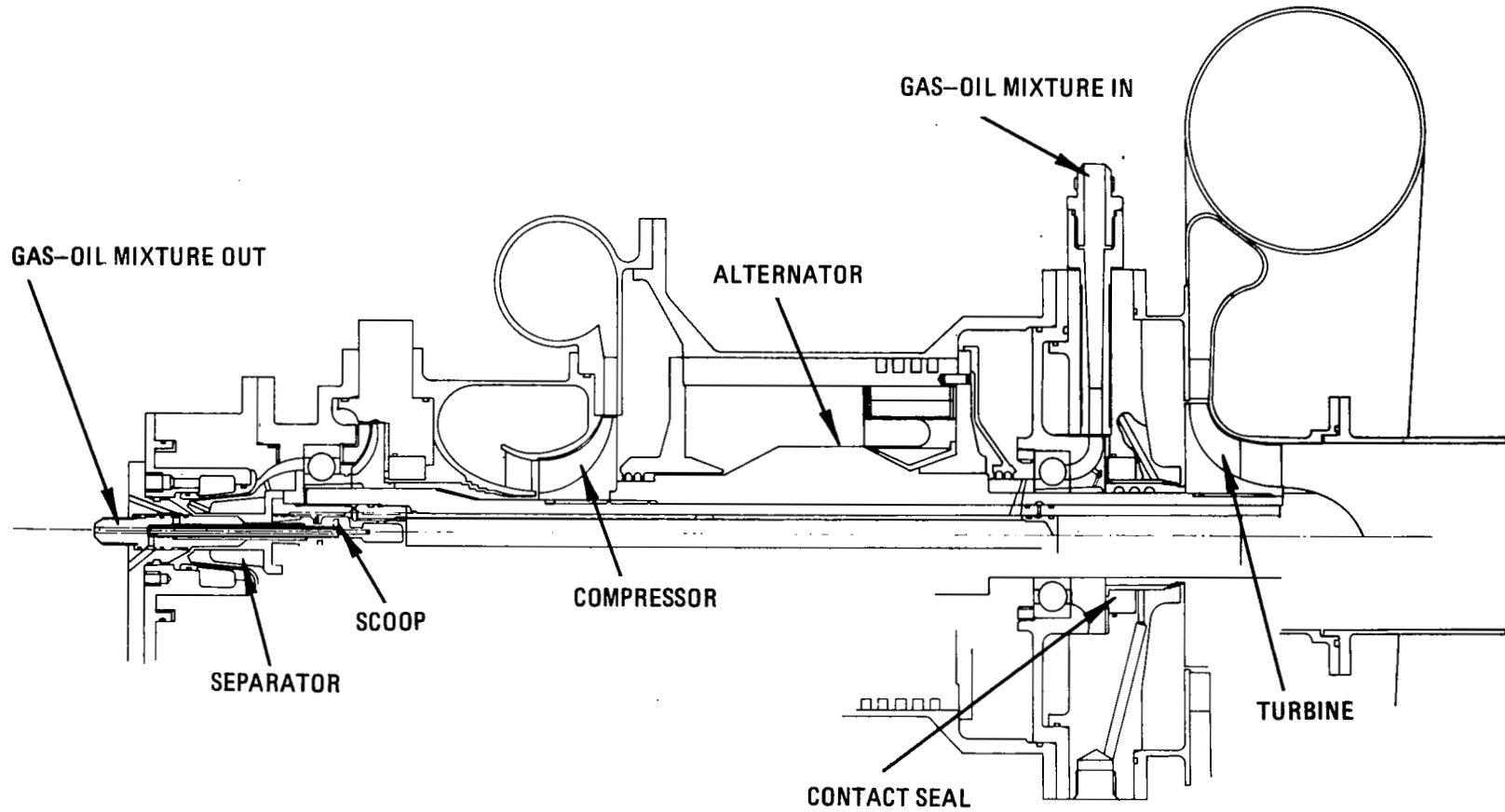


Figure 43 BRU with Rolling-Contact Bearings M-59079

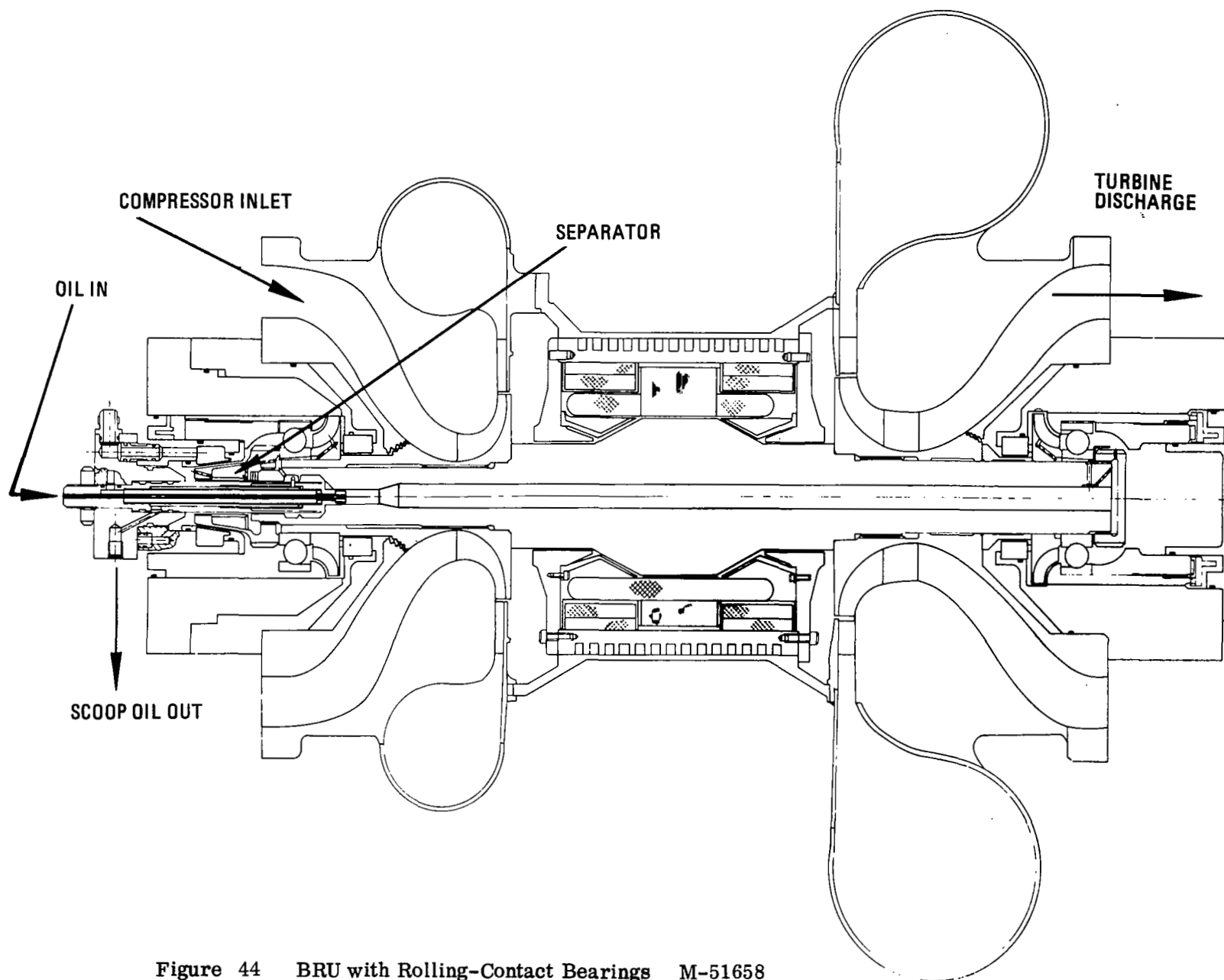


Figure 44 BRU with Rolling-Contact Bearings M-51658



TABLE 15

## Rotor Assembly Critical Speeds (rpm)

Rotor Support Springrate, lb/in	50,000	75,000	100,000	250,000
1st rigid-body critical	10,740	12,600	13,980	18,200
2nd rigid-body critical	20,850	25,830	29,007	41,200
1st bent-shaft critical	55,880	58,290	60,660	71,450

A reduction in the springrate to about 75,000 lb/in would be required for reasonable rigid-body critical speeds. This could be accomplished by using low-springrate bearing mounts. This BRU configuration has the disadvantage of requiring oil to pass through the hot turbine area. Also, this design provides limited oil scoop height with accompanying wake problems and lack of puddle depth.

The outboard-bearing configuration shown in Figure 45 incorporates two separators but only one oil scoop. The oil and gas flow paths in this arrangement are essentially the same as in the previous design except that the gas and oil flow paths through the shaft are isolated from each other. The use of two separators does not affect the basic flow path, but would permit the use of smaller separators at each compartment, because each separator would have to handle only half of the total seal leakage flow. A deviation from the NASA compressor design was incorporated into this configuration for assembly purposes. The compressor wheel bore was enlarged one-half inch. This change has a small effect on critical speed, as shown in Table 16.

TABLE 16

## Rotor Assembly Critical Speeds (rpm)

Rotor Support Springrate, lb/in	50,000	75,000	100,000	250,000
1st rigid-body critical	10,810	12,790	14,290	18,700
2nd rigid-body critical	19,850	24,170	27,740	43,000
1st bent-shaft critical	59,290	61,350	63,380	75,000

As in the previous case, this configuration would require low-springrate bearing mounts to lower the rigid-body critical speed.

In the BRU configuration of Figure 46, oil and gas are introduced and removed at each end of the shaft, eliminating the necessity for passages through the shaft bore, under the compressor and turbine. This design also uses 40 mm bore bearings, but ball diameter has been reduced from 0.5 inch to 0.25 inch, permitting a more compact bearing compartment housing and smoother flow channels at the compressor inlet and turbine exit. The enlarged compressor wheel of the previous configuration was retained in this arrangement. This configuration was

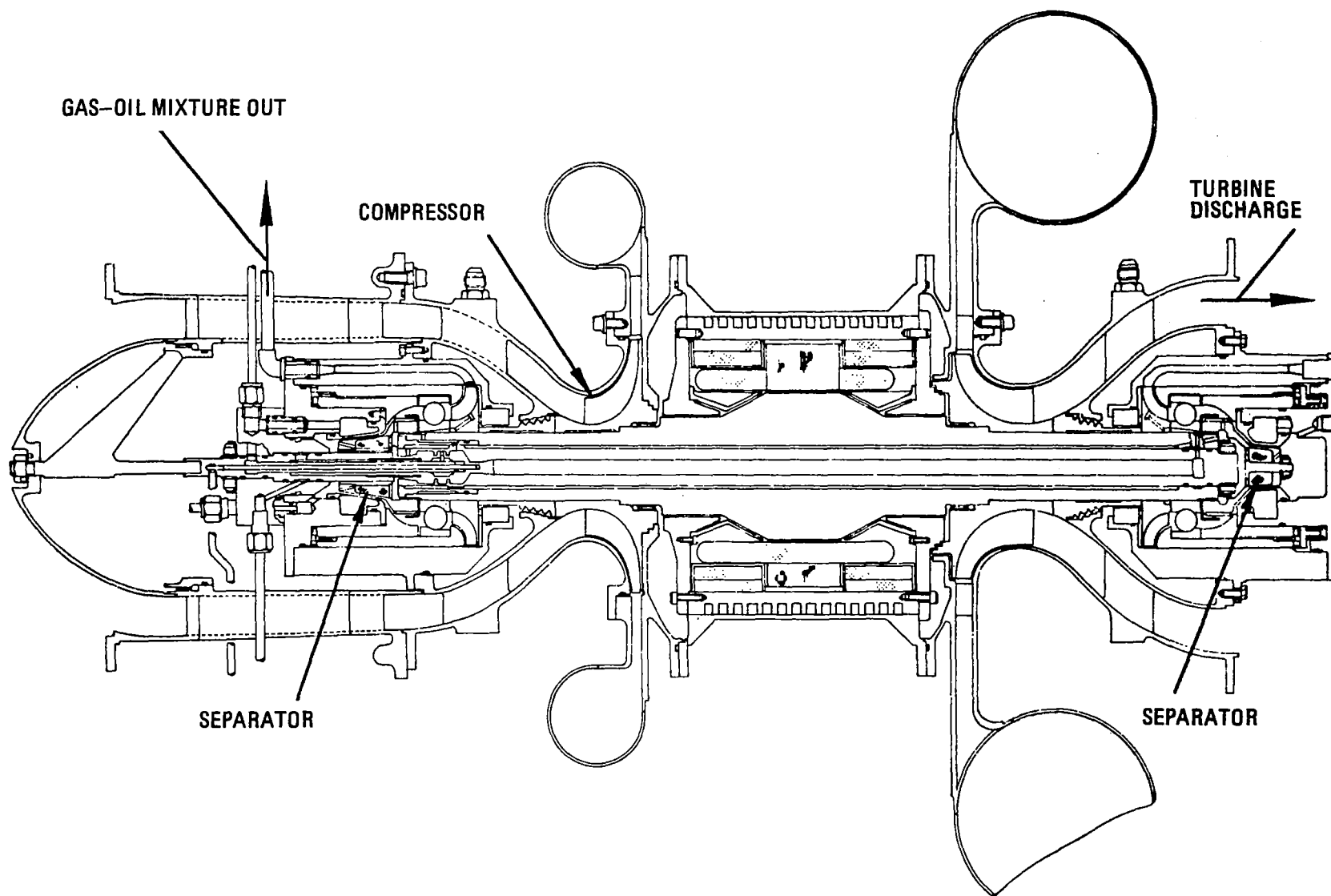


Figure 45 BRU with Rolling-Contact Bearings M-51656

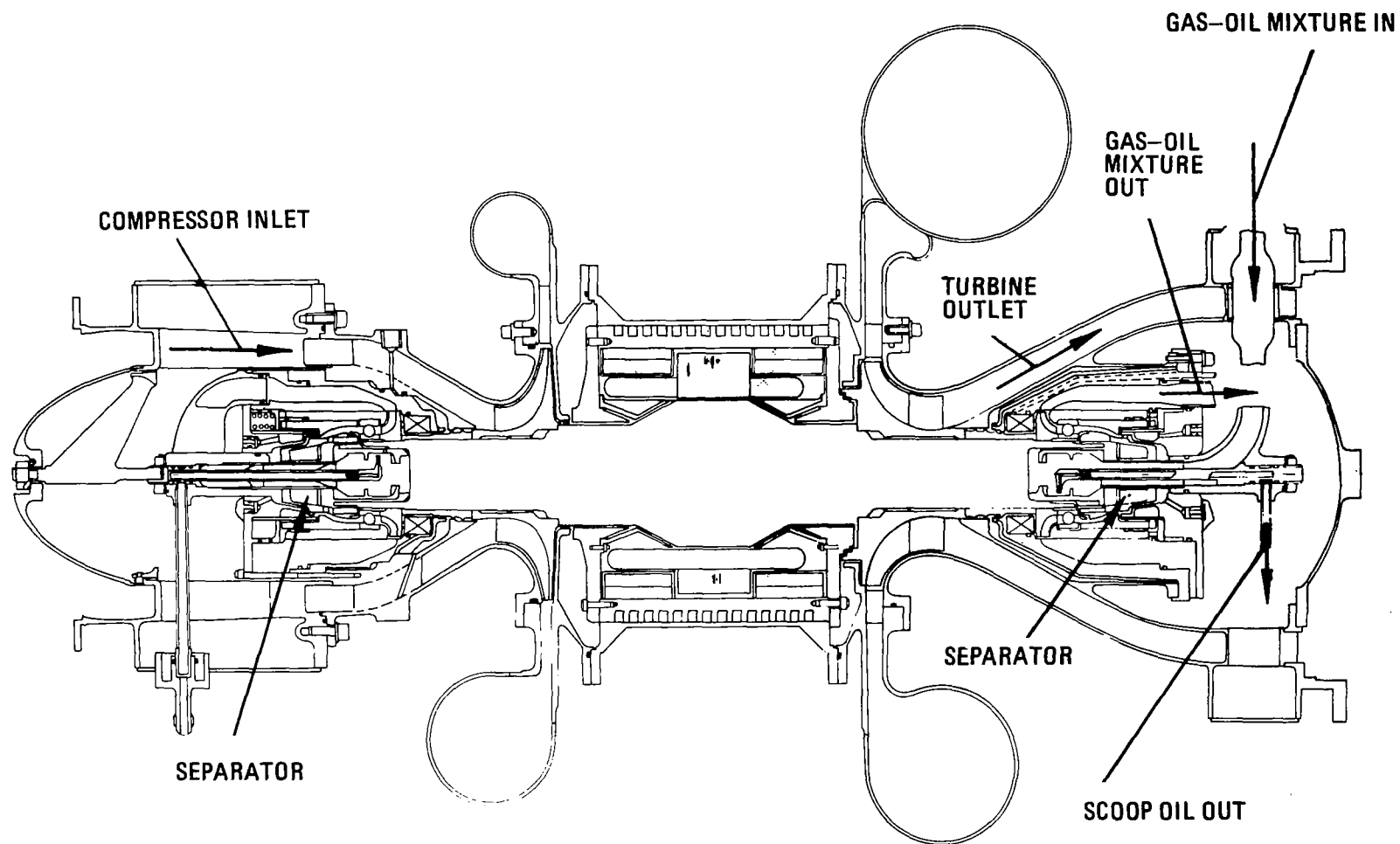


Figure 46 BRU with Rolling-Contact Bearings M-51657

also the first outboard design to incorporate the static pressure oil scoop disc (partial arc) which was introduced in the inboard bearing design of Figure 38 previously. Since this design included two nearly identical bearing compartments, the lubrication system could be split into two isolated loops or could be tied together with a common accumulator. Oil flow through each of the bearing compartments was similar to that previously described. As in the two previous outboard bearing configurations, this design would require low-springrate bearing mounts to control the rigid-body critical speeds. The first bent-shaft critical speed occurred at about 80,000 rpm. The parasitic power losses for this configuration are indicated in Table 17.

TABLE 17  
 Parasitic Power Losses  
 for 40 mm  
 Outboard-Mounted Rolling-Contact Bearings

<u>Power Loss Description</u>	<u>Power Loss, watts</u>
bearing heat generation	330
carbon seal heat generation	680
oil pumping power	63
gas pumping power	25
probe disc drag	27
separator drag	15
Power loss for one bearing compartment -----	1140 watts
Total power loss (two bearing compartments) -----	2280 watts

Oil and gas flow rates for the 40mm design are 71 pounds per hour and 30 pounds per hour respectively.

All previous outboard bearing compartment studies utilized 40 mm bore bearings and concentrated primarily on separator design and integration. Minimum parasitic power losses attained in a 40 mm configuration were 2.25 KW. The next few outboard bearing designs represented the effort to optimize the overall package arrangement and to attain minimum parasitic power losses and to select a reference BRU configuration for further study.

A configuration using two 30 mm bearings was studied and is shown in Figure 47. This configuration incorporated a separator and a static disc (scoop) at each bearing compartment. The total parasitic power loss for this design was 1500 watts. Critical speeds were acceptable with rigid-body critical speed values at about 18,000 and 50,000 rpm and a bent-shaft critical speed at about 95,000 rpm. Further study of this design indicated that the gas flow passages were not large enough through the separator area, requiring an increase in bearing diameter to permit increasing the flow passages. As a result of this 30 mm design study, bearing diameter was increased to 35 mm. To minimize parasitic power losses, one separator was deleted from the design permitting the use of a 20 mm bore bearing at the turbine end. The selection of a 20 mm bearing is discussed later. The resulting configuration is shown in Figure 48.

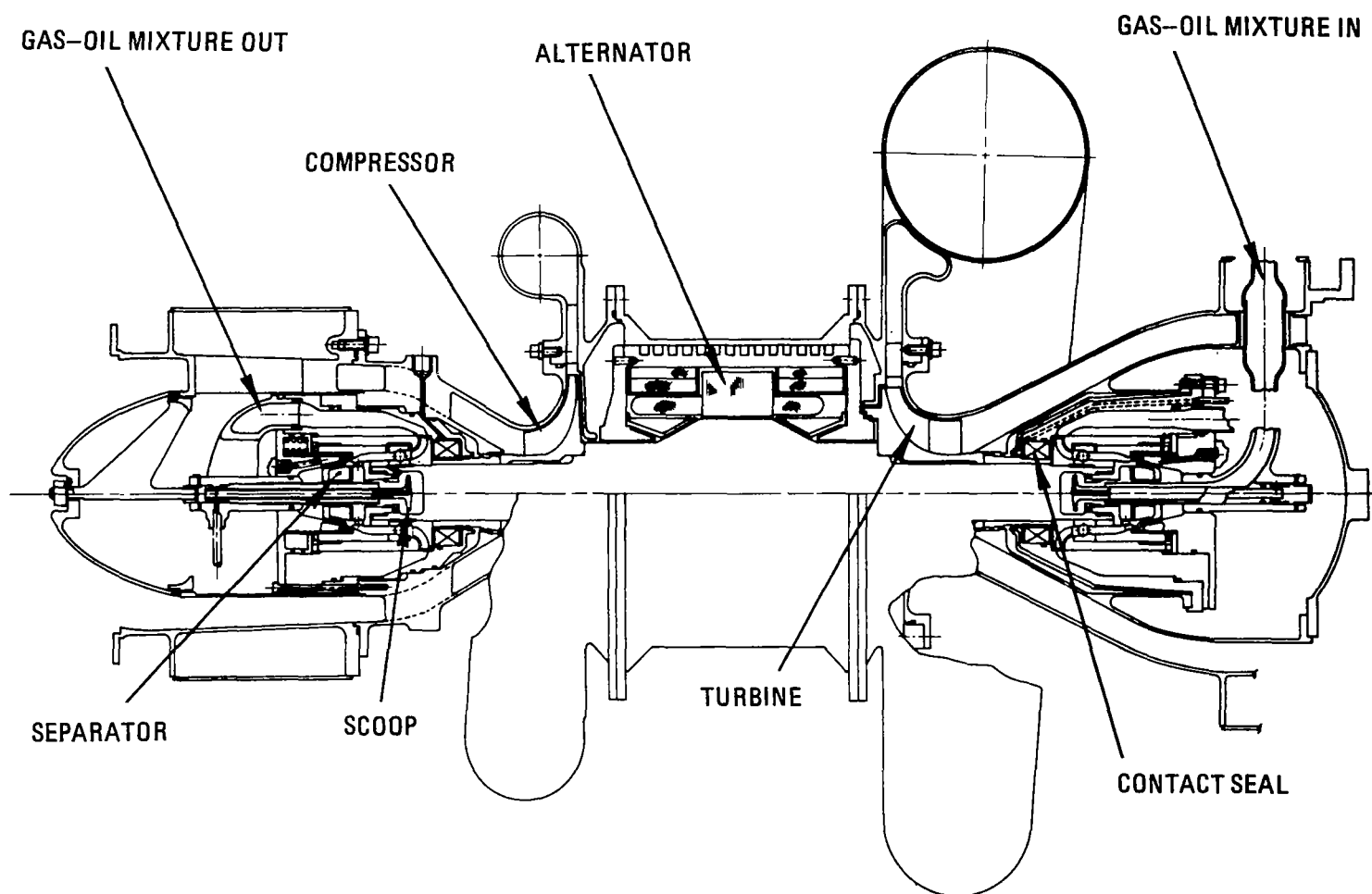


Figure 47 BRU with Rolling-Contact Bearings M-59078

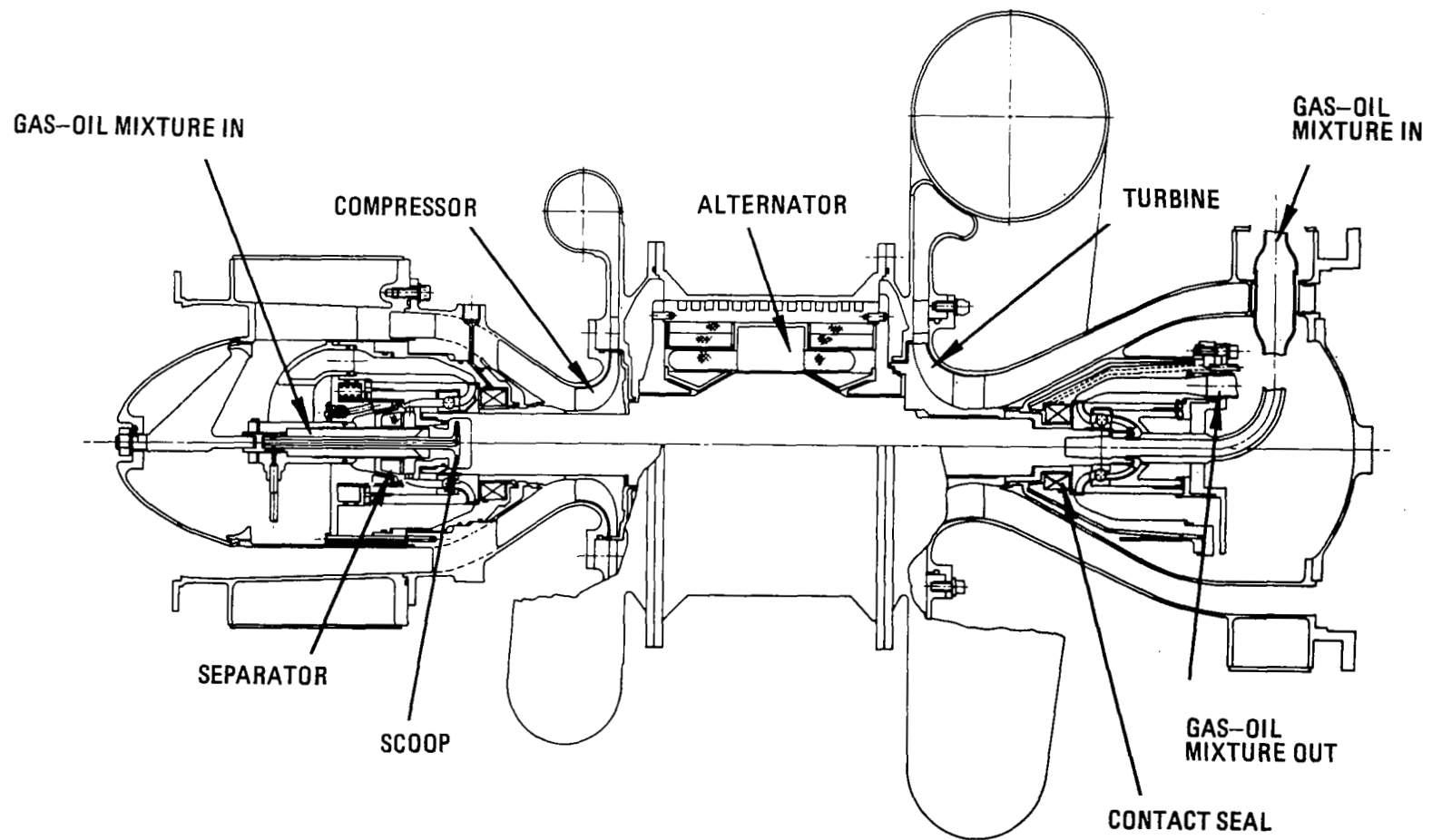


Figure 48 BRU with Rolling-Contact Bearings M-47825

The use of a single separator rather than two separators permits the use of the 20 mm size bearing in the turbine-end compartment, with accompanying reduction in parasitic power. The use of two separators implies that each separator can be designed to handle half of the gas flow of a single separator, thus permitting further reduction in the size of the separator. However, since the separator is already at a minimum practical size with one separator capable of handling the total required flow, the use of two separators was not necessary. This method of reducing parasitic power by using one separator and a smaller bearing compartment is not feasible for an inboard-bearing configuration. If a single separator were used in an inboard-bearing arrangement, oil and gas mixture would have to flow down the shaft to the turbine-end bearing. This method does not permit a reduction in bearing size at the turbine end because the oil cannot flow inward against the centrifugal forces in the rotor. For this reason, an inboard bearing design requires the use of the same size bearing at each end, whether one or two separators are used. This is shown in the shaft sketch of Figure 49.

The final BRU configuration analyzed incorporates no separator in the BRU shaft and represents the minimum possible parasitic power loss for the BRU with rolling-element bearings. A minimum bearing bore of 20 mm was determined for this design because cross-sectional area available in the BRU shaft under the bearing for oil-gas flow passages becomes marginal below this diameter. Figure 50 shows this design. Parasitic power losses for this configuration were 380 watts per bearing compartment for a total loss of 760 watts. The 20 mm bore bearing B<sub>1</sub> life was in excess of 10,000 hours with the rigid-body critical speeds occurring at 11,000 and 33,000 rpm, and the bent-shaft critical speed at about 77,000 rpm. The rigid-body critical speeds could be lowered using soft bearing mounts.

Figures 51 and 52 are schematics of the two possible lubrication systems which could be used with the 20-20 mm outboard bearing configuration of Figure 50. The difference between the two schemes is that the system of Figure 51 uses a separately-driven separator while that of Figure 52 has no separator. The separately-driven separator system remains a closed-loop lubrication, and operates essentially the same as the lubrication system for the 35-20 mm single-separator design. To minimize oil contamination, it is felt necessary to maintain a positive pressure drop across the bearing compartment seals to assure that any gas leakage will result in leakage of cycle gas into the bearing compartment, rather than out-leakage of impure gas. In all of the BRU designs which include a separator, this requirement is met by maintaining working gas inventory through a cleanup system to separate the oil from the leakage gas and return the purified gas to the mainstream of the system. In the no-separator design of Figure 52, the gas leakage is exhausted overboard (vent-to-space line at compressor-end bearing compartment) and the system is replenished with gas and oil from a make-up supply.

At this point in the study, Pratt & Whitney Aircraft recommended the 35-20 mm BRU configuration of Figure 48 be adopted as the reference configuration for further study in this contract. This configuration incorporates a separator providing the power system with added reliability to tolerate increases in seal gas leakage. Also, the integral separator simplifies the

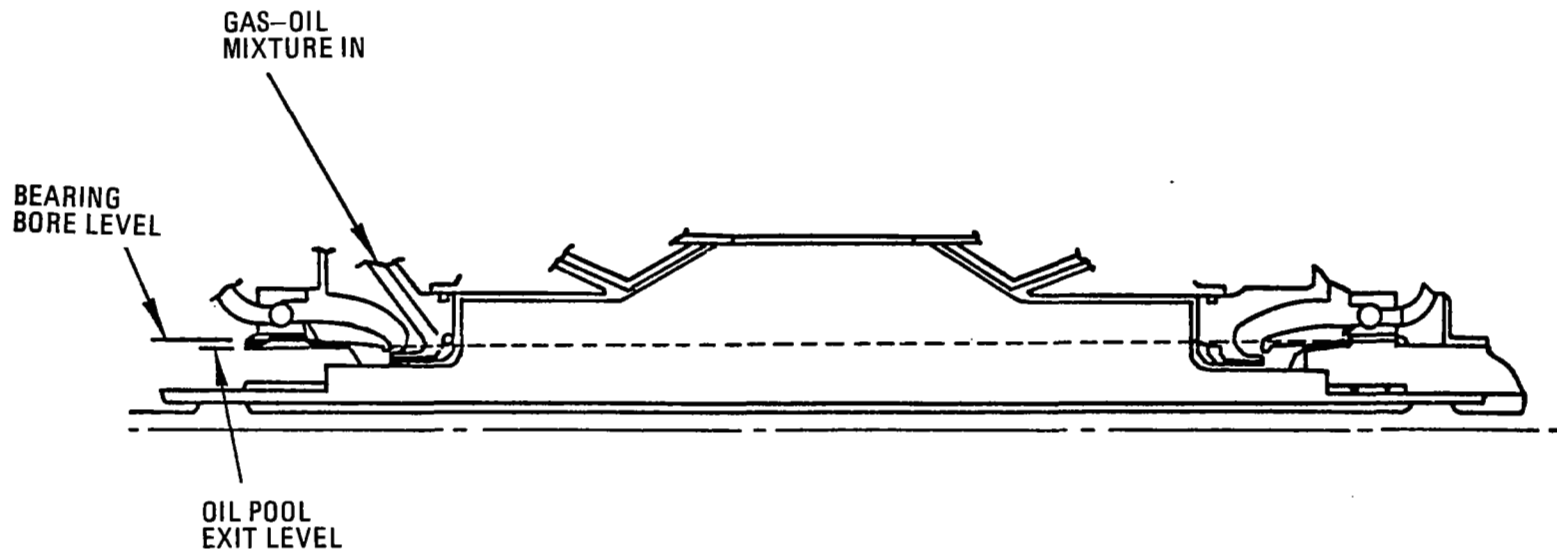


Figure 49 Shaft Section of BRU with Inboard Bearing M-59863



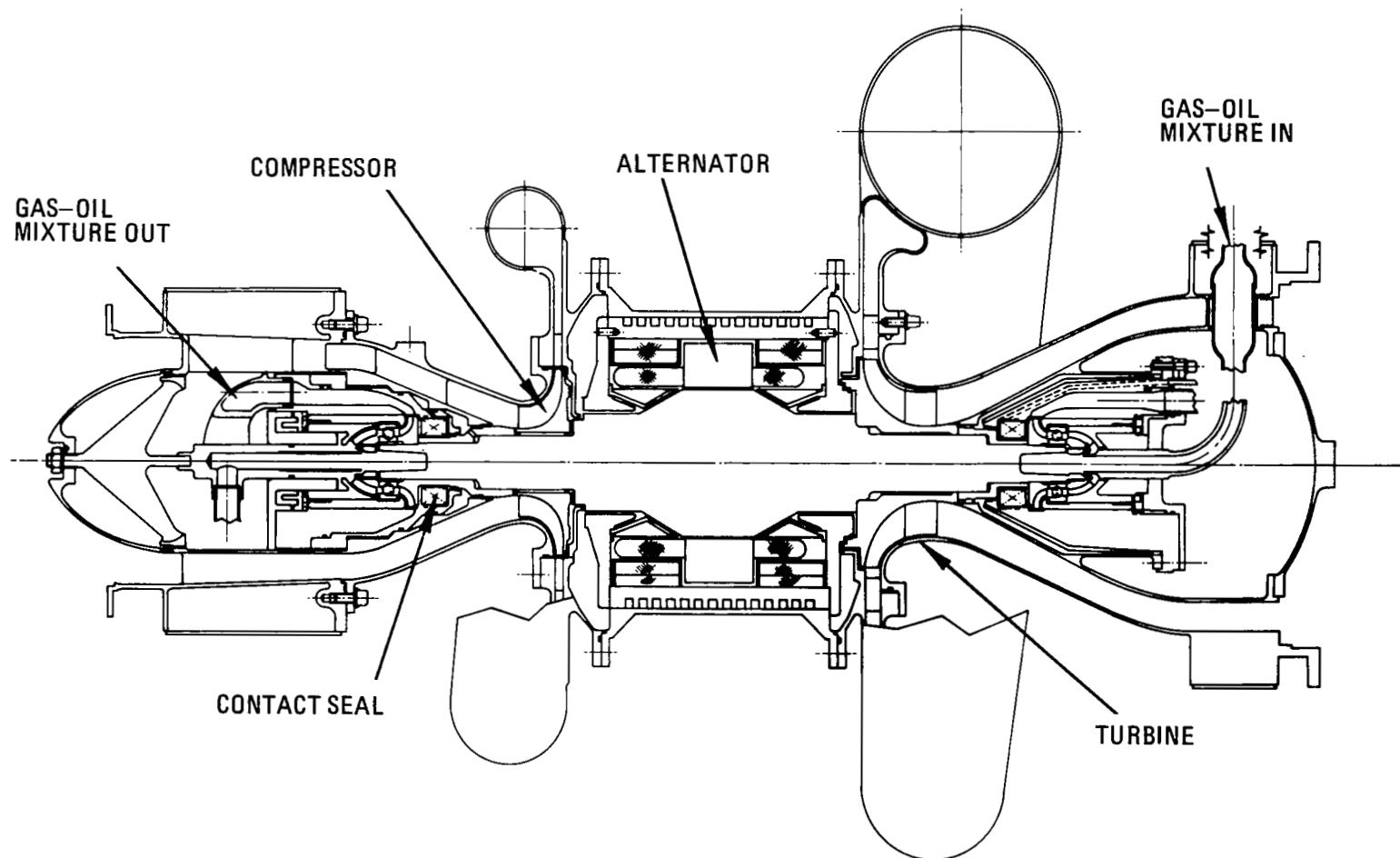


Figure 50 BRU with Rolling-Contact Bearings M-49235

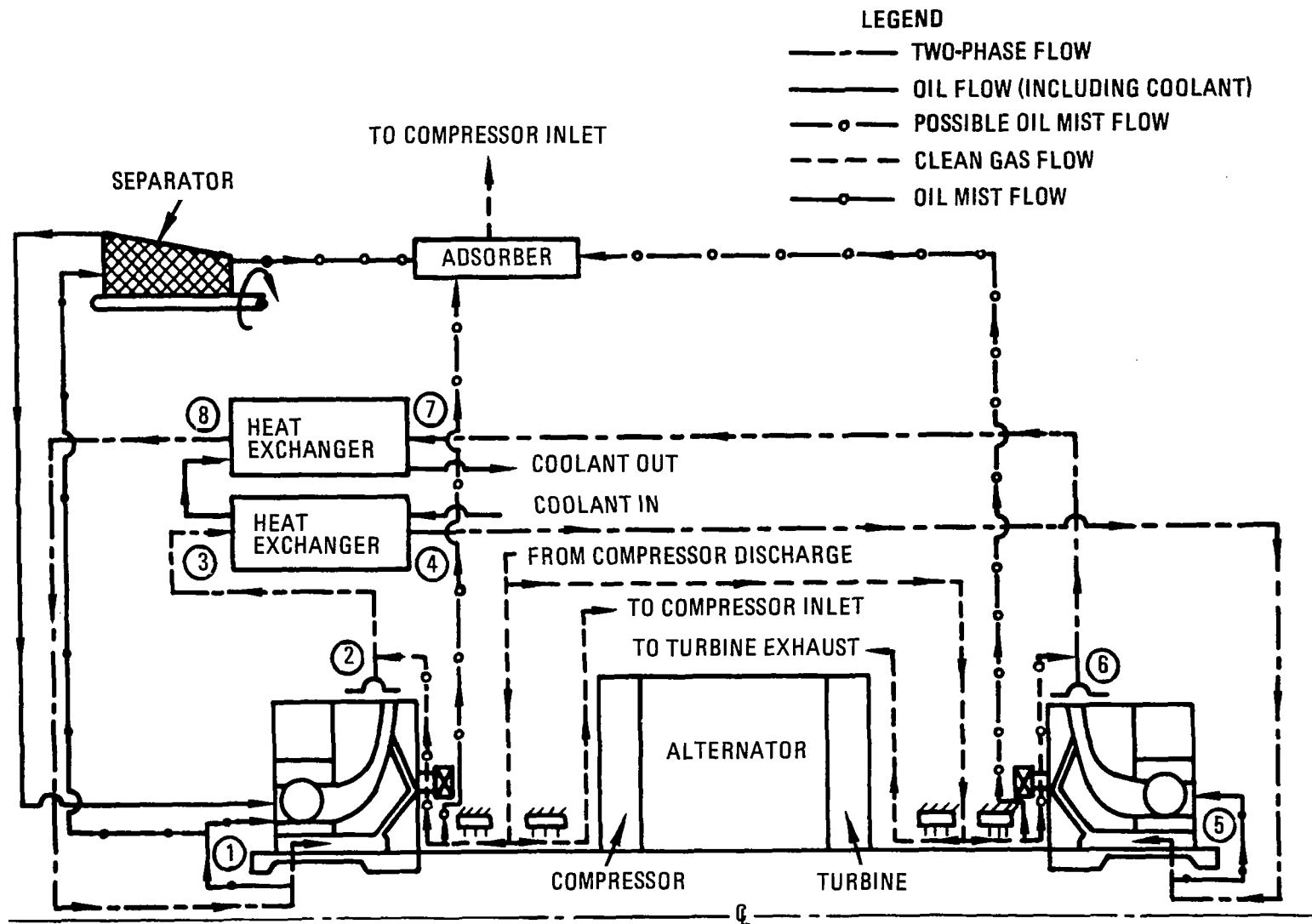


Figure 51 BRU Lubrication System Schematic - Outboard Bearings  
(Externally-Driven Separator) M-59784

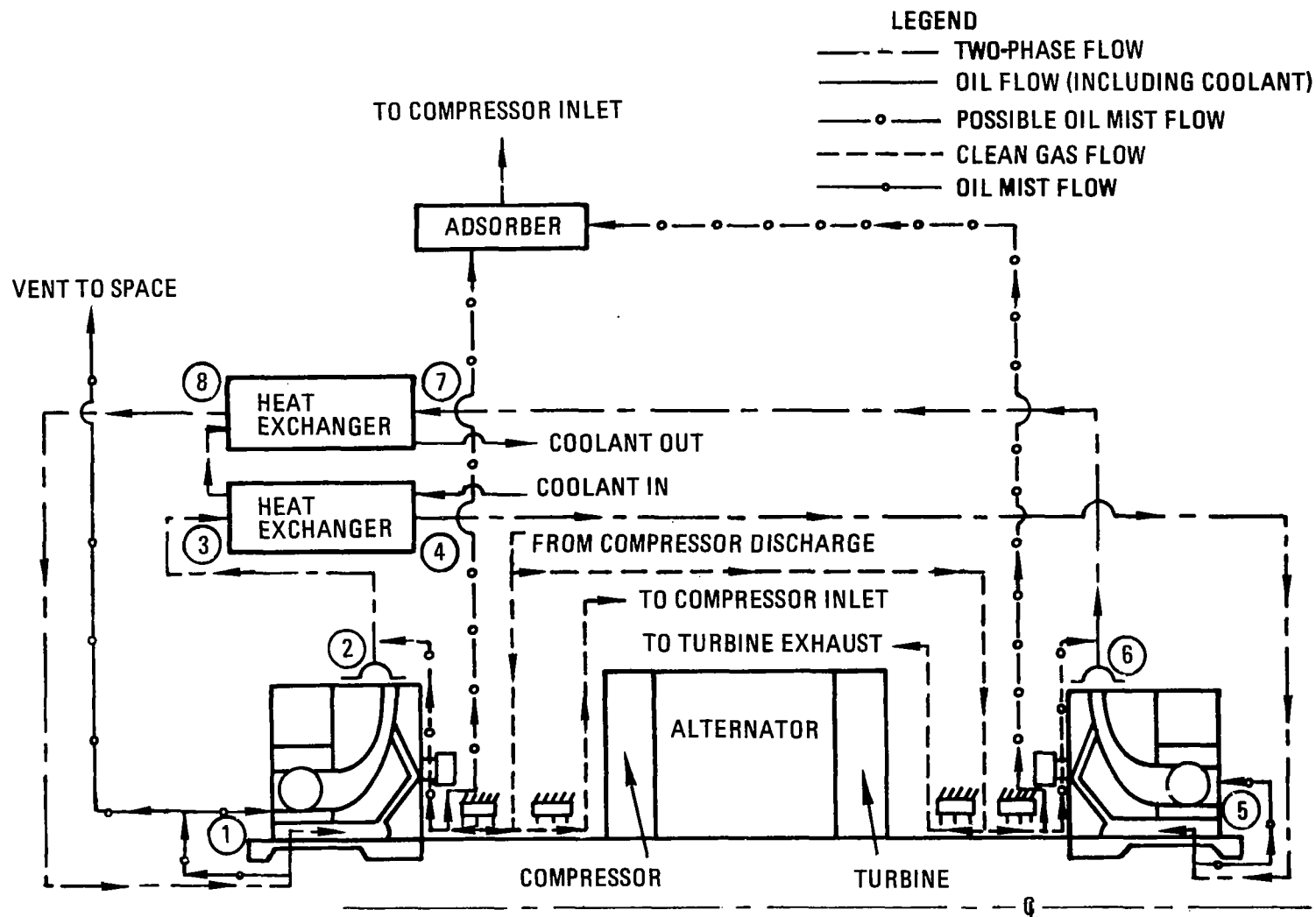


Figure 52 BRU Lubrication System Schematic - Outboard Bearings  
(No Separator) M-59823

overall lubrication system compared to a separately-driven separator. Although a parasitic power loss penalty of about 500 watts appears to result when the separator is incorporated on the BRU shaft, a separately-driven separator either with its own electric motor drive or installing the separator on an existing piece of auxiliary rotating equipment would consume extra power in the small inefficient electric motor and its bearing system, or compromise the BRU lubricant if fluid in the existing auxiliary machinery should leak into the BRU lubricant.